ROCK MAGNETISM AND PALEOGEOPHYSICS

Volume 2

Published by the
Rock Magnetism and Paleogeophysics
Research Group in Japan

December 1974

Tokyo

まえがき

本書は，ＧＤＰ ＩＩ－１－（２）（古地磁気的方法）の活動の，１９７４年末における中間報告として刊行するものである。第１巻はすでに１９７３年１２月に発行された。 以前から，古地磁気グループでは， Annual Report の形で，英文の報告書を刊行してきた。 (Annual Progress Report of the Rock Magnetism Research Group in Japan, 1963, 1964, 1965; Annual Progress Report of the Paleogeophysics Research in Japan, 1967, 1968). これらの Annual Report は，諸外国の研究者の間でかなり広く利用されており，こういつたこれまでの実績を継続するという考えから，ＧＤＰの研究報告であるが，英文で出版することになつた． このため，日本国内の読者諸氏にいく分御面倒をおかけすることになるが，この点御了承いただきたい。

報文の配列の仕方は便宜的なものであるが，一応大まかに（１） 岩石磁気に関する問題，（２） 古地磁気および地かく変動に関する問題，（３） アイソトープ地学および地球の進化に関する問題，（４） 地球磁場に関する問題 に分類してある。

なお本書は，extended abstract 集 をめざしているので，ここにおさめられた報文は progress report 的なものをのぞき，いずれ完全なかたちの論文としていろいろな学術誌に発表される予定である。

１９７４年 １２月

古地磁気学 古地球物理学研究グループ

PREFACE

This is an annual progress report of the Rock Magnetism and Paleogeophysics Research Group in Japan for the year 1974. As the previous annual reports were so, this volume is a collection of summaries or extended abstracts of various research works carried out in our group. Except the ones written as pure progress reports, the papers in this volume will be published in academic journals in full detail and length. This volume can be referenced, but if a paper in this volume is published in another journal, readers are requested to refer the paper from that journal. We hope that this volume will be used as a summary of advance information of recent works on rock magnetism and paleogeophysics in Japan.

We would like to acknowledge the partial financial support for this publication and for the investigations included in this volume from the Ministry of Education as part of the Geodynamics Project. This volume constitutes a scientific report of the Rock Magnetism and Paleogeophysics Research Group in the Geodynamics Project in Japan.

30 December 1974

Masaru Kono
Editor

CONTENTS

ROCK MAGNETISM

PALEOMAGNETISM, TECTONOPHYSICS

ISOTOPE GEOLOGY, EVOLUTION OF THE EARTH AND PLANETS

ORIGIN AND STRUCTURES OF THE GEOMAGNETIC FIELD

ROCK MAGNETISM AND PALEOGEOPHYSICS SYMPOSIA

Two symposia were held in 1974; 14 and 15 March at Geophysical Institute, University of Tokyo, and 15 and 16 July, at Mining Museum, Akita University. Titles of the papers presented at these symposia are as follows:

14 March

N. Niitsuma (Akita Univ.)	Fe-Ti oxides and their alteration
H. Domen (Yamaguchi Univ.)	An estimation of the lattice substituted elements of rocks using rock magnetic data
T. Nomura (Gumma Univ.)	Paleomagnetism of Nohi rhyolites
S. Aramaki (Tokyo Univ.)	Recent topics in petrology
H. Ito and K. Tokieda (Shimane Univ.)	Paleomagnetism of Cretaceous granites in Hokkaido
K. Nakamura (Tokyo Univ.)	Reconstruction of stress fields in the remote past
J. Nishida (Kyoto Univ.)	On thermomagnetic curves of N-type materials
H. Domen (Yamaguchi Univ.)	A study of the archeomagnetic field intensity using old roof tiles

15 March

S. Sugano (Tokyo Univ.)	State of electrons in compounds of transition metals
R. Kubo (Tokyo Univ.)	Fluctuation and response
H. Mabuchi (Tokyo Univ.)	Nucleosynthesis and the origin of the solar system
M. Ozima (Tokyo Univ.)	Origin and evolution of the atmosphere
K. Saito (Tokyo Univ.)	On hot spots
N. Sugiura (Tokyo Univ.)	Magnetic properties of lunar rocks

15 July

H. Kanaya (Geol. Survey)	Radioactivity and magnetic properties of granites
T. Nakajima, K. Yaskawa and N. Kawai (Osaka Univ.)	On the geomagnetic variation during the last 110 thousand years
N. Kawai (Osaka Univ.)	Paloemagnetism and paleoclimate variation
H. Kinoshita (Meteor. Coll.)	Paleointensities obtained from Precambrian (2.6-3.0 b.y.) rocks of Middle India
K. Noritomi (Akita Univ.)	Magnetic properties of volcanic rocks in the Green-tuff areas of northeast Japan
H. Domen (Yamaguchi Univ.)	Construction of a simple, semi-automatic thermomagnetic balance
Y. Shono (Tohoku Univ.)	Ultra high magnetic field and ultra high pressure — generation of extreme states by explosives

16 July

K. Aoki (Tohoku Univ.)	Spinel-peridotites and garnet-peridotites from the mantle
T. Suzuoki (Meteor. Coll.)	An approach to the crust and mantle through hydrogen isotopes
J. Okano (Osaka Univ.)	Preliminary experiments on young-age determination by K-Ar method
M. Ozima and K. Saito (Tokyo Univ.)	Ages of submarine rocks and their geochemical implications
K. Kobayashi (Tokyo Univ.)	Japanese islands seen from the ocean

THERMOMAGNETIC CURVES OF FERROMAGNETIC MINERALS EXTRACTED FROM THE LAVA FLOW OF NISHINOSHIMA-SHINTO, JAPAN

Kan'ichi MOMOSE

Department of Geology, Faculty of Science,
Shinshu University, Matsumoto, Japan.

A quick report is introduced here on the occurrence of native iron within the product from a newly born volcanic island "Nishinoshima-shinto" in the western Pacific(27°15′ N, 140°53′ E).

Fig.1 shows the thermomagnetic curves of ferromagnetic minerals contained within the well-vesiculated lumps of cinder(andesite:SiO_2 -61%) ejected from the craters of the First and Second Cinder Cones.

In the figure, the Curie temperature of the mineral showing a ferromagnetism at high temperatures is at 770°C, and it accords well with that of metallic iron ; hence the occurrence of native iron is unquestion~~k~~able. The mineral that shows a Curie temperature at 770°C is thought, by no means, to be a material as having mixed through the process of separating the experimental samples.

No sooner the assessment by the electron microprobe or the reflection microscope would be finished than the fact will be written for the "Nature".

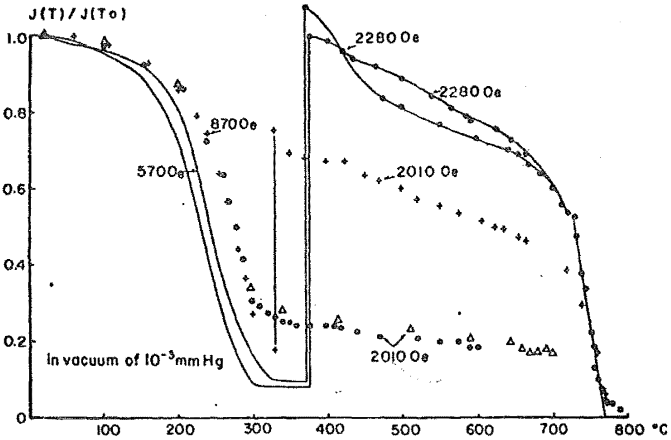

Thermomagnetic curves(heating) for the samples from the first-(indicated by the symbols:● Δ +) and the secnd-(indicated by solid line) cinder cones.

MAGNETIC PROPERTIES OF KIMBERLITE

Masaru KONO

Geophysical Institute, University of Tokyo
Bunkyo-ku, Tokyo 113

Syun-ichi AKIMOTO

Institute for Solid State Physics, University of Tokyo
Roppongi, Minato-ku, Tokyo 106

An oriented kimberite sample was obtained by one of the authors (S.A.) during a field trip of International Conference on Kimberlites held in South Africa in September and October, 1973. The sampling site was at Montrose, about 30 km east of Pretoria and 12 km south of the well-known Premier Mine. The kimberlite pipe at Montrose is thought to be a branch of the Premier Mine pipe, of which age is estimated to be about 1750 m.y. (Jones, 1968).

The stability of natural remanent magnetization (NRM) of this sample was studied by alternating field (a.f.) demagnetization, with peak field of 25, 50, 75, 100, 150, 200, 250, 300 and 400 oersteds. About two-thirds of the NRM was lost at 200 Oe, showing the NRM is not very stable (Fig. 1). The direction of NRM was originally south and downward, but changed to upward after cleaning by 200 Oe (Fig. 2). The ultimate direction after 400 Oe is apparently spurious and indicates that our demagnetizing apparents is not functioning well at high demagnetizing fields. The direction at 250 - 300 Oe may be representative of the "primary" NRM direction.

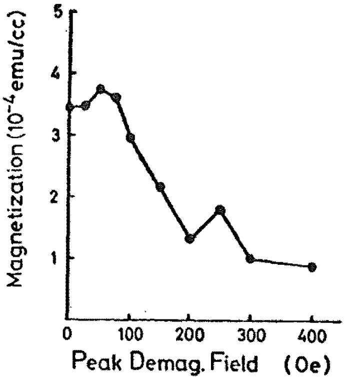

Fig. 1. Change of remanent magnetization intensity in a.f. demagnetization of kimberlite.

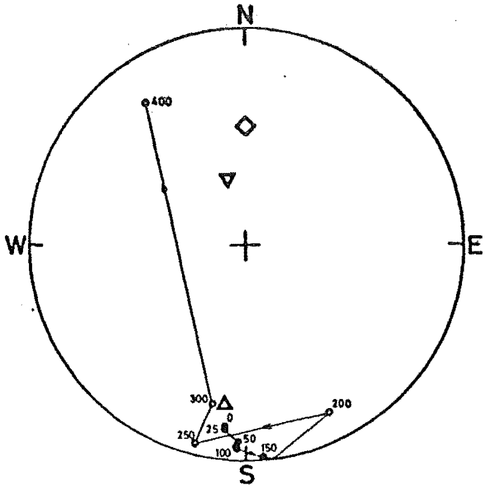

Fig. 2. Direction changes in a.f. demagnetization. Triangle indicates the direction of NRM of Premier Mine kimberlites (Jones, 1968). The present declination is 17°W. Diamond and inverted triangle are axial dipole field and present field direction at the sampling site. Closed and open symbols are, respectively, on the lower and upper hemispheres of equal area projection.

It is far apart from either the present (inverted triangle) or the axial dipole (diamond) directions at the sampling site, and is quite close to the NRM direction of the Premier Mine kimberlites (triangle) reported by Jones (1968). However, as we shall see later, what is meant by this "primary direction" is not so straightforward a matter as Jones has put it.

As this sample contains only a small amount of ferromagnetic minerals, it was crushed to about 200 mesh and ferromagnetics were picked up by a hand magnet. Fig. 3 shows the thermomagnetic curve of the separates under a vacuum of 2 x 10^{-5} torr. It can be seen that a substantial amount of magnetization was lost between 300 and 400°C in the heating and the cooling to the room temperature recovered only about 40 percent of the original magnetization. It is clear that this sample contains magnetite or Ti-poor titanomagnetite as one of the major ferromagnetic minerals, which is shown by the Curie point(s) around 580°C. The irreversible nature of the thermomagnetic curve, however, suggests another component, possibly (titano-) maghemite.

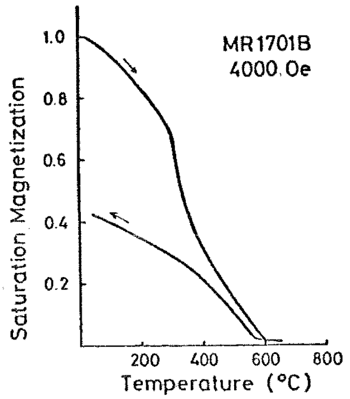

Fig. 3. Thermomagnetic curves of magnetic separates from Montrose kimberlite. Ordinate scale is arbitrary. Measurements were carried out under vacuum (2 x 20^{-5} torr) with a magnetic field of 4000 Oe.

The magnetic separates were subjected to X-ray diffraction analysis using Fe target. The results are listed in Table 1. Except the two small peaks around 40°, the peaks in the diffractogram shows that they come from an almost cubic structure. The lattice parameter calculated from table 1 (8.354 Å) is clearly different from that of magnetite (8.396 Å), and close to the tabulated lattice parameter of γ-Fe_2O_3 (8.338 Å). The 41.9° peak may correspond to (104) diffraction of α-Fe_2O_3.

Table 1. X-ray Diffraction Pattern of Magnetic Separates from Kimberlite

2 (°)	hkl	d (Å)	a (Å)
38.221	220	2.95666	8.3627
40.735	___	2.78124	___
41.90	___	2.70725	___
45.185	311	2.51965	8.3567
55.215	400	2.08882	8.3553
69.222	422	1.70419	8.3488
74.050	333, 511	1.60751	8.3529
81.962	440	1.47602	8.3496
		mean	8.3543 ± 0.0051

Target : Fe   Power : 30kV, 10mA

The sudden decrease of magnetization between 300 and 400°C (Fig. 3) can be interpreted as the break down of Ti-poor titanomaghemite to (titano-) hematite (Nagata, 1961).

Jones (1968), on the basis of a.f. and thermal demagnetization, has concluded that the main ferromagnetic mineral in the Premier Mine kimberlite is magnetite, and that their NRM is thermoremanent magnetization (TRM) which represents the ambient magnetic field direction at the time of the kimberlite intrusion (1750 m.y.). The results of the present analysis, however, cast a doubt about the validity of this interpretation. It is well known that maghemites are formed by low temperature oxidation with possible creation of chemical remanence (CRM) (Ozima, 1971). As Jones emphasized, the fact that the NRM direction is quite different from that of the present geomagnetic field may indicate a reasonable stability of NRM. However, this does not exclude the possibility that the NRM represents a CRM, not TRM, acquired much later than the time of the intrusion. It can be concluded, therefore, that a more careful study is needed before we can obtain the Precambrian field direction from kimberlites.

References

Jones, D.L. (1968) J. Geophys. Res., 68, 6937.
Nagata, T. (1961) Rock Magnetism, Rivised Edition, p. 85.
Ozima, M. (1971) Earth Planet. Sci. Lett., 13, 1.

(To be submitted to Nature)

ON THE SELF-REVERSAL OF TRM IN A HIGHLY OXIDIZED SUBMARINE BASALT

Sadao SASAJIMA and Junichi NISHIDA

Department of Geology and Mineralogy, University of Kyoto
606, Kyoto, Japan

1. Introduction

The self-reversal remanent magnetization of basalts due to N type magnetization was reported first by Schult (1965, 1968), and recently by the present authors (Nishida and Sasajima, 1974). Schult (1971) determined the chemical composition regions of N- and P-type titanomaghemites in the FeO- Fe_2O_3-T_iO_2 ternary diagram neglecting some impure ions substituted in cation sites of spinel. On the other hand, Richard et al. (1973) emphasized a possible mechanism of self-reversal in some cation deficient titanomagnetites ($1.0 \geqq z \geqq 0.6$) substituted by Mg and Al ions in continental basalts.

We have attempted to synthesize the N type ferrite from an appropriate composition of titanomaghemites in a submarine basalt, in order to clarify the causation of N type self-reversal. The basalt sample dealt in this paper, 128D is reported in detail by Ozima et al. (1974). The chemical composition of ferromagnetic separates of the sample is to be located within the N region defined by Schult (1971).

It is the main theme of this report that the self-reversal of TRM produced from 128D is caused by either transformation or unmixing of titanomaghemites involved in it. In this respect it is important to note that Stephenson (1972) computed possible N type curves in Ti-rich titanomaghemites.

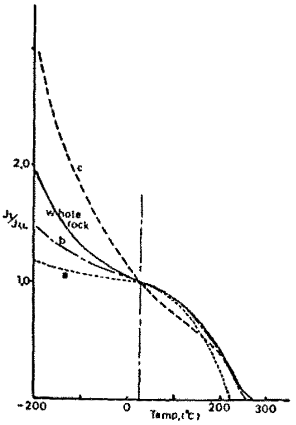

Fig. 1 Thermomagnetic curves of three kinds of fraction separated magnetically: a, pure ferromagnetic grains; b, weakly ferromagnetic fraction c, residual.

2. Experimentals

2.1 Specimens

Description of basalt sample such as locality, rock type, magnetic and chemical properties of ferromagnetic separates obtained from it, and the other data are given by Ozima et al. (1974). Thermomagnetic curves obtained in air and in vacuum of 10^{-5}torr both show remarkably irreversible changes in cooling stage characteristic to titanomaghemites (Ozima and Ozima 1972)

After pulverization of rock sample, we were able to devide magnetically into three characteristic fractions. Fraction (A) is a small amount of relatively strong ferromagnetic separates being presumably derived from phenocrysts and microphenocrysts, whose thermomagnetic curve shows Q or QP type with the Curie point of 225°C. Intensity of saturation magnetization is 6.3emu/g(Fig.2-a). Fraction (B) is a fairly large amount of very weakly magnetic one having the Curie point of 260°C. The spinel grains in (B) fraction are too fine to be separated from surrounding silicates intergrowth with the aid of mortar grind (Bryan, 1972). Fraction (C) is

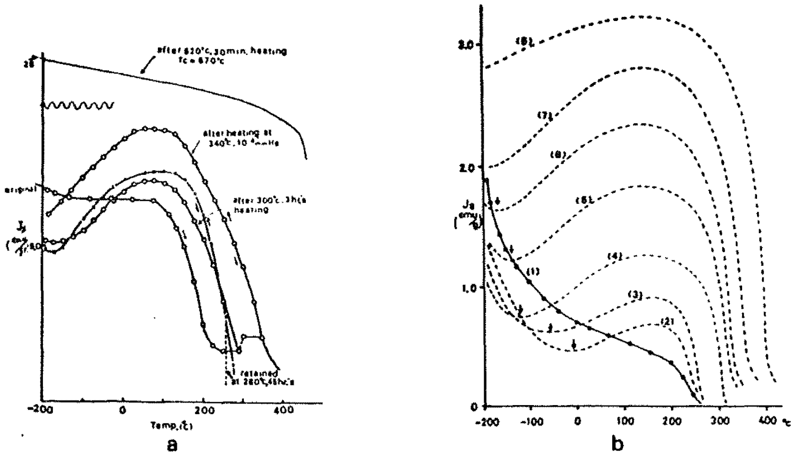

Fig. 2 Changes in thermomagnetic character after different heattreatments (Hex=6500 Oe). (a) and (b); for the fraction A and B respectively. As for (b): 1), original; 2), at 250°C, 30 minutes 10^{-3} Torr; 3), at 250°C, 15 hours, 10^{-2} Torr; 4), at 270°C, 18 hours, 10^{-3} Torr; 5), at 300°C, 1 hour, 10^{-2} Torr; 6), at 320°C, 1 hour, 10^{-3} Torr; 7), at 350°C, 30 minutes, 10^{-4} Torr; 8), at 380°C, 20 minutes 10^{-5} Torr.

the residual part including presumably hemoilmenites; thermomagnetic curve is similar to hyperbolic or paramagnetic character. Thermomagnetic curve of these fractions are shown in Fig. 1 in normalized scale at room temperature.

2.2 Successive heat treatments of (A) and (B) components

A series of heating experiments of (A) and (B) components at moderate temperature have been carried out under controled conditions of atmospheric pressure ($10^{\circ} \sim 10^{-5}$ Torr). Changes in thermomagnetic curves are shown in Fig. 2 (a) and (b). It is needless to say that the reaction responsible for such changes depends on grain size, time of heating, oxygen pressure and temperature of heating, the change of mode of thermomagnetic curves of fraction (B) is significantly different from that of (A), suggesting the former is much unstable than the latter for heat treatments ranging in temperature from 230°C to 380°C. At the first stage of heating of 250°C the original Q type curve of (A) is transformed into P type curve being accompanied with some 50°C increase in Curie point and with some decreases in Js(at 80°K), whereas the original (B) is tranformed into N type (strictly, coexistence of N- and P-types) having about 20°C higher Curie point and a little smaller Js. Such a difference in thermomagnetic changes might be attributable to different degrees of oxidation between (A) and (B) components. And the thermomagnetic behaviour of the rock sample is more likely to be represented by (B) component than (A) component.

2.3 TRM acquired in various heating conditions

Making clear of the correspondence of TRMs to various heat treatments mentioned above, tabular specimens (0.8 x 0.6 x 0.5 cm) were heated at various temperature for 15 minutes in a direct field of 2.5 Oe. the other TRM experiment was performed in various successively increasing fields (40~2800 Oe) keeping a constant temperature of 320°C. The dependencies of TRMs upon

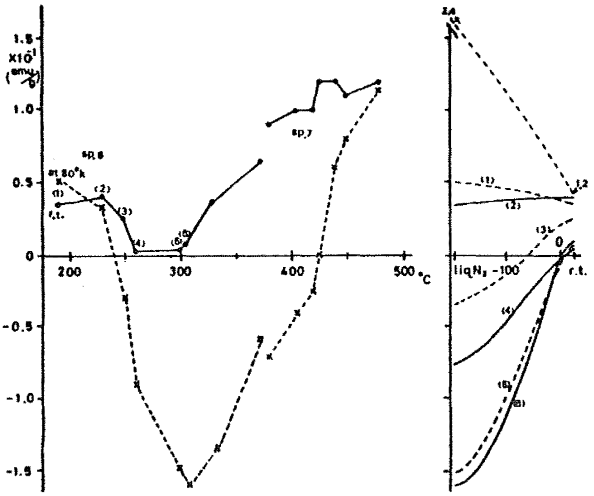

Fig. 3 Relation between self-reversal of TRMs and heating trmperatures.

temperature and applied fields were observed between 80°K and room temperature with an astatic-magnetometer or a fluxgate magnetometer. An example obtained is shown in Fig. 3 (a), (b). Provided that the effect of accumulation of heating time is negligible, each result for specimen no.6 and no. 7 possibly indicates the temperature dependency of the reverse TRM. The dependency of applied field on the intensity of TRM is apparent up to 150 Oe, while for further stronger field up to 2800 Oe no appreciable increase in TRM is observed. And even in a strong field of 2800 Oe the self-reversal was not suppressed. The a.f.-demagnetization of TRM was performed to know coercivity of the self-reversal component. It is noted from results obtained that after the application of 800 Oe alternating field the normal component (parallel to the direct field applied) at room temperature was lessened by two thirds, but the reverse component at 80°K reserved 80% of the original one, suggesting significantly hard character of the reversal.

3. Discussion

As seen in Fig. 2 (b) and Fig. 3, the correspondnece of individual reactions in the same temperature range of 250~320°C is remarkable (reaction I). The former is presumed to be a process producing N type predominantly, and the latter a process yielding the reversal. Such a production of new phases is not so sensitive to atmospheric pressures within a range of $10^0 \sim 10^{-5}$ Torr, however, the rate in higher vacuum is 1.1~1.5 times as large as that in air.

It may be difficult to explain the obtained results simply in terms of the low temperature oxidation or unmixing (inversion). Clarifying the time effect of the reaction producing source material responsible for the self-reversal, another specimen was heated at 320°C for a long time. After more than ten times of successive heat treatments of the specimen over 35 hours the self-reversal property was always kept, though whose compensation temperature was decreased by about 80°C from that for the initial TRM (≒ 0°C). The time dependency of production rate is simply approximated by a logarithmic function of time, suggesting that our data indicate a much more sluggish reaction as compared with that of the submarine basalt already repored by Ozima & Larson (1968). Judging from the production rate, it could be expected that there exist at least a quasi-equilibrium state different from unmixing which predominates above 320°C.

On the contrary, the reaction occurring in the temperature range 320 ~450°C (reaction II) shown in Fig. 3 is assumed to be inversion, a counteractive process, not only disintegrates reversal component (N-type) but also increases normal component (or produce stronger P- and Q-types). An experimental example indicates that the self-reversal of TRM acquired at 420°C for 60 minutes was easily overcome by a rapid growth of the normal component on further 30 minutes heating. It is pointed out in this connection that the abrupt change of N-type magnetization to P-type at 360°C in Kôzuike basalt is also well understood as being in the same category (Nishida and Sasajima, 1974).

Possible interpretations of the reaction (I) may be that (a) the original titanomaghemites, an ensemble of different degrees of oxidation products, invert to N- and P-type non-stoichiometric titanomagnetites and hematite and anatase TiO_2 (Readman and O'Reilly, 1970) as a transitional state, and that (b) the original impure titanomaghemites with Q type random cation distribution (Akimoto model) is transformed into N- and P-type titanomaghemites having ordered (Néel-Shevallier) cation distribution (Stephenson, 1972). According to the theoretical computation made by Stephenson, nonstoichiometric titanomagnetite ($x > 0.6$) with random cation distribution always possesses Q type J-T curve, and in a certain condition cation deficient titanomagnetites with N type is caused by oxidation or cation ordering from Q- or P-type ones. The ferromagnetic minerals dealt in this study seem most likely to be this kind of Q type from petrographic observations of thin section (Bryan, 1972). If this is the case it may be reasonable to suppose that the original titanomaghemites with the disordered cation distribution of our sample might be transformed into the ordered distribution (including Mg and Al ions), resulting in N- and P-type curves at the early stage of heating (Creer and Stephenson, 1972). This view is also supported by the fact that the transformation of random cation distribution into ordered cation distribution gives rise to the increase of Curie point by some 50°C and the decrease in Js (Fig. 2).

We have observed no positive data supporting the self-reversal due to an exchange interaction of two phases by which Ozima and Larson (1968) plausively explained the self-reversal of TRM in some submarine basalts.

References

Bryan, W.B. (1972): J. Geophys. Res. 77, 5812

Creer, K.M. and A. Stephenson (1972): J. Geophys. Res. 77, 3698

Nishida, J. and S. Sasajima (1974): Geophys. J. R. astr. Soc. 37, 453

Ozima, M. and E.E. Larson (1968): J. Geomag. Geoelec. 20, 337

Ozima, M. and M. Ozima (1972): Phys. Earth Planet. Interior, 5, 87

Ozima, M., M. Joshima and H. Kinoshita (1974): J. Geomag. Geoelec. 26, 335

Readman, P.W. and W. O'Reilly (1970): Phys. Earth Planet. Interior 4, 121

Richard, J.C.W., J.B.O'Donovan, Z. Hauptman, W. O'Reilly and K.M. Creer (1973): Phys. Earth Planet. Interior 7, 437

Schult, A. (1965): Beitr. Mineral. Petro. 11, 196

(1968): Earth Planet. Sci. Letters 4, 57

(1971): Zeit. Geophys. 37, 357

Stephenson, A. (1972): Geophys. J.R. astr. Soc. 29, 91

P.S.: Finally, it should be mentioned that the specimen 128D was a piece of dredged basalt kindly given from Scripps Inst. of Oceanography.

ON THE POSSIBILITY OF SELF-REVERSAL CAUSED BY REDISTRIBUTION OF CATIONS BETWEEN TWO SUBLATTICES

Junichi NISHIDA and Sadao SASAJIMA

Department of Geology and Mineralogy, Faculty of Science,
Kyoto University, Kyoto, Japan

1. Introduction

The N-type thermomagnetic curve in some basalts with self-reversal of magnetization below room temperature were so far reported by Schult(1971) and Nishida & Sasajima(1974). The latter authors measured the internal field intensity associated with this self-reversal of remanence, and noticed that the self-reversal of Kozuike basalt is caused by a strong exchange interaction (> 2200 Oe). They also reported that the thermomagnetic curve of this sample showed an irreversible increase in magnetization, Curie temperature accompanied by the change of curve from N-type to P-type at 360 °C in vacuo of 10^{-5} torr. They regarded this phenomenon as being due to the inversion of nonstoichiometric N-type titanomagnetite to Fe-rich P-type spinel.

Schult(1971) observed Fe/Ti ratio of N-type magnetic mineral with microprobe analyser and presumed the magnetic mineral to be a highly oxidized titanomagnetite using Readman et al's(1972) contour diagram for Curie temperature.

In this paper, it is our purpose to consider whether this N-type material is cation deficient titanomagnetite or a kind of product resulted from redistribution of cations.

2. Experiments

Samples used in this study are basalts from Steinberg Göttingen Germany(No 209 after Schult) and Kozuike, Hiroshima Japan. The surface of St 209 is highly weathered. The unweathered part of this rock specimen is devided into two parts; inner zone and outer zone. Outer zone appear reddish brown and inner zone is dark grey. Outer zone of this rock specimen is considered to have been suffered to hydrothermal alteration after the eruption. The thermomagnetic curves of these two zones are shown in Fig.1. The magnetization(J) of outer zone of this specimen decreases hyperbolically with increase in temperature (Fig.1-b). And in the relation of J versus H at nitrogen temperature, it does not attain saturation moment with an external field strength of 10 KOe. From these facts, it seems likely that the magnetic mineral contained in this part is mostly hemo-ilmenite. The thermomagnetic curve of inner zone of the

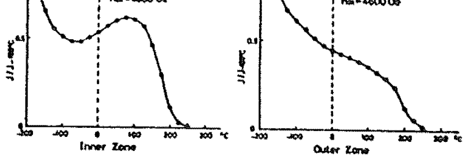

Fig.1 The thermomagnetic curves of inner zone(left) and outer zone(right).

Table 1

Sample	Tc(°C)	a_o(Å)	Ref.
St 209 intensively magnetic	180	8.424	A
St 209 weakly magnetic	170	8.409	B
St 209 residual rock poeder	-	-	C
Kozuike P-type fraction	200	8.462	D
Kozuike N-type fraction	210	-	E

specimen shows so-called N-type magnetization(J-T) curve (Fig.1-a).

The inner zone of this rock specimen was finely crushed in ethyle alcohol, and magnetic concentrates were extracted by a hand magnet. Magnetic concentrates were devided into two parts; intensively and weakly magnetic fractions. Residual rock powder exhibits almost the same thermomagnetic curve as outer zone of the rock specimen. In Fig. 2, thermomagnetic curves of these three magnetic concentrates are shown.

The Curie'temperatures and lattice parameters of ferromagnetic concentrates were measured, and the results are shown in Table 1. In this table is also shown the measured Curie temperatures and lattice parameters of Kozuike basalt.

The X-ray diffractograms of sample E(N-type) did not show any peak except the peak responsible for cubic titanomagnetite phase.

The change of the thermomagnetic curve of sample B at repeated heatings is represented in Fig.3. The initial phase has a Curie temperature of about

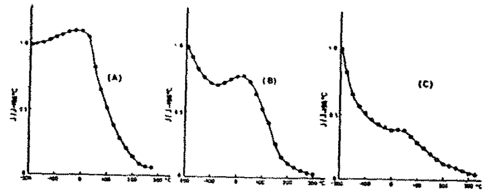

Fig.2 The thermomagnetic curves of three magnetic fractions. A,B and C correspond the Ref. of Table 1.

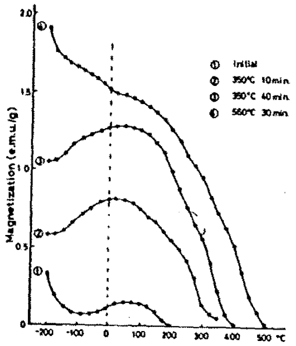

Fig.3 The change of thermomagnetic curve of sample B for repeated heatings.

200 °C and the second phase produced by heating at 350 °C has a Curie temperature of about 400 °C. It is considered that the intensity of the magnetization reaches saturation value when the sample is heated about 40 minute at 350 °C.

The rates of the increase of magnetization were observed at two different temperatures, 310 °C and 330 °C. In Fig.4, the intensities of magnetization versus time at two different temperatures are shown. Here, we can calculate the time constant for the reaction(λ) as performed by Creer et al.(1970) and Ozima et al.(1972). In their expressions, the magnetization J is given by

$J=A\exp(-\lambda t) - B(1 - \exp(-\lambda t))$ ---(1)

From the result shown in Fig.4, we may approximate the time for the reaction as 0.00109 min.$^{-1}$ at 310 °C and 0.00437 min.$^{-1}$ at 330 °C respectively. The magnetizations are plotted against $1 - \exp(-\lambda t)$ as shown in Fig.5. The fact that the magnetization is proportional to $1 - \exp(-\lambda t)$ for calculated value of λ means that the reaction is constant through this experiment.

The time constant for the reaction depends on temperature following Arrhenius relation. Thus it is given by

$\lambda=C \exp(-Es/kT)$ -----(2)

in which Es, C, k and T denotes the activation energy, a numerical constant, Boltzman's constant and the absolute temperature respectively.

The activation energy obtained for the two temperatures following the equation(2) is 2.1 eV per molecule.

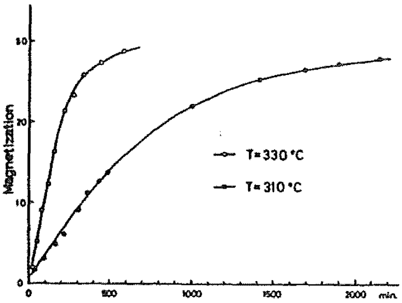

Fig.4 The change of the intensities of magnetization versus time at two different temperatures.

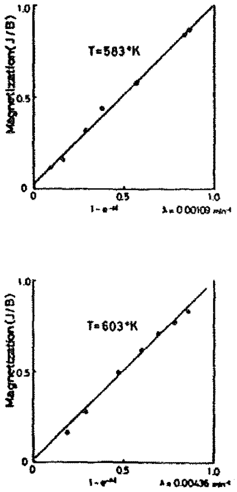

Fig.5 Magnetization as a function of $1 - \exp(-\lambda t)$.

3. Discussion

The authors reported that so-called N-type thermomagnetic curve of Kozuike basalt is the resultants from two different magnetic curves, N- and P-types (Nishida & Sasajima, 1974). Is it possible to consider that N-type thermomagnetic curve is the resultants from two different magnetic phases such as the magnetization curves shown in Fig.2-a and 2-c? In this case, the P-type titanomagnetite grain and superparamagnetic ilmenite must exist separately in the rock. In this configuration, the magnetic interaction between two phases must be magneto-static interaction, and the strong internal field associated with self-reversal reported by the authors cannot be explained. and the fact that we cannot detect the peak responsible for rhombohedral phase from the X-ray diffractogram of sample B also support that there exist cubic titanomagnetite with N-type thermomagnetic curve. Consequently, we may safely assume the coexistence of three magnetic phases in this rock specimen, P-,N-type titanomagnetites and a small quantity of hemoilmenite.

From the lattice parameters and the Curie temperatures of sample A, B and D shown in Table 1, the chemical compositions of these two nonstoichiometric titanomagnetites are located on the ternary diagram $FeO-Fe_2O_3-TiO_2$ by the use of Readman et al's contour diagrams. The chemical compositions of sample A, B and D thus determined are located in N- and Q' regions of the Fig.5 after Schult(1971). Chemical analysis was made on sample D (FeO, Fe_2O_3, TiO_2). The chemical composition of sample D obtained from chemical analysis locates, contrary to our expectation, near ulvöspinel-magnetite join (in preparation). This fact do not support the current idea that the self-reversal due to N-type is concerned with cation deficient titanomaghemite(O'Reilly & Banerjee,1967, Ozima & Sakamoto,1971). It may be supposed as a reason for this discrepancy that the estimated chemical composition by using Readman et al's diagrams differ significantly from the probable point since there are foreign atoms replacing Fe^{++} and Fe^{+++} ions. If there are much foreign ions substituted in titanomagnetite, it can be considered that the self-reversal concerned with N-type magnetization might occur as a result of redistribution of cations between two sublattices(Creer et al. 1972).

The activation energy obtained for the N-type titanomagnetite(2.1 eV per molecule) is one or two order of magnitude larger than those obtained by Creer et al.(1970) and Ozima et al.(1972). Readman et al.(1970) suggested the activation energy, followed by observing the time dependece of magnetization, is not reliable as measuring the weight change. It may be considered that the true value for the activation energy is less than 2.1 eV.

If the irreversible increase in Js and Tc of N-type material is assigned to a function of competition between the degree of unmixing in nonstoichiometric titanomagnetite and multiphase oxidation of titanomagnetite, the activation energy should be far smaller than 2.1 eV. Nicolas(1970) obtained 1.67 eV for the diffusion of Al and Fe between tetrahedral and octahedral sites in the spinels. It should be considered that the irreversible change of N-type thermomagnetic curve could be regarded as a function of competition between the multiphase oxidation of titanomagnetite and redistribution of cations. Further examination of N-type self-reversal is now being in progress.

References

Creer,K.M. & A.Stephenson (1972), J.Geophys.Res.,77,3698.

Creer,K.M., J.Ibbetson & W.Drew (1970), Geophys.J.R.astr.Soc. 19,93.

Nicolas,J. (1970), J.Phys.Chem.Solids,28,847.

Nishida,J. & S.Sasajima (1974), Geophys.J.R.astr.Soc.,37,453.

O'Reilly,W. & S.K.Banerjee (1966), Min.Mag.,36,29.

Ozima,M. & M.Ozima (1972), Phys.Earth Planet.Interiors,5,87.

Ozima,M. & N.Sakamoto (1971), J.Geophys.Res.,76,7035.

Readman,P.W. & W.O'Reilly (1970), Phys.Earth Planet.Interiors, 4,128.

Readman,P.W. & W.O'Reilly (1972), J.Geomag.Geoelectr.,24,69.

Schult,A. (1971), Zeit.Geophys.,37,357.

WHEN DID MAGNETIZATION FIX IN LOOSE SEDIMENTS ?

Katsumi YASKAWA

Department of Physics, Faculty of Engineering Science,
Osaka University, Toyonaka, Osaka 560, Japan

Introduction

The natural remanent magnetization (NRM) of sediment is of course chiefly subject to the ambient geomagnetic field at the time of deposition, but usually the direction of magnetization of each magnetic constituent in the sediments does not coincide exactly with that of the ambient geomagnetic field at the time of its landing on the bottom surface.

The main reason why they are not coincident with each other is that the shape of each grain falling in the water is generally far from the sphere; for example, if a small needle, which is magnetized along its axis, is falling in the water, the axis will be parallel to the direction of the ambient magnetic field until the needle reaches at the bottom, but at the last moment it will rest on the bottom parallel to a horizontal component of the ambient magnetic field, if the bottom has a smooth horizontal surface, or the magnetization of the small needle-like magnetic constituents in any rather coarse sediments cannot be arranged parallel to the direction of the ambient geomagnetic field at the time of their deposition on the smooth bottom-surface.

In fact, it was proved by King (1955) that, as the result of the irregular rotation chiefly due to the gravitational attruction at the time of landing of the magnetic minerals falling through the water, the inclination of natural remanent magnetization of sediments has the tendency to become shallower than the inclination of the ambient geomagnetic field. He showed by experiment that this discrepancy of inclination between natural remanent magnetization of sediment and the ambient geomagnetic field reaches an angle of more than 20 degree. In case that the problems concern only the polarity of geomagnetic field; that is, normal or reversal, the discrepancy between the directions of magnetization and of geomagnetic field at the time of deposition is not so serious, and we may use the magnetic polarity which was obtained from the natural remanent magnetization of any sediments to stratigraphic correlation.

Irving and Major (1964) showed experimentally that very fine particles of ferromagnetic minerals mixed with water and the relatively coarser non-magnetic grains can move in relatively large cavities surrounded with the coarser non-magnetic grains, and rearrange themselves in such a way that their magnetization become parallel to the direction of the ambient magnetic field after deposition, and as the result, the remanent magnetization of the sediments coincides with the direction of magnetic field applied at the time of artificial dehydration. Irving and Major called the remanent magnetization thus obtained "post-depositional DRM (Detrital

Remanent Magnetization)".

Recently Kent (1973) showed experimentally that the natural remanent magnetization of deep-sea sediments seemed to be a kind of the "post-depositional DRM" and that the direction of natural remanent magnetization was exactly parallel to the ambient magnetic field and the intensity of NRM was propotional to that of the magnetic field applied at the time of dehydration. From both Irving and Major's and Kent's experiments it seems to be guaranteed that the remanent magnetization of very fine sediments such as deposited on the bottom of offshore region of a sea or a lake can be regarded as a fossil magnetization of the past geomagnetic field.

Unfortunately they both have recourse to dehydration by artificial drying-up on their experiments to fix a remanent magnetization. The actual process of fixation of magnetization in the natural sediments, however, does not result from dehydration by drying-up but result from gradual dehydration accompanying with the gravitational compaction. Therefore, we cannot directly expect the exact fossil of a past geomagnetic field in the actual sediments even of very fine grains, in spite of the results of these experiments. One of the serious problems are that in the actual sediments lying in the water the dehydration does not occur within a very short period but it will take a considerable long time, and so we do not know when the magnetic constituents are fixed on the process of gradual dehydration due to gravitational compaction.

Thus, it is clear that the time of fixation of magnetization or the time of acquisition of natural remanent magnetization is not coincident with the time of deposition. It must be a little later than deposition. The purpose of this paper is to get an order estimation of the time discrepancy between fixation of magnetization and the deposition for the very fine sediments.

Magnetic moment in viscus liquid

Now let us assume a circular cylinder which is rotating in the liquid. The viscosity momemt acting on the cylinder is expressed as follows:

$$M_v = 4\pi\eta\omega R^2 dx$$

where η is viscosity coefficient of the liquid, ω, R and dx are the angular velocity, the radius and the thickness of the cylinder respectively. Using this equation, we can derive the viscosity moment acting on the sphere rotating in the liquid. Putting a the radius of the sphere, we have

$$R^2 = a^2 - x^2,$$

Integrating R from -a to a, we have the viscosity moment for sphere:

$$M_v = 4\pi\eta\omega\int_{-a}^{a} R^2 dx = \frac{16}{3} a^3\pi\eta\omega.$$

On the other hand, when the magnetic field (H) rotates with angular velocity ω, the moment (M_m), which is expressed as follows;

$$M_m = mH \sin \Delta\theta, \quad (\Delta\theta = \omega t - \theta),$$

is to act on a magnetic particle, where m is the magnetic moment of a magnetic particles and θ is the angle between m and H. The magnetic vector of the magnetic particle in the viscus liquid follows the rotation of magnetic field when M_v is less than M_m, and generally the direction of the vector does not coincide with that of the magnetic field. The vector will always be behind the field by the angle $\Delta\theta$. This delay-angle $\Delta\theta$ will be nearly inverse proportion to the ratio of M_v / M_m and is expressed as follows;

$$\sin \Delta\theta = 4\eta\omega / \kappa H, \qquad (1)$$

where κ is magnetic moment per unit volume of the particle.

Thus, if $\eta\omega$ is sufficiently large or κH is small, we have considerably large $\Delta\theta$. The fixation of magnetic particle in question is in fact subject to this delay-angle $\Delta\theta$; that is, the time discrepancy between at the deposition and the acquisition of the natural remanent magnetization in the sediments can be considered to correspond to this $\Delta\theta$, because, if $\Delta\theta$ becomes 180 degree or the magnetic vector of the particle is behind the rotating magnetic field by 180 degree, the vector can no longer follow the field.

Effect of compaction on the viscosity of very fine sediments

It is known that there is the following relation between the density (ρ) and the shear strength (τ) of the clay:

$$\rho = \alpha \ln \tau,$$

where α is constant. It seems reasonable to regard the shear strength of clay as the maximun limit of its viscosity. Therefore, it may possibly be true that the viscosity of clay is connected with the density by the same kind of relation; that is,

$$\rho = c \ln \eta. \qquad (2)$$

On the other hand, in such soft, loose sediments as at near the bottom surface of the deep sea or of the central region in the lake, the bulk density of homogeneous sediment can be expressed as a function of depth (z) down from the bottom as follows:

$$\rho = \rho_m - (\rho_m - \rho_o) e^{-Az}, \qquad (3)$$

where ρ_m and ρ_o are the densities of the closest packed clay and of the water respectively, and A is a constant.

An estimation of the depth of fixation of magnetic moment

Substituting (2) into (3), we obtain

$$z = \frac{1}{A}\{ \ln (\rho_m - \rho_o) - \ln (\rho_m - c \ln \eta)\} \qquad (4)$$

Now, replacing viscosity (η) in the equation (4) by that in the equation (1); that is,

$$\eta = \frac{\kappa H}{4\omega}\,\Delta\theta,$$

we have

$$z = \frac{1}{A}\{\ \ln(\rho_m - \rho_o) - \ln(\rho_m - c\ln(\frac{\kappa H}{4\omega}\Delta\theta))\}$$

Fig. 1 shows the bulk density of the sediments in Lake Biwa as a function of depth. As ρ_o is the density of water, we can put $\rho_o=1.0$, and using the data in Fig. 1, we can determine ρ_m and constant A in the equation (3); that is, $\rho_m=1.7$ and $A = 0.0003$, where the depth should be measured in centimeter.

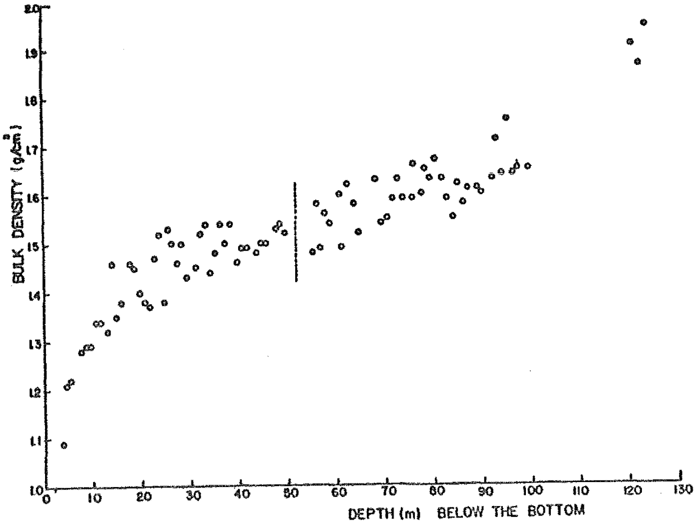

Fig. 1 Bulk densities of the core sample for every meter. The increasing densities with depths show the consolidation effect of the bottom sediments. (A. Yamamoto, S. Kanari, & Y. Fukuo).

To make a minimum estimationof the depth for fixation of magnetic moment, let us adopt the value of τ as that of η in order to determine the constant c. For the clay named M_3 in Osaka Formations, $\rho=1.7$ and $\tau=5$ to $7.5\ \mathrm{kg/cm^2} = 6\times10^6\ \mathrm{dyne/cm^2}$ were experimentally determined (Takenaka, 1974), so that we get 0.11 as the value of constant c using these values. And also to make a minimum estimation, let us adopt $\pi/12$ as the value of $\Delta\theta$ because the amplitude in the secular variation of the geomagnetic field is usually about 30 degree or $\pi/6$ and sometimes much greater.

Then, substituting these values into the equation (4), we obtain the equation

$$z = -3333\ \ln\{\ 2.43 - 0.157\ \ln(\ 0.0654\ \frac{\kappa H}{\omega}\ )\}.$$

The magnetic field (H) in problem is 0.5 Oe as approximate value of the intensity of the geomagnetic field, and assuming that the angular velocity of the geomagnetic field is approximately

$$\omega = 30°/2{,}000\ \mathrm{yrs} = 30°/630720\ \mathrm{sec},$$

we have the relation between the depth of fixation of magnetic particles contained in the sediments and the magnetic moment per unit volume of the particle:

$$z = -3333 \ln (2.43 - 0.157 \ln 687.48 \kappa).$$

In Fig. 2 this relation is shown. Usually the magnetic moment of titaniferrous magnetite is in the order of 10 emu and the depth of fixation for this value is to be a few meters; e.g. 2.24 m for 20 emu and 0 m for 1.37 emu.

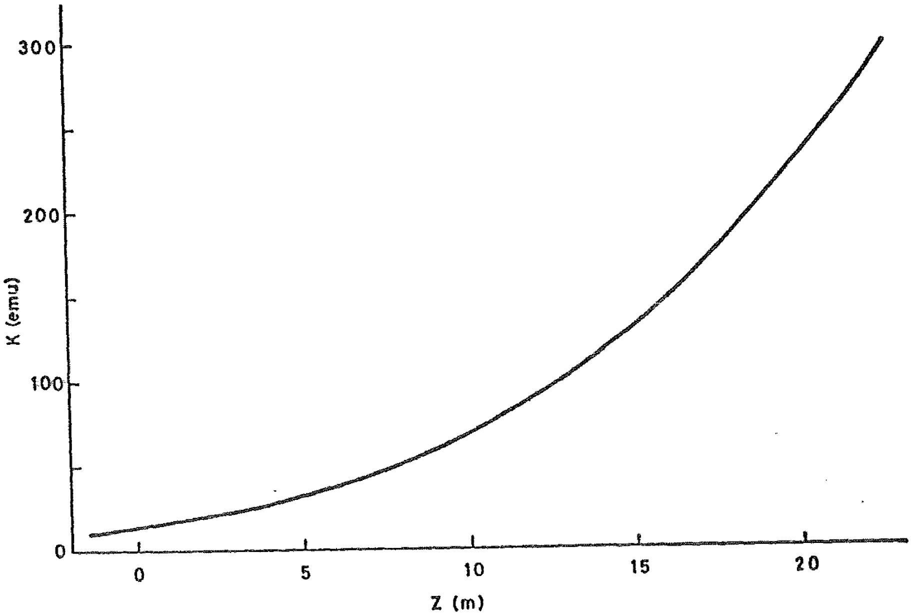

Fig. 2, The depth of fixation of magnetic particle in a certain clay deposit as a function of the magnetic moment of the particle per unit volume.

Reference

Irving, E. and A. Major (1964) Sedimentology, 3, 135.

Kent, D. V. (1973) Nature, 246, 32.

King, R. F. (1955) Month. Not. Roy. Astron. Soc. Geophys. Suppl., 7, 115.

Takenaka, J. (1974) Personal communication.

Yamamoto, A., S. Kanari and Y. Fukuo (1972) "Paleolimnology of Lake Biwa and the Japanese Pleistocene" edited by S. Horie, 1, 37.

(To be submitted to J. Geomag. Geoelectr.

ORIGIN OF NRM OF SAN JUAN VOLCANIC ROCKS FROM COLORADO, U.S.A.

Hidefumi TANAKA and Masaru KONO

Geophysical Institute, University of Tokyo, Bunkyo-ku, Tokyo 113

Introduction

Paleomagnetic study of the San Juan volcanic field was already reported (Tanaka and Kono, 1973). In the present paper, magnetic properties of these rocks are studied and it will be shown that the NRM correctly represents the magnetic field direction at the time of rock formation. The magnetic properties of samples from sixteen cooling units were examined by thermo-magnetic analyses, X-ray diffraction analyses and microscopic observation of polished sections.

Thermomagnetic curves

Change of staturation magnetization J_s with temperature T was studied in a vacuum of about 10^{-5} Torr with a magnetic field of 5 K Oe. Nine out of sixteen samples contain only magnetic minerals with a high Cure temperature T_c (Fig. 1-a), while others contain two phases with a high T_c and a low apparent T_c (Fig. 1-b). Hereafter the former are designated as type I and the latter type II. The term "apparent" T_c is used because the magnetization did not recover on cooling. A histogram of T_c's determined from heating curves only is shown in Fig. 2.

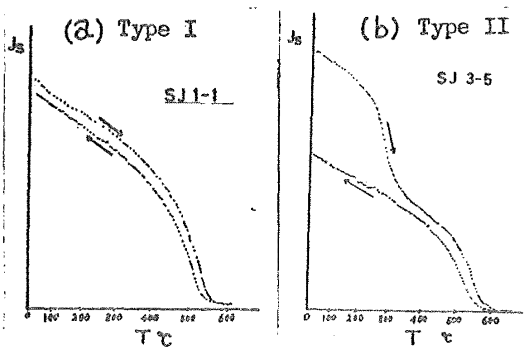

Fig. 1. Example of typical thermo-magnetic curves.

High T_c ranging between 530° and 580°C indicates the presence of almost pure magnetite. Low apparent T_c ranging from 310°C to 380°C can be interpreted in two ways; either the presence of Ti-rich titanomagnetite, or the transition of maghemite to hematite. Thermomagnetic analyses are summarized, together with other data, in Table 1.

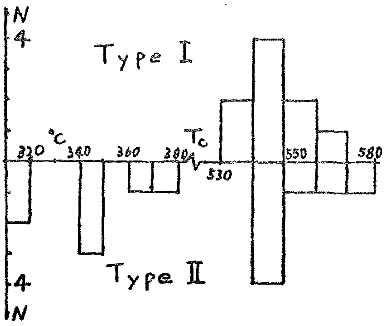

Fig. 2. Histogram of Tc's.

X-ray Diffraction Analyses

The magnetic minerals were extracted from powdered samples by a hand magnet. Four to six diffraction peaks were used to determine the unit cell size (a_o) of the cubic phase. Almost all samples showed the diffraction peaks of rhombohedral phase which could not be separated from

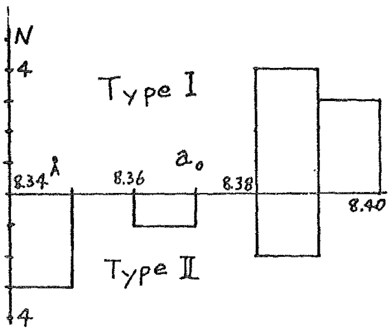

Fig. 3. Histogram of a_0

the titanomagnetite grains. The determined unit cell sizes are shown in Fig. 3 and Table 1. The a_0 of type I samples (~ 8.39 A) are indicative of almost pure magnetite which suggests the occurrence of high temperature oxidation shortly after the rock formation. But some of type II samples have rather small value of a_0 which may suggest a partial conversion of magnetite to maghemite.

Reflection Microscopy

The opaque minerals were studied by using a reflection microscope. Except for one (SJ 2), all the samples have the opaque minerals with ilmenite lamellae exolution, showing evidence of high temperature oxidation corresponding to oxidation states of II or III of Wilson and Watkins (1967). These results are summarized in Table 1 with other data.

Stability of NRM in terms of Magnetic Mineralogy

Stability of NRM can generally be explained by the ordinary criteria such as presented by Larson et al. (1969). For example, SJ 2 with very unstable NRM has only large homogeneous grains. Opaque minerals of SJ 12 which has remarkably stable NRM are highly oxidized and have very fine ilmenite lamellae. But there were no difference of NRM stability between type I and II. Fig. 4 indicates a slight negative correlation between α_{95} of stable remanence and Q ratios. This may mean the existence of lower limit of α_{95} inversely proportional to Q ratio, and this is not so meaningless.

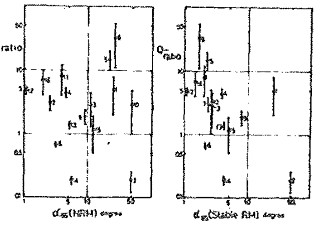

Fig. 4. Q-ratio and α_{95}

Occurrence of Maghemite in Type II Samples

The natural occurrence of titanomaghemites in oceanic basalts and deep-sea sediments is now considered to be quite common (Ozima and Larson, 1970; Ozima and Ozima, 1971; Lowrie et al., 1973; Kent and Lowrie, 1974). But the existence of such minerals in continental igneous rocks seems not to be well recognized. Nevertheless the occurrence of them were shown by many authors using various method (Akimoto and Katsura, 1959; Akimoto and Kushiro, 1960; Sanver and O'Reilly, 1970; Løvlie and Opdyke, 1974). Symons (1973) interpreted, without any detailed analyses, the "kink" of J_s-T curve similar to the ones in Fig. 1-b, as the maghemite-hematite transition point. It should, however, be examined more fully before concluding whether or not maghemitization occurres in type II samples. Evidence of its occurrence in the present samples may be summarized as follows:

1. The kink of J_s-T curve around 350°C, and breakdown of magnetization in cooling curve (Fig. 1-b).
2. Smaller values of a_0 of cubic phase in type II (Fig. 3).

Identification by microscopic analyses has not been carried out yet.

The type II J_s-T curve has the same feature indicative of occurrence of transition of oxidized magnetite to magnetite and hematite (Readman and O'Reilly, 1970).

Table 1

Unit	Age (m.y.)	Polarity	α_{95}*	Type	Js-T curve Tc (°C)	X ray analyses a_0 (Å)	X ray analyses α phase	Microscopic observation**	Formation
SJ 14	22.5	R	4.3	I	553	8.392	trace	II	Sunshine Creek Tuff
SJ 13	26.4	N	4.2	I	549	8.390	trace	II	Fisher Quartz Latite
SJ 12		N	1.1	I	539	8.39	rich	III	Snowshoe Mountain Tuff
SJ 11		N	2.1	II	544 , 342	8.37	trace	III	Nelson Mountain Tuff
SJ 10		R	2.7	I	546	8.387	trace	II	Wason Park Tuff
SJ 9	26.7	R	7.9	II	546 , 363	8.384	none	III	Mammoth Mountain Tuff
SJ 8		R	1.7	I	562	8.393	trace	III	Carpenter Ridge Tuff
SJ 7	27.8	N	2.4	I	562	8.391	trace	II	Fish Canyon Tuff
SJ 15		R	4.9	II	560 , 342			II	Sapinero Mesa Tuff
SJ 6	28.2	R	2.2	II	550 , 316	8.39	none	II	Masonic Park Tuff
SJ 16	28.4	N	1.5	I	553			III	Ute Ridge Tuff
SJ 5	29.8	R	2.3	II	580 , 346	8.34	none	II	Tresure Mountain Rhyolite
SJ 4		N	3.8	I	548			III	
SJ 3		R	2.7	II	575 , 311	8.344	none	II	
SJ 2	32.4	?	49.2	II	542 , 375	8.350	none	I	Summer Coon Rhyolite
SJ 1	34.0	N	25.8	I	558	8.39	rich	II	La Garita Creek Rhyodacite

* α_{95} of stable RM

** number indicates oxidation state by Wilson and Watkins (1967)

Another interpretation for the above two points may be that the Ti-rich phase is unstable to heat treatment and causes the kink of J_s-T curve. Diamagnetic ions such as Mg^{2+}, Al^{3+} decreases the unit cell size (Richards et al., 1973) and about twenty mole percent of almina in magnetite decreases it from 3.9 Å to 3.5 Å (Katsura, personal communication). Study of these problems is intended in the future.

Conclusion

It could be concluded from the evidence of high-temperature oxidation of samples and no difference of NRM stability between type I and type II that the NRM represents the direction of geomagnetic field at the time of rock formation. The two VGP's from type I and type II samples agree within the 95% confidence angle as shown in Fig. 5.

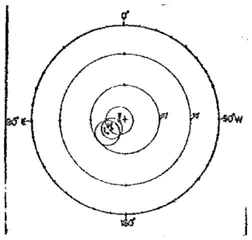

Fig. 5. VGP's from type I (I), type II (II) and mean of them (M).

References

Akimoto, S. and T. Katsura (1959) J. Geomag. Geoelect. 10, 69.

Akimoto, S. and I. Kushiro (1960) J. Geomag. Geoelect. 11,94.

Kent, D. V. and W. Lowrie (1974) J. Geophys. Res. 79, 2987.

Larson, E., M. Ozima, M, Ozima, T. Nagata and D. Strangway (1969) Geophys. J. R. astr. Soc. 17, 263.

Løvlie, R. and N. D. Opdyke (1974) J. Geophys. Res. 79, 343.

Lowrie, W. , R. Løvlie and N. D. Opdyke (1973) J. Geophys. Res. 78, 7647.

Ozima, M. and E. E. Larson (1970) J. Geophys. Res. 75, 1003.

Ozima, M. and M. Ozima (1971) J.Geophys. Res. 76,2051.

Readman, P. W. and W. O'Reilly (1970) Phys. Earth Planet. Interiors (1970) 4, 121.

Richards, J. C. W. , J. B. O'Donovan, Z. Hauptman, W. O'Reilly and K. M. Creer (1973) Phys. Earth Planet. Interiors 7,437.

Sanver, M. and W. O'Reilly (1970) Phys. Earth Planet. Interiors 2, 166.

Symons, D. T. A. (1973) J. Geophys.Res. 78, 5100.

Tanaka, H. and M. Kono (1973) Rock Mag. Paleogeophys. 1, 71.

Wilson, R. L. and N. D. Watkins (1967) Geophys. J. R. astr. Soc. 12,405.

A FURNACE FOR THERMAL DEMAGNETIZATION USING OXYGEN PARTIAL PRESSURE CONTROL TECHNIQUES

Hidefumi TANAKA and Masaru KONO

Geophysical Institute, University of Tokyo, Bunkyo-ku,
Tokyo 113, Japan

Introduction

Recentry it has become a very important problem to distinguish whether or not the characteristics of artificial TRM acquired in a laboratory are identical with those of original NRM. As is well known, errors in the determination of paleointensities are frequently caused by irreversible changes in TRM capacity during heating (Coe and Grommé, 1973; Kono,1974). It is also pointed out that the change is caused by chemical alteration of ferromagnetic minerals, the degree of which depends on the atmosphere in a heating furnace (Khodair, 1974). Significance of oxygen partial pressure (Po_2) to iron-titanium oxide was first clarified by Buddington and Lindsley (1964). The Po_2 values in laboratory furnaces are often quite different from that in magmas or in cooling lavas. Various attempts have been made to evaluate the values of Po_2 in magmas; on the basis of caluculation of equilibrium of volcanic gases (Heald and Naughton, 1962), composition of co-existing iron titanium oxides (Buddington and Lindsley, 1964), equilibrated mole ratio of (FeO)/($FeO_{3/2}$) (Shibata, 1967; Katsura, 1967) or direct measurement by using electrochemical devices (Sato and Wright, 1966). Typical value of Po_2 in magmas is found to be $10^{-7} \sim 10^{-9}$ atms at 1200°C. It is therefore important, first of all, to examine whether an artificial TRM can be produced in a laboratory with exactly the same properties as the original NRM of the sample which was acquired when the rock was formed from molten magma. A furnace for this study was newly constructed and experiments are now in progress.

Gas Mixture Techniques

The atmosphere surrounding the sample is controled by mixing H_2 and CO_2 with variable volume ratios. The value of Po_2 is caluculated by the following equation (Muan and Osborn, 1964).

$$Po_2 = \tfrac{1}{2}K_1 (r-1)\left\{(r-1)+\sqrt{(r-1)^2+\frac{4r}{K_0}}\right\}+\frac{K_1 r}{K_0} \qquad (1)$$

K_0; the equilibrium constant for ($CO_2 + H_2 = CO + H_2O$)
K_1; the equilibrium constant for ($2CO_2 = 2CO + O_2$)
r ; volume gas mixing ratio of CO_2 to H_2

The caluculated Po_2 is shown in Fig.1. At lower temperatures, however, discrepancies exist between Po_2 values obtained from eq.1 and those measured directly by electrochemical fugacity probe. The latter is usually thought to represent the actual Po_2 value. It is, therefore, neccessary to use fugacity probe in the experiments at such low temperatures as 600°C 800°C which is the range of interest of the present study. In the electrolyte

fugacity probe, illustrated in Fig.2, any difference in oxygen fugacity between the inside and outside of the electrolyte wall causes migration of O^{2-} ions in the defect zirconia structure and produces a potential difference between the two electrodes.
The Po_2 is known at any time only by measuring the voltage on a very high-impedence electrometer and caluculating by the thermodynamic equation (Sato, 1971):

$$-\log Po_2 = \frac{E(mv)\cdot 100}{Temp(^\circ K)\cdot 4.96}$$

Gas flow rate and mixing ratio of two gases are varied with substantial long term stability by using a flow meter designed by Katsura (1973) and illustrated in Fig.3.
In principle, the gas flow rate is proportional to the pressure difference between two sides of a capillary.

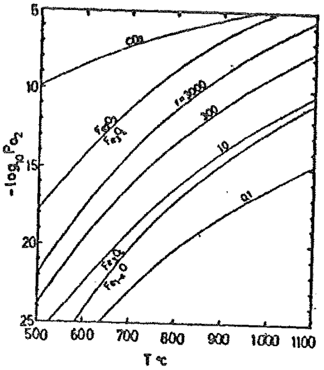

Fig.1 Temperature dependence of Po_2 in Co_2-H_2 system.

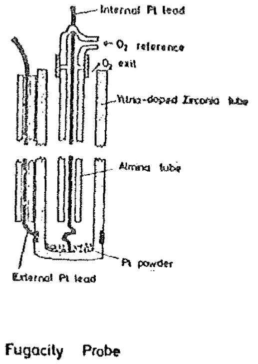

Fig.2 Fugacity probe.

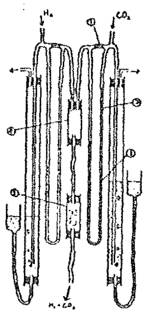

(1) capillary
(2) U-tube
(3) dibutyl phthalate
(4) mixer
(5) drier

Fig.3 Flow meter designed by Katsura (1973).

Furnace for Thermal Demagnetization

Fig.4 illustrates the newly constructed furnace to control the Po_2 in the sample space. Three layer permalloy magnetic shield surrounds the furnace,and a solenoid coil is set inside the shield to apply a magnetic field to the samples. Possible value of Po_2 in the sample space ranges

Fig.4

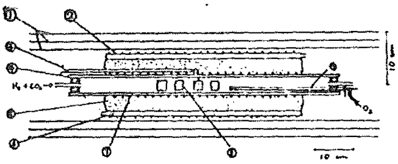

1. magnetic shield
2. solenoid
3. thermocouple
4. furnace
5. asbestos
6. water jacket
7. heater
8. sample
9. probe

frome 10^{-4} to 10^{-25} atm at 800°C.

Experiments and Results

Experiments are now in progress and in this paper an interim report is given. Cylindrical samples 2 cm in diameter and 2.3 cm long were cut from historic lavas in Hawaii and 1950 lava in Oshima. Experimental procedures are as follows.

(1) measure the AF demagnetization spectrum of NRM
(2) give TRM on the demagnetized sample by cooling down to room temperature after heating one hour at 600°C in the controled atmosphere under 0.5 Oe magnetic field
(3) measure the AF demagnetization spectrum of acquired TRM

First, the ratio of intensities of artificial TRM to that of original NRM was measured under different atmosphere conditions for several samples. It can be seen from Table 1 that the TRM acquired in air has larger intensity than the original NRM and for some samples it amounted to twenty times larger than the NRM. Secondly, the shapes of AF demagnetization spectra were compared. In Fig.5 the spectrum of original NRM is represented by a broken line, while the solid line represents that of artificial TRM. It can be said that the TRM acquired in air is magnetically harder than the original NRM. Details will be reported in the future.

sample	atmosphere	ratio
HA 5-1-2	air	2.1
HA 5-2-2	H_2	1.0
HA 5-3-1	CO_2	1.7

Table 1 The ratio of intensity of artificial TRM to that of original NRM

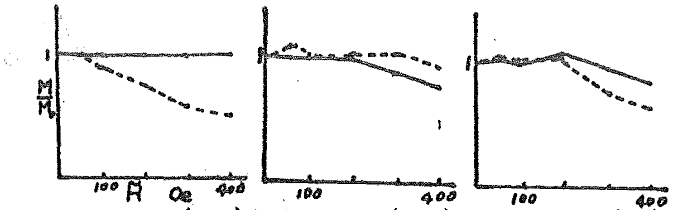

HA 5-1-2 (air) HA 5-3-1 (CO_2) HA 5-2-2 (H_2)

Fig.5 AF demagnetization spectra of artificial TRM (solid line) and original NRM (broken line).

References

Buddington, A. F. and D. H. Lindsley (1964) J. Petrol. 5, 310.
Coe, R. S. and C. S. Grommé (1973) J. Geomag. Geoelect. 25, 415.
Heald, E. F. and J. J. Naughton (1962) Nature 193, 642.
Katsura, T. (1967) Geochem. J. 1, 157.
Katsura, T. (1973) Distribution of elements accompanied the formation of rocks and minerals (in Japanese) p.65.

Khodair, A. A. (1974) EOS 56, 1112.
Kono, M. (1974) J. Geophys. Res. 79, 1135.
Muan, A. and E. F. Osborn (1964) Phase equilibria among oxides in steelmaking (Addison-Wesley) p.48
Sato, M. (1971) Research Techniques for High Pressure and High Temperature (Springer Verlag) p.43.
Sato, M. and T. L. Wright (1966) Science 153, 1103.
Shibata, K. (1967) Bull. Chem. Soc. Japan 40, 830.

REMANENT MAGNETISM OF THE RECONSTRUCTED ANCIENT KILN

Tadashi NAKAJIMA, Masayuki TORII, Nobuyoshi NATSUHARA,
Katsumi YASKAWA, Masahiro TAKAGI, Kiyomitsu IKEGUCHI,
and Naoto KAWAI ---------------- *

Department of Physics, Faculty of Engineering Science,
Osaka University, Toyonaka, Japan

Japanese ancient kiln called Noborigama (Fig. 1) was reconstructed in the field near Sakai city (Fig. 2) in the winter of 1971. The construction was completely imitated to that of an excavated kiln of the 7th century. It was subsequently fired together with many Sue type earthenwares placed in the ascending floor.

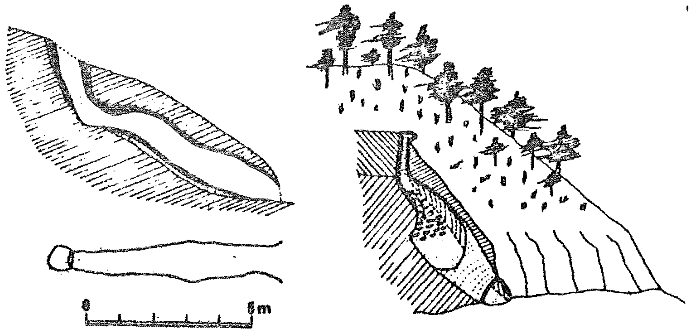

Fig. 1 Reconstructed Noborigama kiln

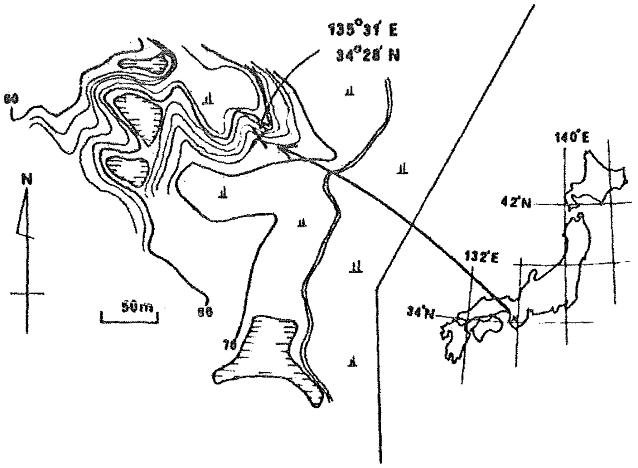

Fig. 2 Locality of the kiln

The purpose of this experiment is first to make clear the thermal condition within the kiln relative to the fuels used, and then to clarify many other archaeological problems in connection with the past ceramic techniques. Besides, we had another aim to know directly the relation between the applied field and the aquired remanent magnetism of baked clays, especially the uniformity and stability of the magnetic vectors.

Prior to the construction, the present geomagnetic field

---

* The other co-operative members of this experiments are as follows; (Archaeology) Hiroshi NAKAMURA, (Ceramists) Hajime ATARASHI, Akira SAINEN.

was measured at the spot. The determined declination, inclination, and intensity are 5°38' W, 46°47', and 46,350 γ, respectively.

Chromel-alumel (CA) and platinum-platinum/ 13% rhodium (PR) thermocouples (7 in number) were embeded in and around the kiln ground as shown in Fig. 3. All thermocouples were protected with sintered alumina sheaths. The PR thermocouple was 0.5 mm in diameter and 1 m in length, respectively. The two leads were connected to the cold-junction placed out of the kiln through two compensating cables which were 4 m in length.

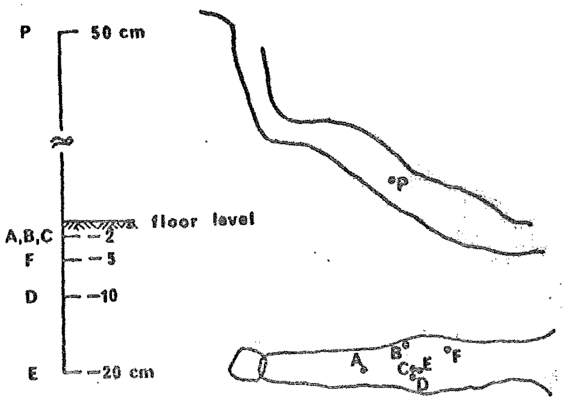

Fig. 3 Position of the hot-junction of thermocouple
P:platinum-plutinum/ 13% rhodium thermocouple
A,B,C,D,E,and F: chromel-alumel thermocouple

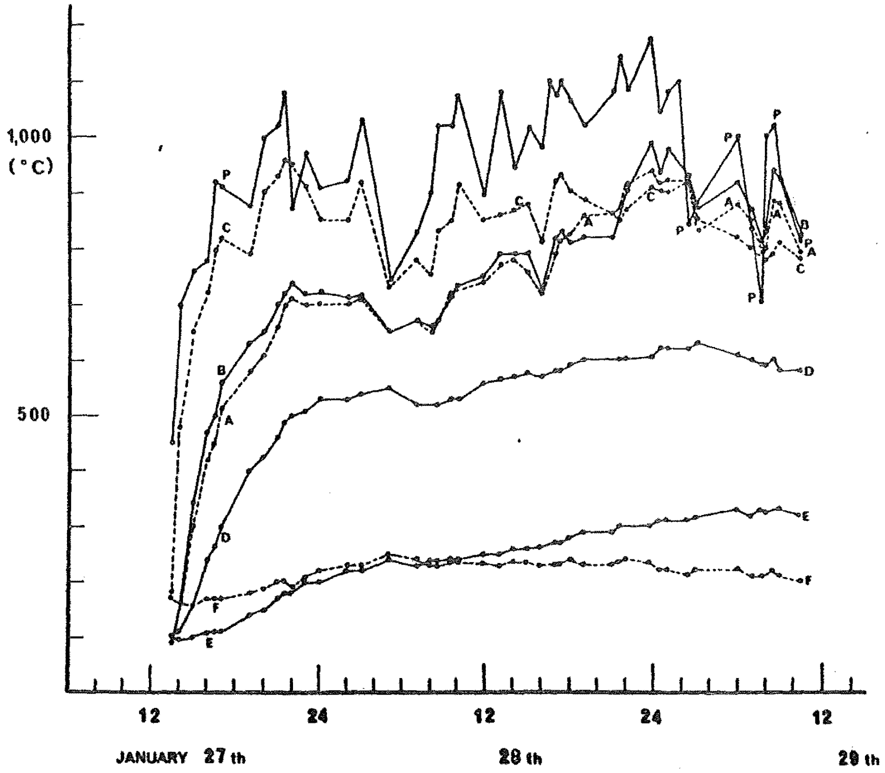

Fig. 4 Result of temperature measurement

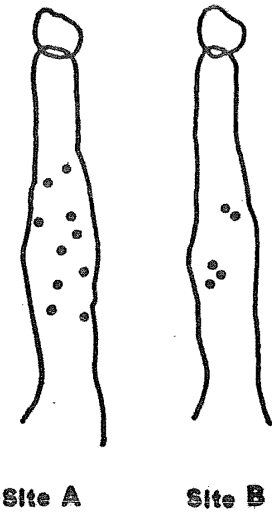

Fig. 5 Distribution of oriented samples

Site A: at the floor level of the kiln
Site B: at the level 20 cm below the kiln floor

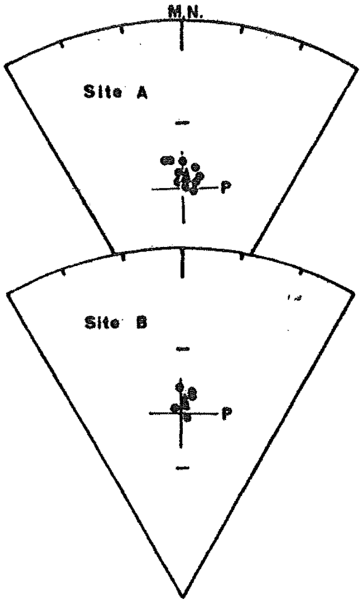

Fig. 6 Direction of NRM (plotted on the schmidt's equal areal projection)

P: present geomagnetic direction

While, CA thermocouples were 2 mm thick and about 5 m long. All the leads were connected directly to a 6 way selector switch which was assumed as the cold-junction, so that all the results reported here have been corrected for the temperature of the switch. Direct-reading temperature meters (CA and PR) were used for the thermo-e.m.f. Change of temperature at each position during the firing was measured from time to time relative to the cold-junctions. All curves showing the respective change are shown in Fig. 4. The maximum temperature was attained in the middle of the ascending tunnel (Position P). It was 1,180°C. On the other hand, the temperatures at the floor level (Positions A,B and C) rose up to about 1,000°C, and at the level 10 cm below the floor (Position D) up to 630°C, which is very close to the blocking temperature of magnetic domain of α-Fe_2O_3. Even at the level 20 cm below the floor (Position E) the temperature was observed up to 350°C. Consequently, in such Noborigama kilns with the same size, relatively thick layer of the floor can be utilized as the reliable specimen for archaeomagnetism. On the other hand, the effect of reheating should not be ignored in the case when the kilns were repeatedly fired.

Naturally grown pine trees with diameter about 10 cm and all other miscellaneous woods in 100 m in radius around the spot were used up, although our firing technique was still insufficient. It, nevertheless, would have been a very serious and severe problem for the ancient ceramists to obtain fuel woods. One of the reason why we can now find so many kiln spots in the district is certainly due to that a new kiln was easier to be made, instead of the enormous fuels to be carried over a long distance.

After the firing, roof of the kiln was removed, and the baked soils on the floor and those below it were carefully sampled, each orientation in situ being referred to both the horizontal plane and the geomagnetic meridian in the sampling site as shown in Fig. 5. The plaster of Paris was used to make even surface of soil on which the orientation was clearly marked. Remanent magnetism of each sample was determined under the astatic magnetometer in Osaka University. The results of measurement are tabulated in Table 1. Schmidt's equal areal projections are used in plotting the direction of NRM (Fig. 6). The plots of NRMs are swarming around a position for the present geomagnetic direction. Mean precision factor k is larger than 470, showing that the magnetization is almost uniform everywhere in the kiln floor. Progressive AC demagnetization method was carried out with respect to the several pilot samples, whose decreasing intensities with increasing field together with the changes of the directions are shown in Fig. 7. Quite uniform distribution of magnetic vectors and obtained high coercive force in each sample show that the particular baked earths may be used quite safely for the representation of the past geomagnetic field.

Table 1

Results of magnetic measurement

	Site A	Site B	A + B
Decli.(°E)	-5°02'	-4°48'	-4°53'
Incli.	43°22'	43°31'	43°25'
α_{95}	2°25'	3°23'	1°46'
k	411	513	471
N	10	5	15
Intensity (x10^{-4} CGSemu/gr)	45	6	32

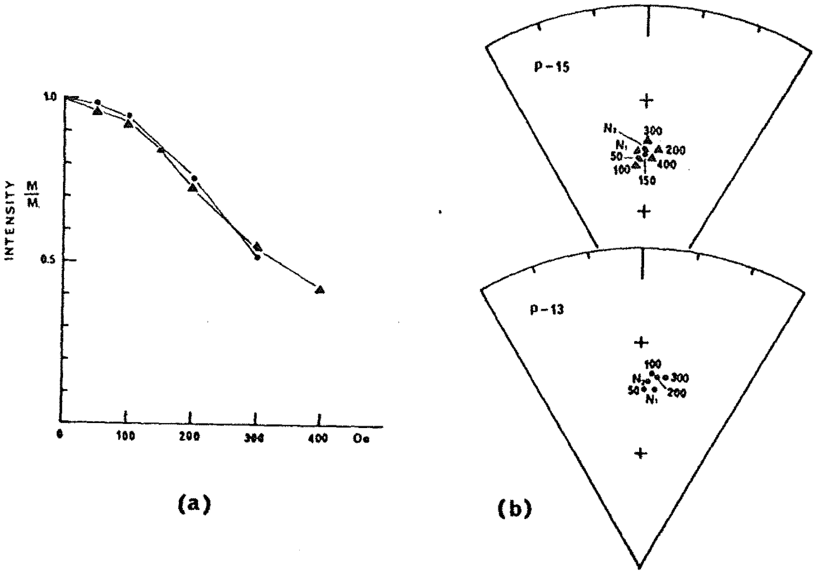

(a)

(b)

Fig. 7 Alternating field demagnetization curves

A BRIEF NOTE ON THE REMANENT MAGNETIC MEASUREMENT OF THE DILUVIAL DEPOSITS IN YAMAGUCHI PREFECTURE, WEST JAPAN.

Haruo DOMEN and Hiroshi MUNEOKA

Institute of Physical Sciences, Faculty of Education
Yamaguchi University, 753 Japan.

Since 1967, the present authors have been engaged in the paleo/rock magnetic study on the tephra in Diluvial deposits widely spreaded in southern Yamaguchi Prefecture, Japan (Domen 1968, Domen and Kawano 1969, Domen et al 1970, Domen 1971, Kawano and Domen 1971).

The questioned tephra deposits are called by the name of 'Ube volcanic ash' which originated with the eruptions of Mt. Aso in the central Kyushu Island, west Japan at about 33,000 years before present, and which has been well known to be correlated to the Yame clay and the Aso pyroclastic flow in the northern Kyushu Island and also to the Musashino loam at the Kwanto district in the central Japan.

These ash deposits have generally deposited having the few centimeters to few meters in thickness and it seemed to be divided into two layers such as the upper redish brown layer and lower white one roughly speaking. Recently, one more couple of such a two-tone-colored layers beneath the above-mentioned alternative colored layers has been found at a certain locality in the central part of southern Yamguchi Prefecture. That is to say, the whole ash deposits may be classified into two layers; upper and lower, and each layer might be devided into two-tone-colored sub-layers B and W respectively; such as the upper brown layer(Bu in abbreviation), upper white (Wu), and the lower brown (Bl), lower white (Wl) in the descending order. Individual locality mainly shows the single couple of B and W layers and it is very difficult to distinguish whether the couple of B-W in outcrop may be belonged to the upper group or lower one.

The magnetic study about the individual deposit has now been undertaken in order to clarify finding any correlation among them, and to make clear the causation how to appear the two-tone-colored band, and also the paleomagnetic study (mesgeomagnetic study; Domen and Kawano 1969) has been carrying on.

Over 100 oriented samples were newly taken from 6 districts. The specimen sampled was taken as a cylindrical which has both the diameter and height of 6 cm. by the aid of the cylindrical vessel made of polyvinyle chloride.

All of specimens were submitted to their nrm measurements by means of an ordinal astatic magnetometer. The af demagnetization of these specimens, and also the thermomagnetic and X-ray analyses of the ferromagnetic constituents separated from the ash specimen magnetically by means of a strong hand magnet in the room temperature are being carried on.

The table 1 shows these sampling localities together with data concerning the nrm measurements.

However the adequet numbers of samples had been collected and bunch of the magnetic data have been piled up since 1967, it is very hard to recognize any correlation among the individual deposit layers and even the magnetic characteristics of these of balk specimens and also of ferromagnetic constituents are still under examination. Any conclusive result has not been deduced yet. The further investigations, expanding the sampling area have to be required.

Table 1. NRM data at individual localities, Yamaguchi Diluvial tephra newly sampled.

Locality	Color	Nos. of samples	N R M			
			D(E)	I(D)	$\alpha_{95\%}$	k
Jumonji	B	6	8.4°	4.9°	35°	5
"	B	6	-5.8	44.6	7	102
"	W	4	-67.8	23.8	14	45
Oyama	B	12	-30.6	32.9	15	10
Kibe	B	10	4.0	30.8	15	11
Iwanaga	B	17	8.4	32.1	5	52
"	W	10	-7.9	33.4	9	27
Kurumaji	B	8	5.1	32.0	10	30
"	B	8	-5.6	56.0	4	161
"	W	8	0	50.5	7	75
Yuno-to	B	6	-1.6	36.2	16	19
"	W	6	-16.7	34.4	23	10

References

Domen, H. (1968) 1967 Annual Prog. Report of Palaeogeophys. Res. Group in Japan, 74-75.

Domen, H. and M. Kawano (1969) Bul. Fac. Educ. Yamaguchi Univ., 18 (Part 2), 23-33 (in Japanese).

Domen, H., H. Muneoka and M. Kawano (1970) ibid, 19 (Part 2), 23-26 (in Japanese).

Domen, H. (1971) ibid, 21 (Part 2), 1-14.

Kawano, M. and H. Domen (1971) Dai Yonki (Quaternary) No. 16 (in Japanese).

PALEOMAGNETISM ON THE WATER-LAID VOLCANIC ASH LAYERS IN THE OSAKA GROUP, SENNAN AND SENPOKU HILLS, SOUTHWESTERN JAPAN

Masayuki TORII*, Shusaku YOSHIKAWA and Minoru ITIHARA

Depertment of Geosciencs, Faculty of Science, Osaka City Universtiy, Sugimoto-cho, Osaka City, 558
(* present address: Dept. of Phys., Fac. of Engineering Sci., Osaka Univ.,
Machikaneyama-cho, Toyonaka City, 560)

The Osaka Group, one of the typical Plio-Pleistocene Series in Japan, crops out in the hills around the Osaka plains and is mostly composed of clay, silt and sands. Also several ten water-laid volcanic ash layers are intercalated in these sediments as key beds. The paleomagnetism on these ash layers was studied by several investigators, and their results showed that the Osaka Group was formed from the Gauss normal epoch to Brunhes normal epoch (Kawai, 1951; Ishida et al., 1969; Komyoike Reserch Group, 1970).

Recently, the tephrostratigraphic study was carried out in detail at Sennan and Senpoku hills, southern parts of Osaka prefecture. And the precise stratigraphy was newly establised on the Osaka Group in these areas, whose total thickness is about 400 m intercalating forty or more water-laid volcanic ash layers (Itihara et al., 1975).

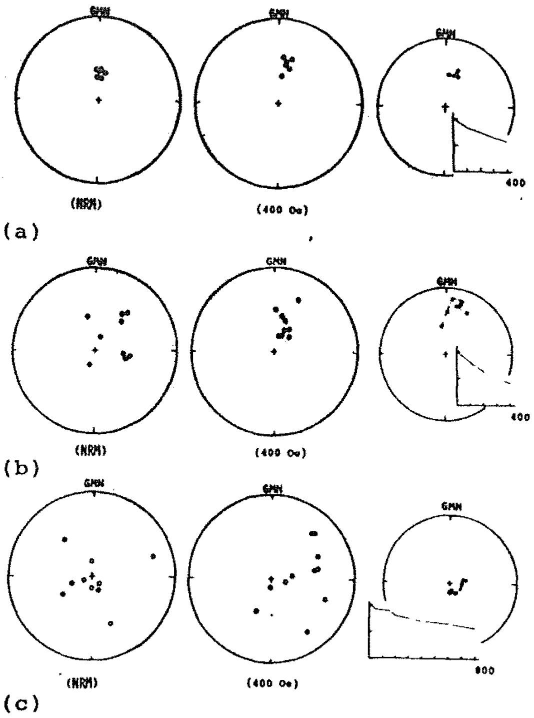

Fig.1 Some examples of the a.f. demagnetization. (a), (b) and (c) are descrived respectively in the text.

The thickness of these ash layers are ordinarily 10 cm more or less and the nature of them ranges between rhyolitic and andestic. The remanent magnetization of the ash layers is considered to be detrital origin. And yet, the ashes are very coarse in grain and have a rather rapid depositional rate in comparison with clay or silt. For the purpose of the paleomagnetic stratigraphy, it is favorable to measure the remanence of clay or silt because of their continuous deposition, while the ash layers are intercalated at intervals. However, the present authors found the remanence of clay or silt of the Osaka Group considerably weak and unstable

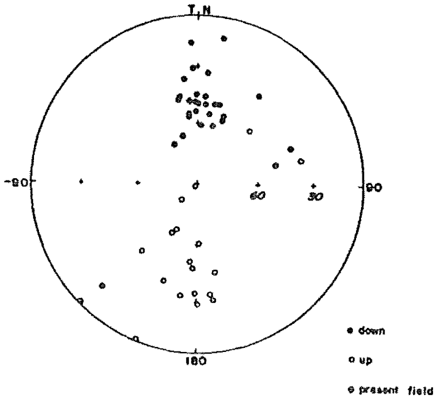

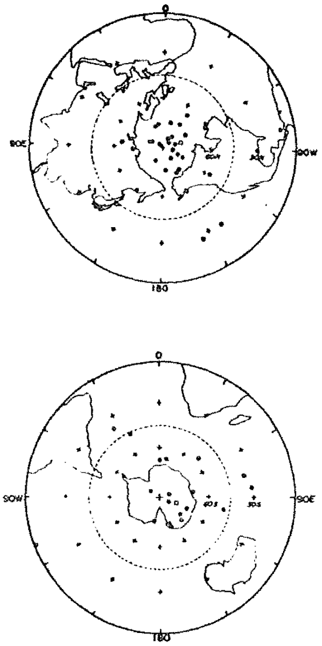

Fig. 2 (left) The mean direction of each ash layer plotted on Schmidt's net after the a.f. demagnetization and the bedding correction.

Fig. 3 (right) The VGPs are plotted on the polar Schmidt's net.

compared with that of the volcanic ash layer. Therefore we have collected about seven hundred oriented ash samples at sixty sites round the both hills.

After the field collection, hand samples were cut into cubes of 3.5 × 3.5 × 3.5 cm coated each side with plaster of Paris in the laboratory. Then paleomagnetic measurements were made with an astatic magnetometer. The intensities of natural remanent magnetization lay in the range $10^{-5} \sim 10^{-7}$ cgs emu/cc. Most of them were the order of 10^{-6} cgs emu/cc. To examine the stability of the remanence, the progressive alternating field demagnetization up to 1200 Oe (peak, the maximum case) was carried out on each pilot sample picked up from every ash layer.

The results of the a.f. demagnetization were classified as

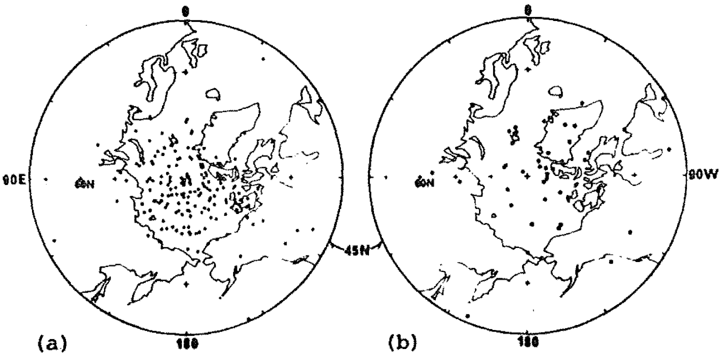

(a) (b)

Fig. 4
The VGPs except intermediate polarities plotted on the northern hemisphere.
(a) igneous rocks
(b) volcanic ash layers of the Osaka Group

follows; (a) stable against the a.f. demagnetization (b) soft components removed apparently with the a.f. demagnetization (c) unstable or scattered after a.f. demagnetization. Some typical examples of these results are illustrated in Fig. 1, but (c) is rather exceptional in this study. In most of the ash layers, apparent viscus components seemed to be removed with the a.f. cleaning up to 400 Oe (peak). Each mean direction of every site was then calculated, and after the bedding correction, the virtual geomagnetic pole (VGP) was also determined. They are shown in Fig. 2 and Fig. 3, respectively.

Even if we can eliminate unstable components with a.f. cleaning, it is uncertain that the mean remanent direction of each ach layer is strictly coincident with the past geomagnetic field. To solve this problem, we compared the VGPs of our results with those of the igneous rocks in the age range Pliocene to Pleistcene collected from all parts of the world (Irving, 1964; McElhinny, 1973). This procedure is shown in Fig. 4. Though there is rather large deviation in our results in comparison with those of the igneous rocks, these two tendencies of the distribution resemble each other.

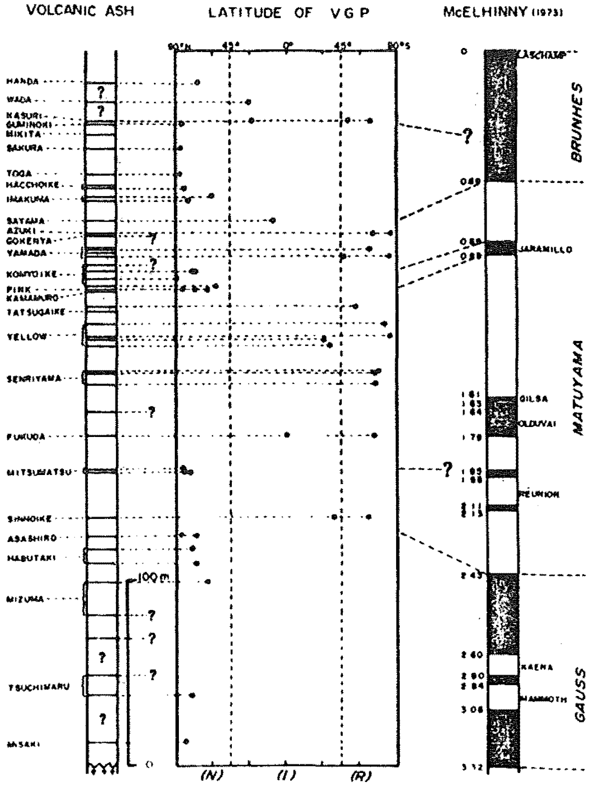

Fig. 5 The latitude of the VGP are correlated with the geomagnetic polarity epoch time scale. Left column indicates the horizons of the ash layers.

Thus we correlated the polarity of the VGP (ψ) of each ash layer (i.e. $90°N \geq \psi \geq 45°N$, normal; $90°S \geq \psi \geq 45°S$, reversed; $45°N \geq \psi \geq 45°S$, intermediate) with the geomagnetic polarity epoch time scale (McElhinny, 1973) for the purpose of the stratigraphic correlation. These resuluts are illustrated in Fig. 5 and described as follows.

(1) The boundary between the Brunhes normal and Matuyama reversed epochs (0.69 m.y.) was correlated with the horizon of the Sayama volcanic ash layer which revealed intermediate polarity.

(2) The boundary between the Matuyama reversed and Gauss normal epochs (2.43 m.y.) lay between the Sinnoike and Asashiro volcanic ash layers.

(3) The Jaramillo normal event was clearly detected. On the other hand, normal polarity was found out in the lower part of the

Matuyama epoch, and it may be correlated with the Olduvai or Réunion normal event.

(4) The Kasuri volcanic ash layer whose absolute age reported to be 0.38 m.y. with the fission-track method (Nishimura and Sasajima, 1970) revealed reversed polarity after the a.f. cleaning (Torii, 1973). Though this ash was somewhat magnetically unstable, it suggests the possibility of quite short interval of reversed polarity that belongs to the Brunhes normal epoch.

This work is still continued on the Osaka Group in the other districts.

References:

Irving, E. (1964) Paleomagnetism and its Application to Geological and Geophysical Problems (John Wiley & Sons, New York)

Ishida, S., K.Maenaka and T.Yokoyama (1969) J. Geol. Soc. Japan, 75, 183.

Itihara, M., S. Yoshikawa, T. Hayashi, K. Inoue and K. Nakajima (1975) J. Geosci. Osaka City Univ., 18, (in preperation)

Kawai, N. (1951) J. Geophys. Res., 56, 73.

Komyoike Reserch Group (1971) *Chikyu-kagaku*, 25, 201. (in Japanese)

McElhinny, M.W. (1973) Palaeomagnetism and Plate Tectonics (Cambridge University Press, Cambridge)

Nishimura, S. and S. Sasajima (1970) *Chikyu-kagaku*, 24, 222. (in Japanese)

Torii, M. (1973) Rock Magnetism and Paleogeophys., 1, 65.

A PROGRESS REPORT ON PALEOMAGNETIC STUDY ON CENOZOIC ROCKS FROM NORTHERN KYUSHU ISLAND, WEST JAPAN

Haruo DOMEN and Hiroshi MUNEOKA

Institute of Physical Sciences, Faculty of Education
Yamaguchi University, 753 Yamaguchi, Japan

The volcanic rocks of northern Kyushu Island, west Japan range in age from Miocene to Pleistocene, were partly submitted to paleomagnetic study.

One hundred sixty six oriented hand samples from thirty five sites at four districts were collected. These NRMs were measured by means of an astatic magnetometer and some of them were cleaned out their soft components in the alternative demagnetizing field.

About one half of the samples were collected from the

Table 1. Polarity of NRM of the Cenozoic rocks from the northern Kyushu Island, west Japan.

Saga	Himeshima	Kunizaki	Oita
	Up. Pleisto. $\frac{8}{54}$ N		Up. Pleisto. $\frac{3}{22}$ N
Pleisto. $\frac{2}{10}$ R,O			
		Low. Pleisto. $\frac{1}{14}$ R	
		Up. Plio. $\frac{1}{4}$ O	
Plio. $\frac{17}{53}$ N,R,O			
Up. Mio. $\frac{3}{9}$ R,O			

'Ref.'

Geologic Age

$\frac{\text{Nos. of Sites}}{\text{Nos. of Samples}}$ Polarity*

* N: Normal NRM
R: Reversed NRM
O: Oblique NRM

Saga district at the western part of northern Kyushu Island and the others from the eastern four districts; say Himeshima (an islet opposed easterly to the Kunizaki district mentioned below), Kunizaki and Oita district respectively.
The western samples were collected at exactly the same locality in the Saga district, where the magnetic investigations had been carried out by Creer and Ispir (1970).

In the Saga district, these Cenozoic basalts, which cover the geologic age from upper Miocene to Pleistocene, are magnetized in either the normal or reversed direction of the NRM. And also the oblique directions of NRM are sometimes found in this district. In the Himeshima district, the NRM from Pleistocene shows the normal. For the Kunizaki district, the NRM direction appears in both reversed and oblique for the lower Pleistocene and for upper Pliocene respectively. The NRM for the Oita district is normal for the upper Pleistocene.

These are shown in the table 1 together with numbers of both sampling sites and samples at the individual district.

Reference

Creer, K.M. and Y. Ispir (1970), Geophys. J. R. astr. Soc., 127-148.

PALEOMAGNETIC EVIDENCE OF THE DURATION OF THE METALLOGENETC EPOCH OF KUROKO DEPOSITS.

Hirotomo UENO

Institute of Mineralogy, Petrology and Economic Geology
Faculty of Science, Tohoku University
Sendai, 980, Japan

The Kuroko strata-bound polymetallic sulphide deposits are apparently related to Middle Miocene submarine acidic volcanism of the Green Tuff region (Horikoshi, 1969; Tatsumi et al., 1970; Matuskuma and Horikoshi, 1970; Horikoshi and Sato, 1970; Kajiwara, 1970) (Fig. 1). Most of the Kuroko deposits occur in the upper part of the Nihsikurosawa stage (13-14 m.y.) of the Middle Miocene (Sato, in press). An attempt to determine the length of involved time from the magnetic polarity of associated rocks is now described.

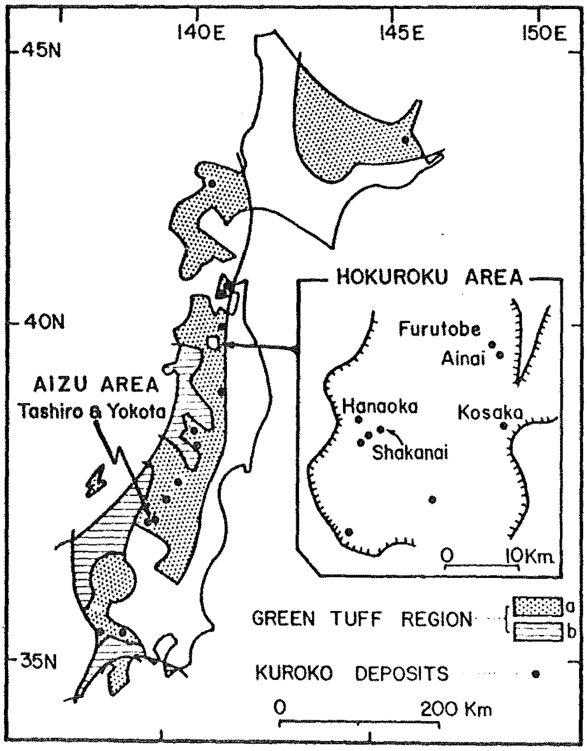

Fig. 1. Distribution of Kuroko deposits. (a) zone of Miocene volcanism, (b) zone of Neogene folding.

Most of the results have been obtained from red ferruginous chert, which commonly overlies the Kuroko ore in beds 1 to 10 m in thickness. Chert deposition seems to have been the last stage in the Kuroko mineralization process(Sato, 1968). The chert consists of quartz (10-600μ diameter) and very fine-grained hematite, with minor pyrite and barite. The average grain size (Stokes, 1948; Warren and Averbach, 1950) of the hematite determined from Furutobe and Kosaka mines (Fig. 1) are 150Å and 95Å respectively. The initial grain size between the single-domain and superparamagnetic range is usually assumed to be about 290Å(Nagata, 1968) so much of the hematite is probably superparamagnetic. Nevertheless a substantial number of larger grains must be present because the remanent magnetization is very stable. The remanent intensity drops only a few per cent, and the directions remain unchanged, after demagnetization in alternating fields of 600 oe (Fig. 2). Also hysteresis loops in fields up to 19000 oe show essentially a straight-line increase, with no tendency to saturation. The magnetization is probably a chemical remanent magnetization (Kobayashi, 1959).

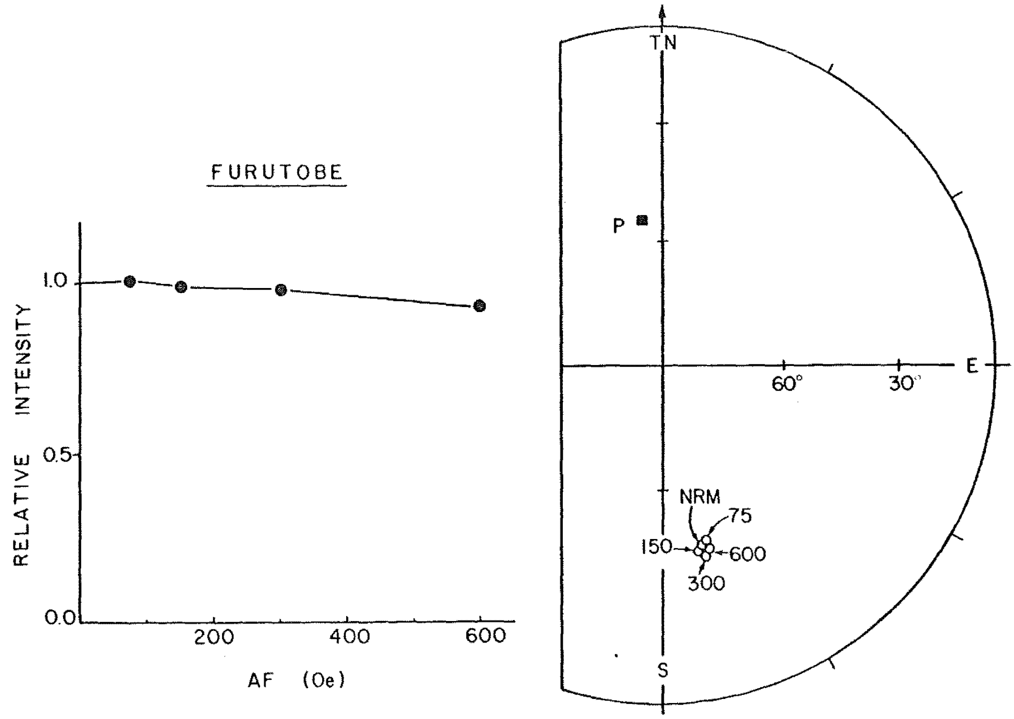

Fig. 2. Changes in direction and intensity during a.f. demagnetization of ferruginous chert. The directions are plotted in an equal-area net. Each direction is labelled with the a.f. strength in oersted. Circles denote upward directions. P is the present geomagnetic field direction (down).

Oriented samples of cherts and other rocks were collected from the Hokuroku and Aizu areas (Fig. 1). The Hokuroku area contains the greatest concentration of Kuroko deposits, and all mines have similar geological sections, except for the occurrence of basalt (B_1) at Furutobe (Fig. 3). Two marker mudstone beds (M_2 and M_1)

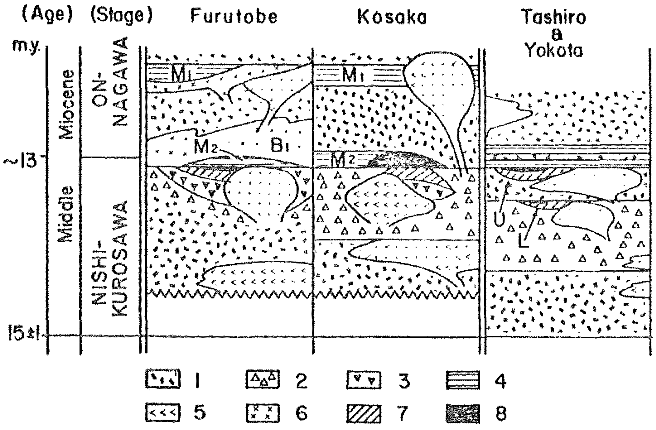

Fig. 3. Geological columns of the Furutobe and Kosaka mining districts in the Hokuroku area, and the Tashiro and Yokota mining districts in the Aizu area. 1 Tuff. 2 Tuff breccia. 3 Volcanic breccia. 4 Mudstone. 5 Rhyolite. 6 Basalt. 7 Kuroko ore body. 8 Ferruginous chert. L Lower ore bodies. U Upper ore bodies. For explanation of M, M_2 and B see text. The ages are from Ikebe et al. (1972).

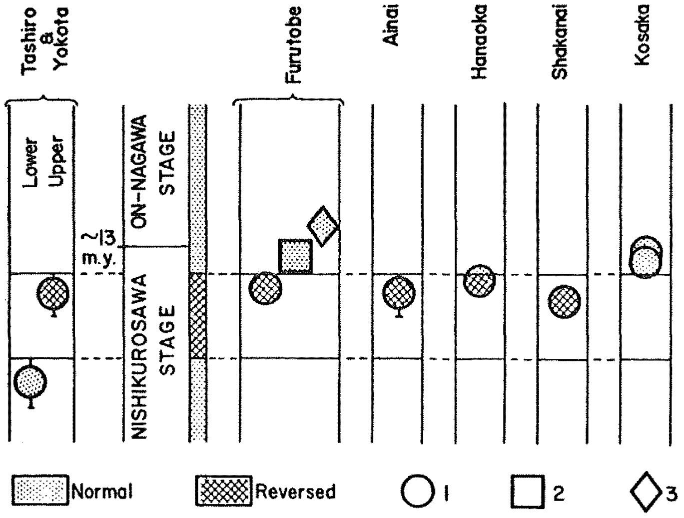

Fig. 4. Polarities plotted on the basis of known stratigraphic sequence. 1 Ferruginous chert. 2 Mudstone. 3 Basalt. Upper and Lower are the upper and lower ore bodies in the Aizu area.

allow the ore horizons to be completed (Fig. 3). The lower half of M_2 has microfossils of the Nishikurosawa stage, and the upper half of M_2 has microfossils of the On-nagawa stage (Otagaki, 1966). At furutobe mine in the Hokuriku area the sequence is Kuroko ore, ferruginous chert, mudstone M_2 and basalt B_1 (Tanaka and Lu, 1969) (Fig. 3). The chert has reversed magnetization (10 samples, mean intensity 500 μG, Fig. 2), the mudstone has normal magnetization (3 samples, intensity 50 μG, remanent coercivity 200 oe), and the basalt has normal magnetization (3 samples, intensity 2000 μG, remanent coercivity 150 oe). At Ainai mine (Ishikawa and Yanagizawa, 1971) the ferruginous chert has reversed magnetization (5 samples, intensity 50 μG). At Hanaoka mine the chert both normal and reversed magnetization (2 normal samples, 6 reversed samples, intensity 30 μG). At Shakanai mine the ferruginous chert that occurs in lower part of the body has reversed magnetization (3 samples,intensity 200 μG). At Kosaka mine the ferruginous chert occurs in the mudstone M_2 (Suzuki et al., 1971) (Fig. 3). Samples taken from directly above, and at some distance from, Kuroko ore have normal magnetization (9 samples, intensity 100 to 800 μG).

The Tashiro and Yokota mines in the Aizu area have similar geological sequences (Shimada and Hirabayashi, 1972). There are two mudstone layers, the lower contains microfossils of the Nishikurosawa stage, and the upper microfossils of the On-nagawa stage exactly as in the Hokuroku area (Fig. 3). The Aizu area is exceptional in that there are two different ore horizons. There is an upper ore body at the same horizon as in the Hokuroku area, and a lower one (Fig. 3). Two layers of chert overlays directly both upper and lower ore bodies. Ferruginous chert associated with the upper ore bodies has reversed magnetization (6 samples, intensity 50 μG), but that associated with the lower ore bodies has normal magnetization (6 samples, 50 μG).

The polarity results are plotted on the basis of the known stratigraphy in Fig. 4. All the Kuroko deposits, except the lower ore bodies in the Aizu area, appear to have been formed in one reversed polarity interval. Soon after the formation of the Kuroko deposits the geomagnetic field changed from reversed to normal. Lower ore bodies in the Aizu area were apparently formed in the preceding normal interval. The upper part of the Nishikurosawa stage seems to have been laid down in an interval of reversed polarity. This is cinsistent with evidence of the short reversal interval in the upper part of the Nishikurosawa stage from measurements on volcanic and sedimentary rocks in the Green Tuff region (Noritomi et al., 1970; Ueno, in press).

If the magnetic stratigraphy of the Middle Miocene were perfectly known the exact time interval of forming Kuroko deposits could be determined from the evidence summarized in Fig. 4. Of course this is not yet possible, but an estimate can be made from the time scale of Heirtzler et al.(1968). On this scale five reversed intervals occur between 12 to 15 m.y. ago and they have an average duration of 0.2 m.y.. Since the Kuroko deposits, except for a few exceptional deposits which in the diferent horizon, were formed in a single polarity interval within that time span it is reasonable to conclude that they were laid down in a time of less than 0.2m.y.. These results give support to the supposition that the Kuroko ores are of syngenetic origin (Sato, 1968; Horikoshi, 1969). They also indicate that they were deposited essentially contemporaneously in both the Aizu and Hokuroku areas over a distance of 300 km apart.

References

Heiritzler, J.R., Dickson, G.O., Herron, E.M., Pitman, III, W.C., and Pichon, X.L. (1968) J. Geophys. Res., 73, 2119-2136.
Horikoshi, E. (1969) Min. Deposita, 4, 321-325.
Horikoshi, E., and Sato, T. (1970) in Volcanism and Ore Genesis (edit. by Tatsumi, T.), 181-195 (Univ. Tokyo Press, Tokyo).
Ikebe, N., Takayanagi, Y., Chiji, M., and Chinzei, K. (1972) in Pacific Geology No. 4 (edit. by Minata, M.), 39-78 (Tsukiji Shokan, Tokyo).
Ishikawa, Y., and Yanagizawa, Y. (1971) Mining Geol. (Tokyo), 21, 138-149 (inJapanese).
Kajiwara, Y. (1970)in Volcanism and Ore Genesis (edit. by Tatsumi, T.), 197-206 (Univ. Tokyo Press, Tokyo).
Kobayashi, K. (1959) J. Geomag. Geoelec., 10, 99-117.
Matsukuma, T., and Horikoshi, E.(1970) in Volcanism and Ore Genesis (deit. by Tatsumi, T.), 153-179 (Univ. Tokyo Press, Tokyo).
Nagata, T. (1961) Rock Magnetism (Maruzen, Tokyo).
Noritomi, K., Sato, S., and Hayashi, K. (1970) Res. Inst. Underground Resources, Akita Univ., 39, 32-73 (in Japanese).
Otagaki, T. (1966) Mining Geol. (Tokyo), 16, 237-248 (in Japanese).
Sato, T. (1968) Mining Geol. (Tokyo), 18, 241-256 (in Japanese).
Sato, T., Mining Geol. (Tokyo) Special Issue, 6, (in Japanese).
Shimada, I., and Hirabayashi, T. (1972) Mining Geol. (Tokyo), 22, 329-346 (in Japanese).
Stokes, A.R. (1948) Proc. Phys. Soc. London, 61, 382-391.
Suzuki, Y., Tanimura, S., and Hashiguchi, H. (1971) Mining Geol. (Tokyo), 21, 329-346 (in Japanese).
Tanaka, T., and Lu, K.I. (1969) Mining Geol. (Tokyo), 19, 312-332 (in Japanese).
Tatsumi, T., Sekine, Y., and Kanehira, K., (1970) in Volcanism and Ore Genesis (edit. by Tatsumi, T.), 3-47 (Univ. Tokyo Press, Tokyo).
Ueno, H., Econ. Geol. (in Press).
Warren, B.E. and Averbach, B.L. (1950) J. Appl. Phys., 21, 595-599.

(Submitted to Nature)

PALEOMAGNETISM AND K-Ar AGES OF HIMEJI VOLCANICS

Masaru KONO, Minoru OZIMA and Kiyoshi WADATSUMI

Geophysical Institute, University of Tokyo, Bunkyo-ku, Tokyo 113
and Himeji Institute of Technology, Shosha, Himeji City 671-22

1. Introduction

The existence of a long normal polarity interval in the upper Cretaceous seems to have well been established both by marine magnetic anomalies (Larson and Pitman, 1972) and by paleomagnetic correlation on land (McElhinny and Burek, 1971). Up to the present, paleomagnetic data for Cretaceous in Japan are not very numerous (Nagata et al., 1959; Sasajima and Shimada, 1965) and the rocks are not dated systematically. A remarkable nature of these reported data is that almost all have normal polarity for natural remanent magnetization (NRM).

The Himeji acid volcano-plutonic complex covers a wide area in Hyogo and Okayama Prefectures, and their stratigraphy has been studied in detail by Kishida and Wadatsumi (1967). Some volcanic rocks of this complex have already been studied paleomagnetically (Sasajima and Shimada, 1965; Sasajima et al., 1968), and they are reversely magnetized. We began the present study with the hope to establish the paleomagnetic stratigraphy of upper Cretaceous and, if possible, to date the boundaries of extended normal interval. The results are, however, not quite simple due, perhaps, to the complex thermal history of this suite.

2. Paleomagnetism

About six samples were collected from each cooling unit as drill-cut cores or as hand samples. The sampling locarities were distributed along the coast of the Seto Inland Sea near Aioi City and near the prefecture boundary about 20 km northwest of Ako City. The angular errors involved in orienting the core samples are less than one degree, while those for hand samples may be as large as five degrees. A specimen 2.5 cm in diameter and 2.2 cm long were cut from each sample and used for paleomagnetic studies.

After the measurement of NRM, each specimen was demagnetized in alternating fields (a.f.) in steps with peak field values of 50, 100, 200, 300, and 400 Oe. "Stable component" direction of NRM was determined as the mean direction of magnetization at the a.f. demagnetization stage where the angular dispersion (α_{95}) was the smallest. Stability of NRM to a.f. cleaning was classified by the scheme of Kono et al. (1972); Class A (B) are cooling units with $\alpha_{95} < 8^{\circ}$ (20°) for NRM and less than 5° (10°) for stable components, while Class C (D) are units with $\alpha_{95} < 15^{\circ}$ ($>15^{\circ}$) for stable components. If the α_{95} was larger than 30° at the best convergence, the unit was classified as unstable and paleomagnetic results were not considered. Results of a.f. demagnetization as well as virtual geomagnetic poles (VGP) corresponding to magnetic field directions of stable components are listed in Table 1. The stability of Himeji volcanics to a.f. demagnetization is rather low compared to that of ordinary volcanic rocks. For instance, about half or more units belonged to Classes A or B in the study of Deccan Trap basalts (Kono et al., 1972) or of San

Table 1. Summary of Paleomagnetic Data of Himeji Volcanics

Unit	N R M				Class	Stable Remanence						Virtual Geomagnetic Pole			
	N	I	D	α_{95}		AF	N	I	D	α_{95}	K	Lat.	Long.	dp	dm
Aioi Sequence															
HM 3	6	-76.4	10.1	109	Unstable										
HM 4	6	-57.1	179.7	15.7	C	200	6	-57.4	174.4	14.0	23.7	-84.5	261.6	15.0	20.5
HM 5	7	-57.2	137.4	19.8	D	50	7	-57.2	137.0	19.3	10.7	-55.5	242.4	20.5	28.2
HM 6	6	-13.9	115.7	180	Unstable										
HM 7	8	-27.1	167.0	61	Unstable										
HM 8	6	-53.2	182.7	11.8	C	50	6	-54.4	182.3	11.4	35.7	-88.1	37.8	11.3	16.0
HM 9	6	-29.9	169.3	55	Unstable										
HM11	7	-40.0	173.4	11.7	B	200	7	-43.8	173.3	8.8	48.4	-79.2	168.5	6.8	10.9
HM 1	4	-45.1	177.5	85	Unstable										
HM 2	5	-45.3	77.7	75	Unstable										
HM10	6	-11.1	230.1	55	D	200	6	-13.1	228.8	18.2	9.9	-40.3	64.1	28.2	54.4
HM12	6	-24.9	160.6	43	Unstable										
Takidani Sequence															
HM13	6	-76.3	294.5	10.0	B	200	6	-78.4	294.0	9.0	55.8	-23.8	336.5	16.1	17.1
HM14	6	-65.1	250.4	6.3	A	400	6	-65.8	251.0	4.9	190	-37.1	6.8	6.5	8.0
HM15	6	-75.7	213.3	6.9	B	200	6	-75.4	212.0	6.3	116	-56.0	340.3	10.5	11.5
HM16	6	-48.8	288.0	8.2	B	200	6	-52.5	289.4	6.1	120	-4.8	6.8	5.8	8.5
HM20	6	-70.9	252.5	5.0	A	300	6	-71.5	255.3	4.8	194	-36.2	356.1	7.4	8.5
HM21	4	-22.1	174.2	5.9	A	200	4	-22.4	176.1	2.0	2140	-66.5	143.8	1.1	2.1
HM22	6	-60.1	215.6	9.8	B	200	6	-65.5	206.2	7.3	85.6	-66.7	3.0	9.6	11.8
HM23	6	-52.9	205.5	13.0	C	100	6	-54.2	204.2	12.6	29.3	-70.2	37.9	12.4	17.7
HM24	6	-17.1	193.7	26.1	D	300	6	-21.6	191.3	25.5	7.8	-64.2	108.1	14.2	26.9
HM25	6	-41.3	201.0	34.5	D	200	6	-62.4	200.4	17.3	15.9	-72.0	8.8	21.1	27.0
HM17	5	12.0	320.7	75	Unstable										
HM18	6	49.0	344.3	66	Unstable										
HM19	5	20.3	245.8	85	Unstable										
HM26	6	-32.6	219.3	14.0	C	50	6	-39.8	220.9	14.6	22.0	-52.4	52.2	10.5	17.5
HM27	6	-47.0	217.5	30.0	C	100	6	-58.4	242.1	14.9	21.2	-41.2	20.0	16.3	22.0
HM28	6	7.0	185.2	58	Unstable										
HM29	6	69.9	284.0	116	Unstable										
HM30	6	14.6	152.7	64	Unstable										
HM33	6	-19.7	327.8	92	Unstable										
HM32	6	-73.2	291.0	29.9	Unstable										
HM33	6	-47.8	269.1	6.7	B	200	5	-51.5	266.1	7.4	108	-20.5	18.7	6.8	10.0

Juan Volcanics (Tanaka and Kono, 1973), while only 9 out of a total of 33 cooling units belong to these two superior classes in the present study.

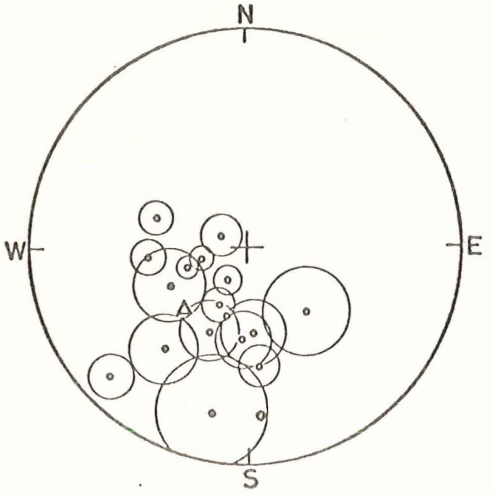

Fig. 1. Mean directions of stable components of NRM with 95 % confidence cones. Triangle indicates the NRM direction reported by Sasajima and Shimada (1965). Upper hemisphere of equal area projection.

Directions of stable components for Classes A-D cooling units are shown in Fig. 1 together with the cones of 95 % confidence (α_{95}). Although some units show large dispersion angles, which obscures the results, it is nevertheless clear that the directions are quite scattered so that their dispersion can hardly be attributable to ordinary paleosecular variation.

Fig. 2 illustrates the VGP's of Himeji Volcanics. Also shown in this figure are the Cretaceous and Paleogene poles determined from southwest Japan by Sasajima and Shimada (1965). The scatter of the VGP's is quite large as anticipated from Fig. 1, and it seems meaningless to calculate the mean VGP position for all the cooling units. The arrows connecting VGP's in Fig. 2 show the successive cooling units (from older to younger)

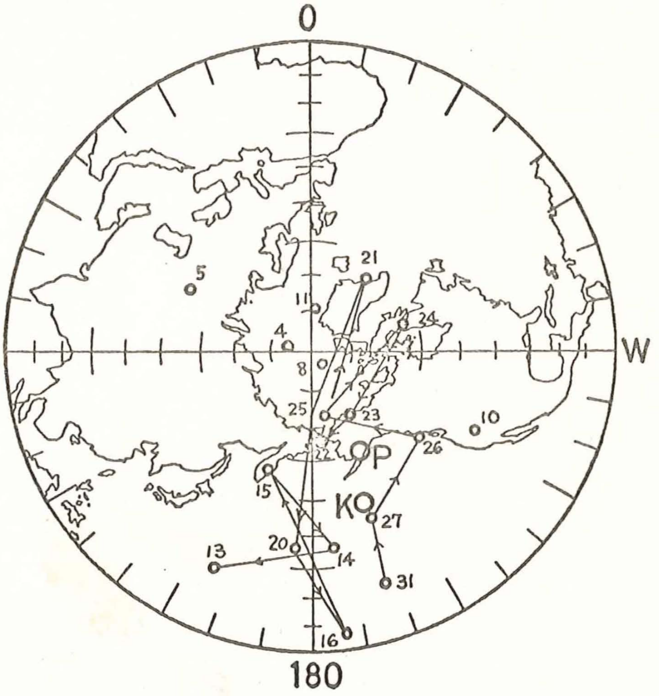

Fig. 3. VGP's for Himeji Volcanics. Those connected by arrows are for successive cooling units of Takidani sequence. Paleogene (P) and Cretaceous (K) poles from southwest Japan are after Sasajima and Shimada (1965).

in Takidani sequence. The movement of VGP shown by these arrows is more like that observed in geomagnetic reversals (Dunn et al., 1971) or in geomagnetic excursions (Doell, 1972) than ordinary secular variation. The meaning of the scatter of NRM directions and VGP's will be discussed later.

3. K-Ar Dating

Samples from seven cooling units were dated by K-Ar method. Samples for K-Ar dating was selected on the basis of minimum alteration of phenocrysts. However, a slight alteration of biotite was inevitable even in these samples.

Potassium content was determined by flame photometry. The error in K analyses is estimated to be less than 2%, based on the analytical error for the standard sample JB-1.

About three grams of total rock sample were used for argon extraction. Quantitative determination of radiogenic ^{40}Ar were carried out by isotope dilution method, using ^{38}Ar spike of about 10^{-6} ccSTP by means of a Reynolds-type mass spectrometer, with corrections for air contamination applied assuming $(^{40}\mathrm{Ar}/^{36}\mathrm{Ar})_{\mathrm{air}} = 295.5$ for the isotope ratio of Ar.

Results are shown in Table 2 and Fig. 3. In Table 2, samples are listed in the stratigraphic order.

Table 2. K-Ar Age Data

Sample	K	$\frac{(^{40}\mathrm{Ar})_{\mathrm{air}}}{(^{40}\mathrm{Ar})_{\mathrm{total}}}$	$(^{40}\mathrm{Ar})_{\mathrm{rad}}$	$\frac{(^{40}\mathrm{Ar})_{\mathrm{rad}}}{^{40}\mathrm{K}}$	Age
	%	%	$\times10^{-11}$mol/g	$\times 10^{-3}$	m.y.
HM 8-5	$\left.\begin{matrix}3.62\\3.64\end{matrix}\right\}3.63$	14.6	46.77	4.236	71.0
HM 2-C	$\left.\begin{matrix}2.65\\2.59\end{matrix}\right\}2.62$	70.4	21.53	2.700	45.6
HM13-4	$\left.\begin{matrix}3.56\\3.59\end{matrix}\right\}3.58$	26.9	43.37	3.981	66.8
HM16-4	$\left.\begin{matrix}2.77\\2.79\end{matrix}\right\}2.78$	27.9	36.39	4.301	72.1
HM18-B	$\left.\begin{matrix}0.65\\0.61\end{matrix}\right\}0.63$	67.7 42.1	6.477 6.137	3.378 3.201	56.9 53.9
HM23-1	$\left.\begin{matrix}3.48\\3.48\end{matrix}\right\}3.48$	12.2	44.71	4.222	70.8
HM30-3	$\left.\begin{matrix}2.79\\2.93\end{matrix}\right\}2.86$	17.6 14.4	37.83 34.31	4.346 3.942	72.9 66.2

$\lambda_e = 0.585\times10^{-10}\ \mathrm{yr}^{-1}$, $\lambda_\beta = 4.72\times10^{-10}\ \mathrm{yr}^{-1}$, $^{40}\mathrm{K/K} = 1.19\times10^{-4}$

4. Discussion

Stratigraphic relations of the sampled cooling units are shown in Fig. 3. Tenkadaiyama lavas and Ako Formation in Aioi sequence were sampled without clear relation among themselves, while in other sequences the cooling units appear one after another along roadcuts and stratigraphic positions of individual

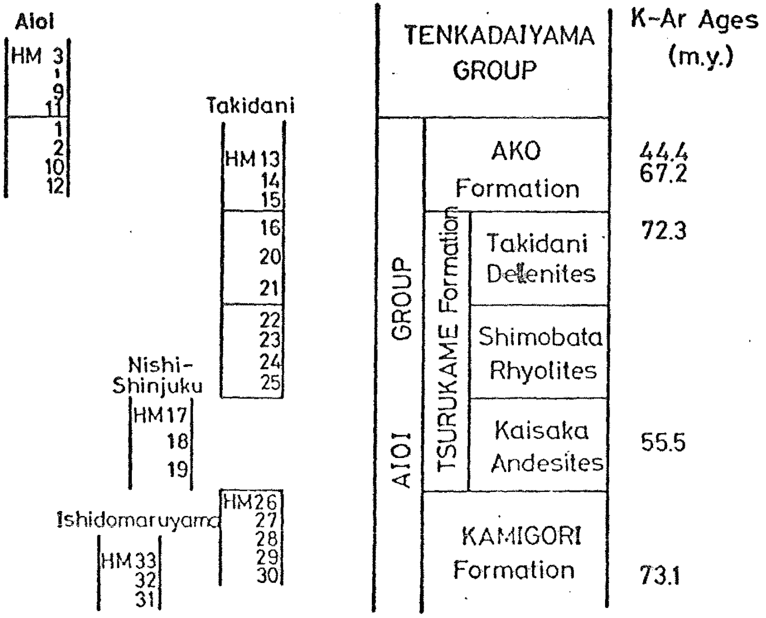

Fig. 3. Stratigraphic relations of sampled units after Kishida and Wadatsumi (1967). Part of the K-Ar age data are also shown.

units are unambiguously determined as shown in Fig. 3. The K-Ar ages, however, do not well fit in the stratigraphic order. As the degree of alteration of minerals are quite similar in all the dated samples (S. Aramaki, personal comm., 1974), we must seek for other reasons for the discordant ages in Table 2 and Fig. 3. One possible explanation may be that the younger ages of HM 2 and HM18 have bigger errors than other dates, because of higher air contamination or lower K content. If we disregard these data, we might conclude that the whole Aioi Group rocks were formed at about 70± 3 m.y.

Seki and Hayase (1974) recently reported ages of Himeji Volcanics by Rb-Sr method. They obtained a good whole rock/mineral isochron of 67.5 ± 5.9 m.y. for the Tenkadaiyama group. For the Aioi Group, five whole rock samples give an isochron of 105 ± 16 m.y., while mineral ages of about 70 m.y. are indicated. We may therefore conclude that the K-Ar ages and paleomagnetism of these rocks represent a short time interval about 70 m.y. ago. However, it is quite difficult to conclude at this stage whether NRM directions really represent a geomagnetic reversal or excursion.

References

Cox,A. and G.B.Dalrymple(1967) J. Geophys. Res. 72, 2603.
Doell,R.R.(1972) Geophys. J. 26, 459.
Dunn,J.R., M.Fuller, H.Ito and V.A.Schmidt(1971) Science 172,840.
Kishida,K. and K.Wadatsumi(1967) Prof. Shibata Commem. Pap. 241.
Kono,M.,H.Kinoshita and Y.Aoki(1972) J. Geomag. Geoelectr. 24, 49.
Larson,R.L. and W.C.Pitman(1972) Geol. Soc. Am. Bull. 83, 3645.
McElhinny,M.W. and P.J.Burek(1971) Nature 232, 98.
Nagata,T,S.Akimoto,Y.Shimizu,K.Kobayashi,H.Kuno(1959) Proc.Jap.Acad.
Sasajima,S. and M.Shimada(1965) Ann.Prog.Rept.Rock Mag.Japan 133.
Sasajima,S.,J.Nishida, M.Shimada(1968) Earth Planet.Sci.Lett. 5,135.
Seki,T. and I.Hayase(1974) Shitsuryo Bunseki 22, 55.
Tanaka,H. and M.Kono(1974) Rock Mag. Paleogeophys. 1, 71.

(to be submitted to J. Geomag. Geoelectr.)

REMANENT MAGNETIZATION OF IBARAGI GRANITIC COMPLEX

Hiroshi KANAYA and Kazuo NORITOMI

Geological Survey of Japan, 135 Hisamoto-cho Takatsu-ku Kawasaki-shi Kanagawa, Japan.

Institute of Mining Geology, Mining College, Akita University, Gakuen-cho 1-1, Tegata, Akita, Japan.

1, Introduction

The Ibaragi granitic complex of Cretaceous age is located in Osaka Prefecture of southwestern Japan. Ito (1963) had studied their natural remanent magnetization (NRM) on the samples collected from six points in the southwestern part of the complex, and reported the existence of normal, reverse and intermediate remanent magnetization. He attempted to make clear the displacement of geomagnetic pole but geological information of this complex was not sufficient.

Recently the granitic complex has been investigated in detail by many workers of Reserch Groupe of the Ibaragi granitic complex. In following the progress in the geological studies, the authors collected samples from more than fifty points for the study of natural remanent magnetization. Preliminary results will be given in this note.

2, Geological Setting

The geology of the Ibaragi granitic complex has been described in detail by Tainosho (1971). The complex intrudes into the Paleozoic formation consisting of sandstone with some shale, chert and volcanic rocks. The complex is divided into two units: the Nose pluton and the Myoken pluton. The former is approximately 5.5 by 10 Km in size and the latter has dimensions of 2 by 6.5 Km, both trending N 30°W.

Rb-Sr ages demonstrate two distinct stages; 96 m.y. for the Nose pluton and 78 m.y. for the Myoken pluton (Ishizaka, 1971). K-Ar ages are, however, 74 to 76 m.y. for both plutons (Shibata, 1971). The younger K-Ar ages of the Nose pluton is considered due to the heat effect of the later intrusion of the Myoken pluton.

The granitic rocks are petologically classified into four major types: 1) coarse to medium grained quartz diorite, 2) coarse grained granodiorite, 3) fine grained adamellite of Nose pluton, 4) fine to very fine grained adamellite of the Myoken pluton. The intrusive succession of the granitic rocks is considered in this order from 1 to 4. The generalized geological map of the granitic complex is shown in Figure 1.

3, Sampling and laboratory procedure

Oriented samples were collected at fifty-three sites in the Nose pluton. From a 6-7 Kg sample, three specimens were cut with a diamond drill in the laboratory. Each specimen has a diameter of 2.54 mm and height of 25.4 mm. Magnetization of specimens was measured by a Spinner magnetmeter.

4, Results and conclusion

The directions of NRM and remanent magnetization after A.C demagnetization are shown in Figure 2A and 2B on basis of rock types. The following conclusions were drawn:
1) The direction of quartz diorite samples are scattered. A.C demagnetization of 200 oe, their orientation converged but not as much as had been expected.
2) The normal and reverse directions of NRM on granodiorite samples are well grouped. Six samples collected near the margin show the direction of northeast to the present magnetic north and the remainder magnetized reverse. But three samples near the contact with quartz diorite revealed the different directions before and after the A.C demagnetization. After A.C demagnetization, much samples remained constant in their direction.
3) The directions of NRM on adamellite samples are grouped, but slightly scattered, and clockwise rotation of about 50° is seen to the granodiorite. After A.C demagnetization, two samples changed their direction to opposite side against the initial direction.

The scattering of the plots on quartz diorite may be explained by heat effect of later intrution such as could be caused the intrusions of the granodiorite or adamellite. Geological and chronological evidence support this interpretation. The difference in the directions between granodiorite and adamellite is rather difficult to explain. It may indicate the displacement of the geomagnetic pole during that time or the rotation of granodiorite and surroundings before the intrusion of adamellite. Geological reasoning for the latter interpretation is not clear, but further studies are necessary for the interpretation of the problem.

References

Ito, H. (1965) Paleomagnetic study on a granitic rock mass with normal and reverse natural remanent magnetization. J. Geomag. Geoelectr, 17, 113- 120.
Ishizaka, K. (1971) A Rb-Sr isotopic study of the Ibaragi granitic complex, Osaka, Japan. J. Geol. Soc. Japan 77, 731-740.
Shibata, K. (1971) K-Ar age of the Ibaragi granitic complex. Chikyu-Kagaku (Earth Science) 25, 306-356.

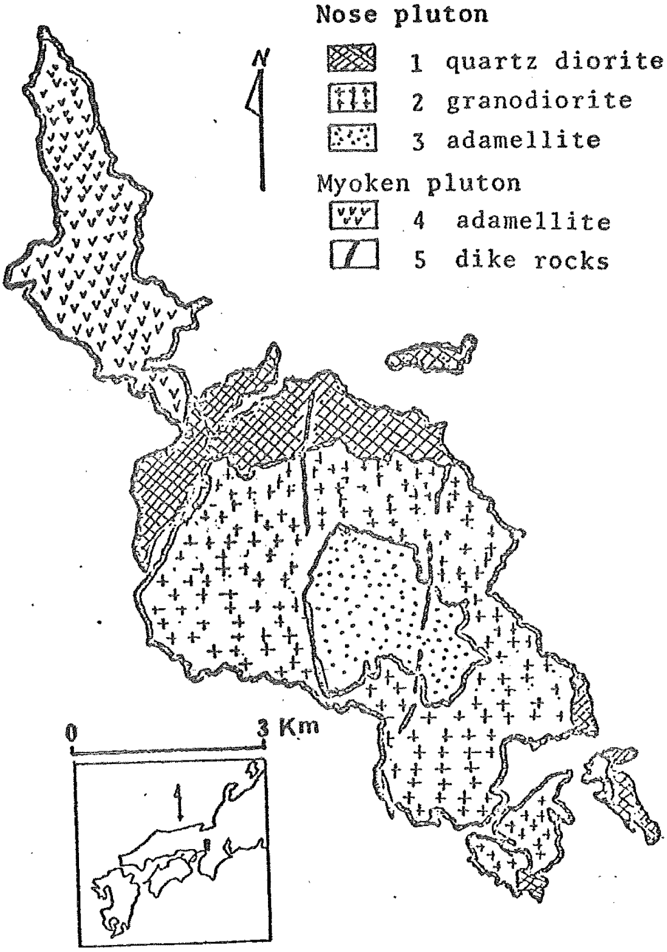

Fig. 1. Generalized geological map of the Ibaragi granitic complex.

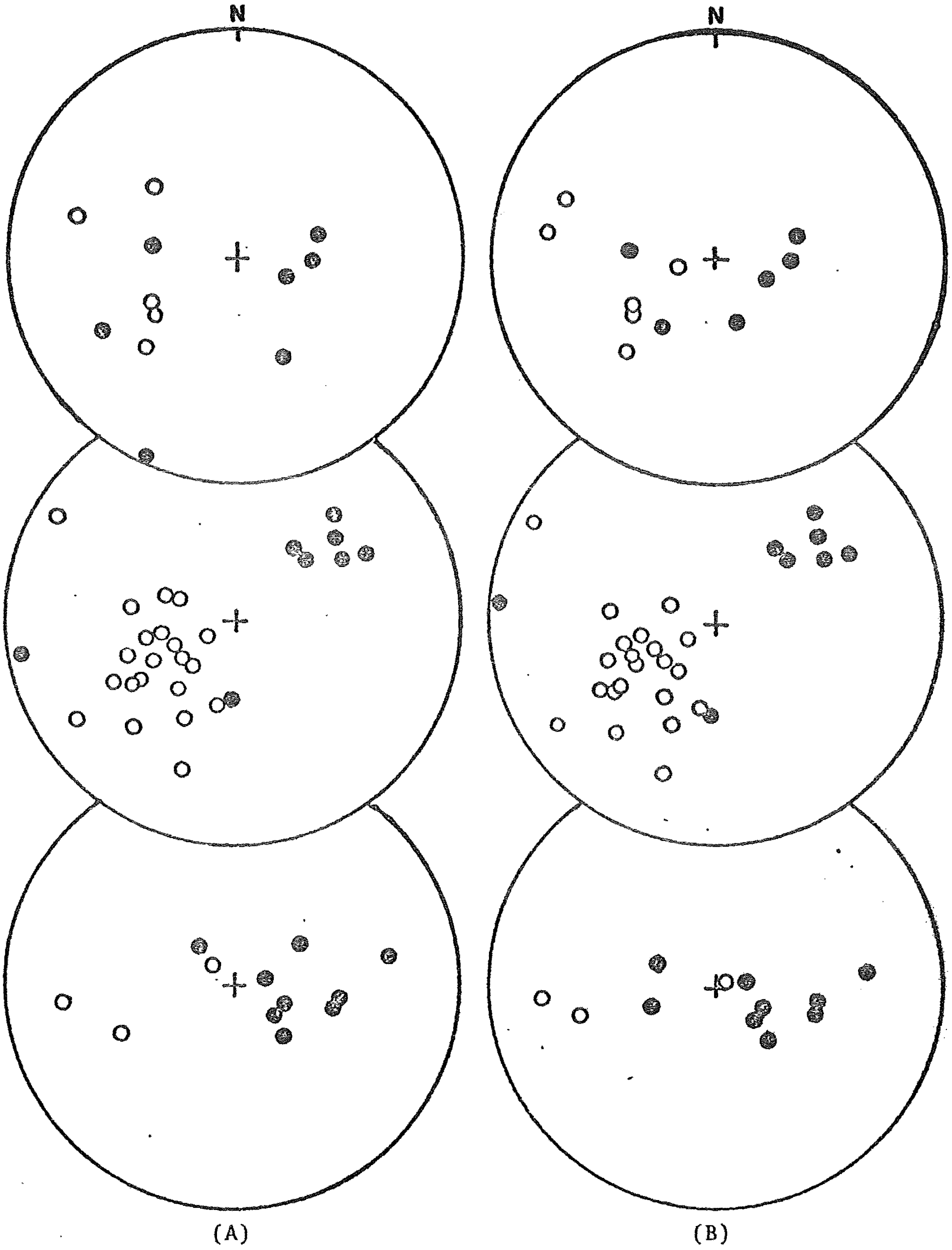

Fig. 2. Direction of NRM and of remanent magnetization after A.C demagnetization of 200 oe.
(A) Direction of NRM. upper; quartz diorite, middle; granodiorite, lower; adamellite.
(B) After demagnetization of 200 oe of each sample.
● lower hemisphere ○ upper hemisphere

TILTING OF HOKKAIDO ISLAND AND KITAKAMI MOUNTAINS DEDUCED FROM THE NRM OF CRETACEOUS GRANITIC ROCKS

Haruaki ITO and Katsuyasu TOKIEDA
Physics Department, Shimane University, Matsue, Japan

Oriented rock samples have been collected over a wide area of the Hokkaido Island and a part of northeast Japan. Collecting sites are shown in Fig.1. The rocks are mainly the upper Cretaceous in age and rock types are almost granitic intrusions ranging from dioritic to granitic. The NRM of samples is measured by a spinner magnetometer and is demagnetized in the alternating field of 100 oe and 200 oe. Results of measurements of the NRM are summarized in Table 1 and 2. Table 1 is data of samples with the stable NRM, which has a circle of confidence less than 20°. Table 2 is a list of sampling sites showing non or unstable NRM.

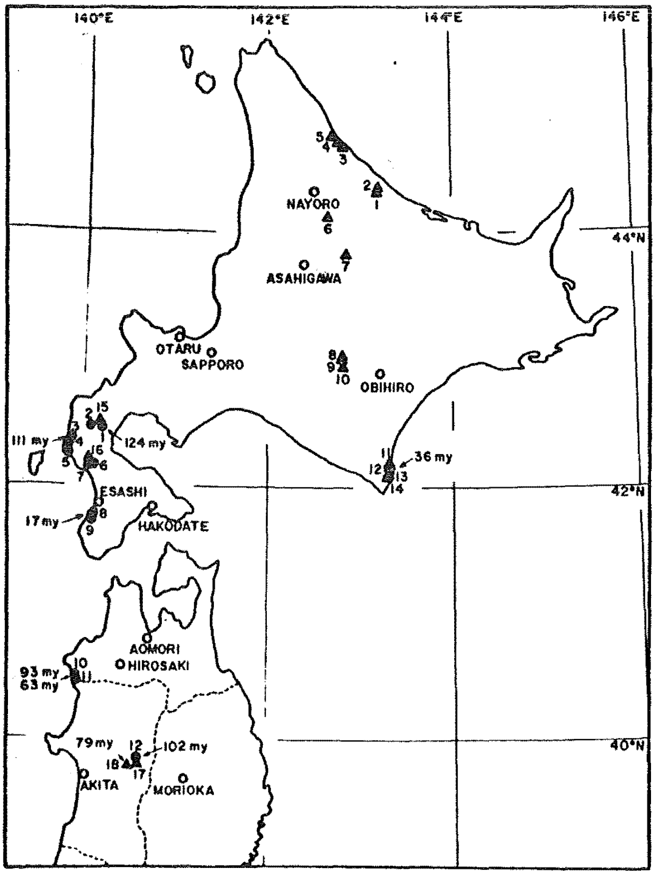

Fig.1 Sampling sites. Numbered solid circles represent the sites where samples with the stable NRM are collected. Triangles represent the sites where samples with non or unstable NRM are collected.

As seen in Table 1, the Cretaceous rocks in Hokkaido are normally magnetized and the direction of the NRM has been considerably deviated to the east. This result is strikingly different from that of the northeast Japan obtained by Kawai et al.(Kawai et al.,1971a). On the other hand, the age of granitic rocks in the southwestern part of Hokkaido seems to coincide with that of granitic rocks of Kitakami mountains in northeast Honshu (Kawano and Ueda,1967).

Recently Kawai et al.(1971b) pointed out that the Hokkaido Island has rotated clockwise relative to the main Island of Japan, from paleomagnetic studies of various kinds of rocks. Our result is likely to support the idea of the clockwise rotation of Hokkaido Island. However, when we give our attention to other areas of northeast Japan than the Kitakami mountains, we are able to find rocks with a remanent direction which is inconsistent with the paleomagnetic results from the Kitakami mountains.

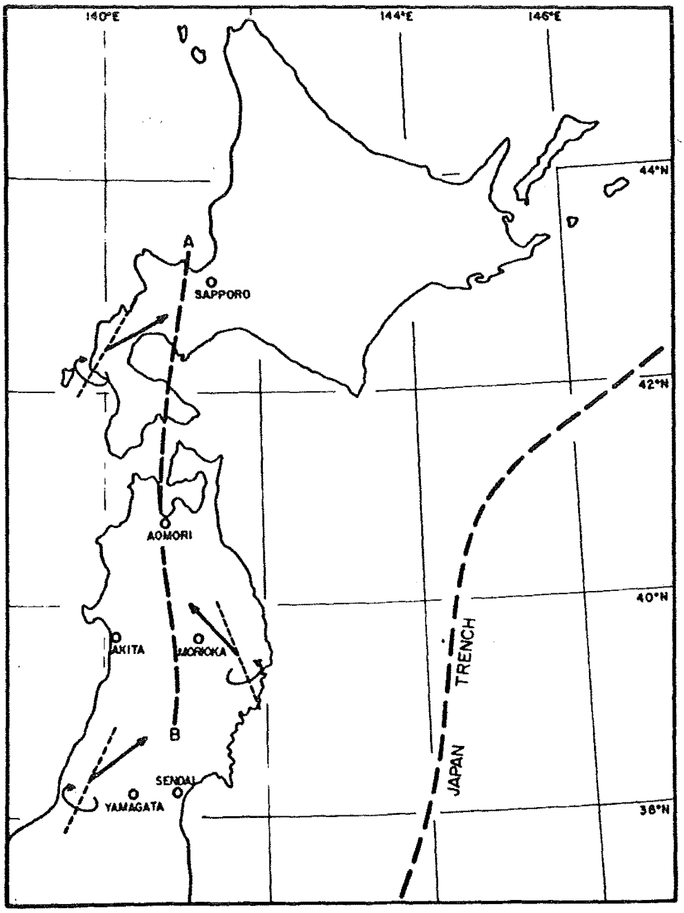

Fig.2 Tilting deformation of Hokkaido Island and northeast Japan inferred from the NRM

Assuming that a deviation of the NRM has been given rise to by any tilting of a rock body (Ito,1975), it is suggested that the difference in declination for the NRM of granitic rocks collected from the southwestern part of Hokkaido and for the present field is due to a tilting deformation of the Japanese Islands. The direction of the NRM estimated from Cretaceous granites at 14 sites in the Kitakami mountains (Kawai et al., 1971a) shows 42° in declination and +48° in inclination, and also that from 2 sites(71 and 85 my in age) in the Asahi mountains is 53° in declination and +32° in inclination (Kato and Muroi,1965). Provided that a rotation axis at each area was in the horizontal plane, each block of Hokkaido, Kitakami and Asahi mountains should be to have rotated about the dotted line as seen in Fig.2. This shows that the southwestern part of Hokkaido is to tilt to the west direction and the Kitakami mountains to the east. It is noticeable that the direction of the rotation axis of the Kitakami mountains is nearly parallel to that of "old" trench which is deduced from gravity anomalies (Tomoda and Segawa,1971). From these results and considerations, an anticlinal axis as AB in Fig.2 is introduced into the deformation of land mass deduced from the NRM direction of the Cretaceous granitic rocks.

References

Ito,H.(in press): On an interpretation of the direction of natural remanent magnetization,Mem.Fac.Lit.Sci.Shimane Univ.Nat.Sci.,8

Kawai,N., T.Nakajima and K.Hirooka(1971): The evolution of the Island arc of Japan and the formation of granites in the Circum-Pacific belt,J.Geomag.Geoelect.,Vol.23,267-293

Kawai,N., T.Nakajima, M.Torii, K.Hirooka and K.Yaskawa(1971): On a possible land block movement of Hokkaido relative to the main Island of Japan,J.Geomag.Geoelect.,Vol.23,243-248

Kawano,Y. and Y.Ueda(1971): K-Ar dating on the igneous rocks in Japan(VI) - Granitic rocks,summary -,J.Jap.Asoc.Min. Petr.Econ.Geol.,Vol.57,177-187

Tomoda,Y. and J.Segawa(1971): Gravity anomalies in the adjacent seas of Japan,Kagaku,Vol.41,68-74,(in Japanese)

Kato,Y. and I.Muroi(1965): Paleomagnetic studies of the Cretaceous granitic rocks in northeastern Japan,Ann.Progr. Rept.Rock Magnetism Res.Group Japan,179-187

Table 1

	Locality	φ	λ	N	Rock kind	Age	D	I	Jn	Θ	K
1	Mirika	42°27'	140°11'	5	Granodiorite	124 my	293°	+36°	$4.32x10^{-6}$	11.7°	43.5
2	Imagane	42°28'	140°05'	5	Granodiorite	Cretaceous	38°	+50°	$6.83x10^{-6}$	10.1°	58.4
3	Udomari	42°21'	139°47'	5	Granodiorite	111 my	41°	+68°	$3.21x10^{-5}$	14.7°	28.2
4	Udomari	42°21'	139°47'	5	Granodiorite	111 my	70°	+62°	$4.80x10^{-5}$	18.5°	18.1
5	Kudo	42°14'	139°47'	5	Granodiorite	Cretaceous	65°	+30°	$8.96x10^{-6}$	9.2°	70.1
6	Kenichi-gawa	42°10'	140°03'	4	Granodiorite	Cretaceous	82°	+55°	$5.52x10^{-6}$	10.0°	85.5
7	Kenichi-gawa	42°09'	140°03'	5	Granodiorite	Cretaceous	71°	+54°	$5.72x10^{-6}$	8.3°	85.7
8	Kaminokuni	41°42'	140°02'	5	Quartz Diorite	17 my	199°	-10°	$2.54x10^{-5}$	2.0°	1538.5
9	Kaminokuni	41°42'	140°02'	5	Quartz Diorite	17 my	339°	+42°	$2.76x10^{-4}$	6.4°	141.3
10	Mokurenji	40°27'	139°57'	5	Granodiorite	93 my	90°	+76°	$1.67x10^{-5}$	19.5°	16.4
11	Mokurenji	40°27'	139°57'	5	Granodiorite	93 my	343°	+21°	$4.16x10^{-6}$	8.2°	88.3
12	Tazawako	39°47'	140°39'	5	Granodiorite	102 my	325°	+64°	$1.40x10^{-5}$	18.0°	18.8

φ: Present latitude of sampling site
λ: Present longitude of sampling site
N: Number of specimens
D: Declination of NRM_{100}
I: Inclination of NRM_{100}
Jn: Intensity of NRM_{100} (emu/cc)
Θ: Radius of 95 percent circle of confidence
K: Fisher's precision factor

Table 2

	Locality	ϕ	λ	Rock kind	Age	Jn
1	Okoppe	44°20'	143°07'	Granite	Cretaceous	$1.43x10^{-5}$
2	Okoppe	44°22'	143°06'	Granite	Cretaceous	$< 1.41x10^{-6}$
3	Esashi	44°44'	142°47'	Granite	Cretaceous	-
4	Esashi	44°44'	142°46'	Granite	Cretaceous	-
5	Esashi	44°48'	142°42'	Granite	Cretaceous	-
6	Okushibetsu	44°08'	142°39'	Granite	Cretaceous	$< 1.00x10^{-7}$
7	Sounkyo	43°49'	142°52'	Granite	Cretaceous	$3.93x10^{-6}$
8	Karikachi-toge	43°08'	142°46'	Granite	Cretaceous	$< 1.10x10^{-6}$
9	Karikachi-toge	43°09'	142°46'	Granite	Cretaceous	-
10	Shimizu	42°58'	142°48'	Granite	Cretaceous	-
11	Erimo-misaki	42°11'	143°20'	Granite	33 my	$6.20x10^{-7}$
12	Erimo-misaki	42°11'	143°20'	Granite	33 my	$7.65x10^{-6}$
13	Erimo-misaki	42°11'	143°20'	Granite	33 my	$< 2.00x10^{-6}$
14	Erimo-misaki	42°10'	143°19'	Granite	33 my	$< 1.00x10^{-7}$
15	Mirika	42°30'	140°11'	Granodiorite	124 my	$< 1.00x10^{-7}$
16	Kenichi-gawa	42°10'	140°03'	Granodiorite	Cretaceous	$4.86x10^{-6}$
17	Tazawako	39°47'	140°39'	Granodiorite	102 my	$1.54x10^{-5}$
18	Tazawako	39°47'	140°36'	Granite	79 my	$3.63x10^{-5}$

ϕ: Present latitude of sampling site

λ: Present longitude of sampling site

Jn: Intensity of NRM_{100} (emu/cc)

PALEOMAGNETISM OF CRETACEOUS GRANITES IN SOUTH KOREA

Haruaki ITO and Katsutasu TOKIEDA
Physics Department, Shimane University, Matsue, Japan

Isotope ages of granitic rocks obtained so far in Korea were compiled and published by Section of Mineralogy, Geological Survey of Korea, in 1972. We mainly collected samples of Cretaceous granitic rocks in south Korea to examine a geomagnetic reversal pattern during the Cretaceous and to estimate a relative block movement with the Japanese Islands. Oriented hand samples have been collected from 13 sites in granitic rocks without the gneissore or shistore. The initial directions of the NRM of samples were slightly scattered. However, after demagnetization to 100 oe, the directions were well grouped around a point which may be an original direction of the remanent magnetization. The mean directions of the NRM after demagnetization of 100 oe are shown in Fig.1 and data of measurements are summarized in Table 1. Curie point determinations demonstrated that the dominant magnetic phase was a magnetite in stable samples investigated.

Declinations of the mean direction of the NRM at each sampling site are shown in Fig.2. Samples with the stable NRM are normally magnetized in all and the directions of remanent magnetization deviate slightly from the present field direction (6.5° west in declination and 51° in inclination at Daegu) to the east. This result is different from the NRM directions obtained from the Cretaceous rocks in southwest Japan(Kawai et al.,1971). This fact may show that the Japanese Islands have moved relative to the land mass of Korea.

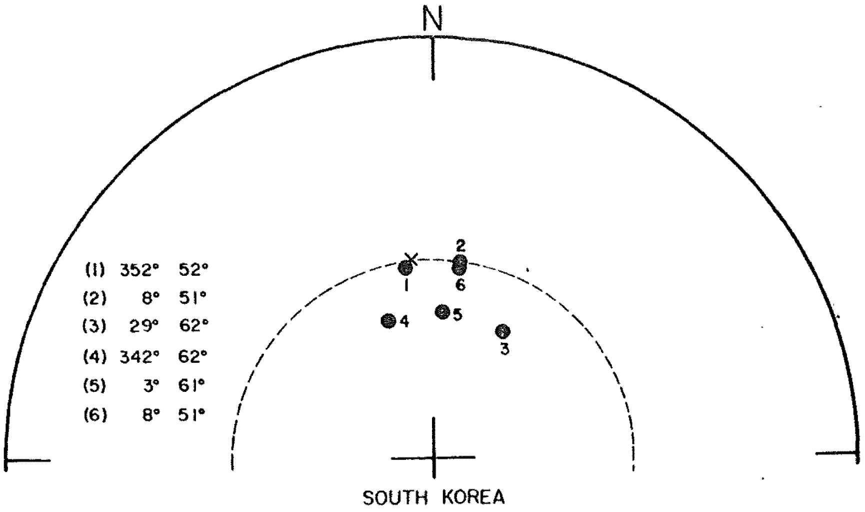

Fig.1 Mean directions of the NRM at each sampling site after demagnetization of 100 oe. The number represents the sites shown in Table 1.

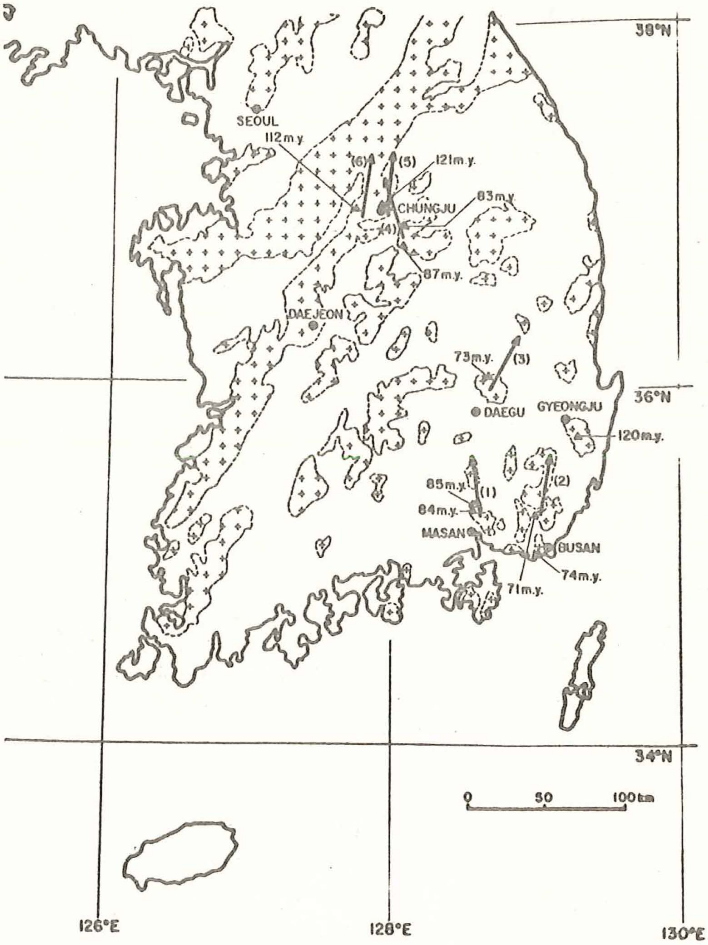

Fig.2 Geological map in south Korea. Sampling sites and mean declinations of the NRM of samples collected are shown by numbered arrows.

Geological Survey of Korea(1972): Isotope ages and geological map of Korea,1972.7.

Kawai,N.,T.Nakajima and K.Hirooka(1971): The evolution of the Island arc of Japan and the formation of granites in the Circum-Pacific belt,J.Geomag.Geoelect.,Vol.23,267-293

Table 1

	Locality	ϕ	λ	N	Rock kind	Age	D	I	Jn	Θ	K
1	Masan	35°16'	128°38'	10	Granite	84.8 my	352°	+52°	$1.52x10^{-4}$	4.7°	105.2
2	Yangsan	35°18'	129°05'	10	Granite	Cretaceous	8°	+51°	$1.90x10^{-5}$	10.0°	24.5
3	Daegu	35°57'	128°44'	5	Granite	73 my	29°	+62°	$6.42x10^{-5}$	11.1°	48.0
4	Yeonpung	36°47'	128°56'	5	Granite	87.8 my	342°	+62°	$3.85x10^{-6}$	13.5°	32.9
5	Chungju	36°56'	127°56'	5	Granite	121 my	3°	+61°	$4.45x10^{-6}$	8.7°	78.6
6	Eumseong	36°52'	127°38'	10	Granite	153-163 my	8°	+51°	$1.51x10^{-6}$	6.9°	46.6

ϕ: Present latitude of sampling site
λ: Present longitude of sampling site
N: Number of specimens
D: Declination of NRM_{100}
I: Inclination of NRM_{100}
Jn: Intensity of NRM_{100} (emu/cc)
Θ: Radius of 95 percent circle of confidence
K: Fisher's precision factor

A PRELIMINARY EXPERIMENT ON QUANTITATIVE DETERMINATION OF NOBLE GASES WITH A QUADRUPOLE TYPE MASS SPECTROMETER

Osamu MATSUBAYASHI, Minoru OZIMA, and Ichiro KANEOKA

Geophysical Institute, University of Tokyo, Bunkyo-ku, Tokyo 113, Japan.

1. Introduction

Recently several workers (Mazor and Fournier 1973, Fisher 1970, and others) have been searching for the noble gases representative of the earth's deep interior. Fisher (1974) have reported that the noble gas abundance pattern in the glassy margin of some submarine basalts resembles to 'planetary primordial' type observed in meteorites. On the other hand Dymond and Hogan (1973) have observed the noble gas abundance pattern of 'solar primordial' type in glassy tholeiites. They noted that neon is much more abundant than is expected in a rock equilibrated with seawater. Hence it is very important to examine further the noble gas abundance pattern in the deep-sea basalts which may be indicative of the mantle noble gas composition, because such information would be very vital to understand an atmospheric evolution process. In addition, the study may reveal various elementary processes of noble gases acting on the deep-sea basalts, such as incorporation of noble gases in solidifying silicate melt under the deep sea condition, secondary effects by seawter, the noble gas inventory in the sea, and so on. (Dymond and Hogan 1974). For these purposes we have installed a quadrupole type mass spectrometer Type MSQ-500 of ULVAC Corporation. Although the quadrupole type mass spectrometer has relatively high sensitivity, suitability of such an instrument for the quantitative determination of a trace amount of noble gases has not been fully explored. In the present short note, we report a preliminary experimental result on the reliability of quantitative analyses of noble gases with a quadrupole type mass spectrometer.

2. Instruments and procedure

The quadrupole type mass spectrometer is equipped with a channeltron electron multiplier and a conventional D.C. amplifier as an ion detecting system. The spectrometer is evacuated with an ion pump and a titanium getter pump, which enable us to obtain a pressure as low as 10^{-9} torr. Pressure rise in a static condition after an hour is no more than 10^{-8} torr. The lowest detectability for noble gases is about 10^{-12} cm^{3}STP for Xe, Kr, and ^{22}Ne, and is about 10^{-8} cm^{3}STP for ^{40}Ar. The detectability of Ar is mainly limited by the background component, whereas the limits of Xe, Kr, and ^{22}Ne are imposed by the noise in the electronic system. In the case of He, reliability of quantitative analyses is questionable, especially for smaller amount ($\lesssim 10^{-8}$ cm^{3}STP), owing to diffusion through glass walls of the present system.

The extraction-purification system is usually baked at about 300°C for several hours and a pressure of less than 10^{-7} torr can be attained. The sample gases are cleaned on a hot Ti sponge held at about 900°C. The purified heavy noble gases (Ar, Kr, and Xe) are kept on the charcoal at the liquid nitrogen temperature and the remaining fraction (He and Ne) is introduced into the spectrometer for the analysis. After the He-Ne fraction was evacuated, the heavy noble gases are released from the charcoal by warming it at boiling water temperature.

3. Calibration of atmospheric noble gases

Quantitative analyses of noble gases in air of about $5x10^{-3}$ cm^3STP were repeated to examine the reproducibility of the measurements over the period of four months. The results are shown in Table 1. The reproducibility of Xe measurements is rather poor since relatively large memory obscured the results. In the later analyses, however, the background in Xe was considerably reduced and the reproducibility became much better.

Table 1. The reproducibility of measurements of the same amount of noble gases in the air over the period of four months.

isotopes	^{4}He	^{22}Ne	^{36}Ar	^{40}Ar	^{84}Kr	^{132}Xe
amounts in cm^3STP (mean of 5 analyses)	$2.6 x10^{-8}$	$7.9 x10^{-9}$	$1.6 x10^{-7}$	$4.6 x10^{-5}$	$2.8 x10^{-9}$	$1.1 x10^{-10}$
1 sigma error	19%	15%	13%	14%	19%	50%

To construct a calibration curve of the sensitivity, the initial gas obtained by purifying the air sample was successively divided into smaller volumes by means of a pipet system. The smallest volume after the fourth pipeting was about $5x10^{-8}$ cm^3STP, which should contain about 0.04, 0.5, 4600, 9, and $2.6x10^{-11}$ cm^3 STP of Xe, Kr, Ar, Ne, and He respectively. Fig.1 shows the calibration curves for noble gas isotopes ^{40}Ar, ^{4}He, ^{22}Ne, ^{84}Kr, and ^{132}Xe in the air sample. For the quantitative determination of neon, ^{22}Ne is suitable because the interference of doubly-charged Ar becomes severe for ^{20}Ne. The solid lines in the figure represent theoretical ones for the successive pipeting. Reproducibility becomes worse for the smaller volumes due to the background. Since the amount of noble gases in submarine basalts (one gram) generally covered by the range for which the calibration was made (see Fig.1.), we can safely estimate an error in an anlysis of a rock sample on the basis of these calibration curves. The largest error, which is usually seen for the smallest volume, amounts to a factor of two. Since the difference in the relative abundance of noble gases between the 'primordial noble gas'component in meteorites and the terrestrial one is more than an order of magnitude, reproducibility in the present instrument is good enough to resolve the two compositions.

4.Examination of blanks

Before an analysis of a rock sample, hot blank was examined. The temperature and the time of heating of the crucible were the same as those for the actual analysis of the basaltic rock sample, about 1200°C and 20 min.. It has been revealed that the blank of Ne is always high and almost comparable to the amount of Ne in basaltic rocks. A large fraction of the Ne blank seems to originate from the hot Ti sponge, in spite of repeated outgassing at a

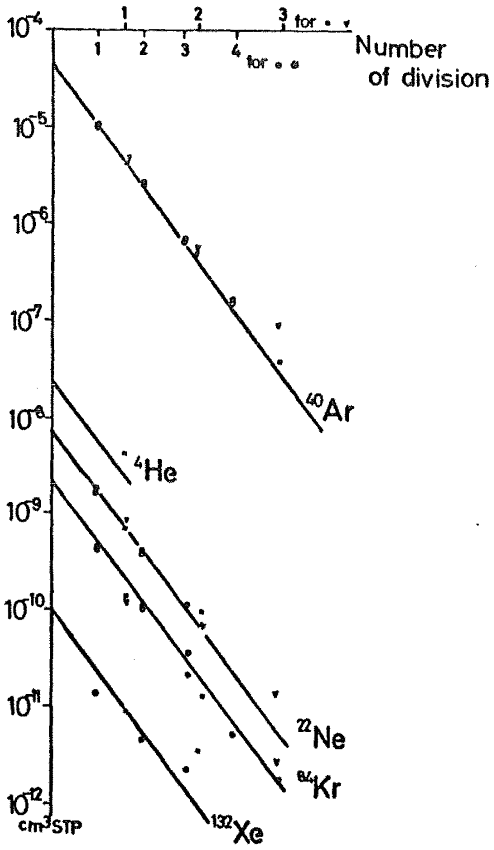

Fig. 1. Calibration curves of atmospheric noble gases.

The ordinate indicates the value measured with the mass spectrometer by peak height comparison, and the abscissa the number of division. Analyses were made on Jul. 26(open circle), Aug.3(cross),Sep. 18(solid circle),and Oct.16(v) 1974.

higher temperature (~1200°C). As seen in Table 2, the blank of other noble gases were no more than 15 percent of those evolved from a basaltic rock of one gram. In Table 2 the cold blank is also included. The cold blank means here that the procedure is the same as an actual analysis of basalt except that Ti furnace and Mo crucible are kept at room temperature.

Table 2. Typical hot and cold blanks in cm³STP (see the text).

isotopes	^{4}He	^{22}Ne	^{36}Ar	^{40}Ar	^{84}Kr	^{132}Xe
hot blank	1x10^{-8}	2 x10^{-10}	1.5 x10^{-9}	4 x10^{-7}	1 x10^{-11}	1 x10^{-12}
cold blank	8x10^{-9}	8 x10^{-12}	9 x10^{-11}	1.6 x10^{-8}	$\lesssim 10^{-12}$	$\lesssim 10^{-12}$

5. Summary

The quadrupole type mass spectrometer may be a powerful tool to study the noble gas abundance pattern in submarine basalts. The blank level in the present extraction-purification system seems to be good enough to do such analyses except for Ne. It is an urgent problem to be solved that we should reduce the amount of Ne blank. Then we can approach the problem of noble gases in the earth's deep interior.

References

Dymond, J. and L. Hogan (1973) Earth Planet. Sci. Letters 20, 131.
Dymond, J. and L. Hogan (1974) J. Geophys. Res. 79, 877.
Fisher, D.E. (1970) Earth Planet. Sci. Letters 9, 331.
Fisher, D.E. (1974) Geophys. Res. Letters 1, 161.
Mazor, E. and R.O. Fournier (1973) Geochim. Cosmochim. Acta 37, 515.

Sr ISOTOPIC STUDIES OF VOLCANIC ROCKS FROM THE ISLAND ARC IN THE WESTERN PACIFIC

Jun-ichi Matsuda, Sigeo Zashu, and Minoru Ozima

Geophysical Institute, University of Tokyo
Bunkyo-ku, Tokyo 113, Japan

1. Introduction

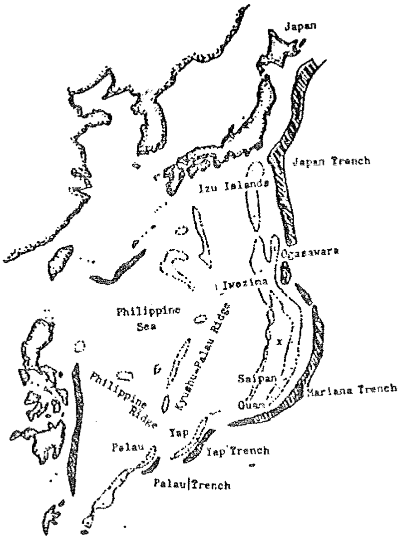

fig.1

The island groups from Izu to Palau which are separated from the Asian continent by the marginal basin of the Philippine Sea, are chiefly composed of volcanic rocks of predominantly andesitic composition and limestones, whose ages range from the Eocene to Recent (Shiraki, 1971). Karig (1971; 1971) discussed the origin and development of these areas that oceanic basins behind the island arcs are extentional in origin and new oceanic crust is being formed behind volcanic arc. The dredged samples from the inter-arc basin (Mariana trough) showed the similar characteristics to those of the mid-ocean spreading ridge basalts (Hart, 1970; Hart et al., 1972). The ($^{87}Sr/^{86}Sr$) ratios of ridge basalts range from 0.7010 to 0.7030 having a mean value of 0.7026, whereas ($^{87}Sr/^{86}Sr$) ratios of oceanic-island and island arc basalts range from 0.7030 to 0.7060 with a mean value of 0.7038 (Peterman & Hedge, 1971). Ridge basalts are more depleted in trace elements than oceanic island basalts. The depletion is larger for elements with larger ionic radius, resulting in high K/Rb ratios (Engel et al., 1965; Gast, 1968). Therefore, ridge basalts are distinguished from island arc and oceanic island basalts by their low ($^{87}Sr/^{86}Sr$) ratios and high K/Rb ratios. The Mariana trough basalts showed low ($^{87}Sr/^{86}Sr$) ratio $<$ 0.7030 and their results seem to support the Karig's hypothesis. In this paper the systematic measurements of ($^{87}Sr/^{86}Sr$) ratios of the rocks from Izu, Ogasawara, Iwojima, Mariana, Yap, and Palau Islands are reported (Fig. 1).

2. Samples

The rock types of the samples are shown in table 1. Most of these samples are volcanic rocks, though the sample from

Yap Islands is a greenshist. The Yap Islands occupies a unique geological position having exposures of pre-Tertialy metamorphic basement (Shiraki, 1971). Volcanic rocks from the other islands have ages ranging from Eocene to Recent. The K-Ar ages forsome samples are in table 1 (Kaneoka et al., 1970).

table 1

sample		rock type	K-Ar age (m.y.)*
Oshima	56091919	Hypersthene-bearing augite andesite	≲0.42
	56093015D	Pyroxene quartz diorite	< 2.14
	NI60030903b	Non-porphyritic basalt	< 2.41
Kozu-shima	NI60071803	Altered ryolite	0.28
Hachijo-jima	NI55071806	OlivineOhypersthene-augite gabbro	2.12
	NI67091704	Ferrohypersthene-ferropigeonite-ferroaugite	<0.14
Chichi-jima	R382	Augite-hypersthene andesite	26.0
Haha-jima	NI69021002	Augite-orthopyroxene andesite	39.3, 41.4
Iwo-jima	NI69021002	Augite-olivine trachyandesite	0.03
Saipan	131B5	Dacite flow	
	7141D	Porphiritic andesite	
Guam	1-7	Fine grained basalt	
	2-4		
Yap		Greenshist	
Palau	1	Olivine-augite basalt	
	6-A	Dike basalt	
	12	Flow basalt	
	14	Dike basalt	

*(Kaneoka et al., 1970)

3. Results

The results are listed (table 2). The error in ($^{87}Sr/^{86}Sr$) ratio indicates the difference from the mean value for the repeated analyses. The mean value were normalized to 0.7080 for the Eimer and Amend standard sample. Using the Rb/Sr ratio and the K-Ar age (in the case of weathered sample, fossil age - 50 m.y. were assigned),.we calculate the initial ($^{87}Sr/^{86}Sr$) ratios. However, the difference between the measured ($^{87}Sr/^{86}Sr$) ratio and the initial ($^{87}Sr/^{86}Sr$) ratio were almost negligible for all samples, because of the low Rb/Sr ratio and the relatively young age of the sample. For comparisonwe also list the average value for the Mariana trough basalt in table 2 obtained by another authors (Hart et al., 1972).

table 2

sample		$^{87}Sr/^{86}Sr$	K	Rb	Sr	K/Rb	$(^{87}Sr/^{86}Sr)_0$
O-shima	56091919	0.7039±2	2820				
	5609315D	0.7033±1	5030	12.8	204	393	0.7033±1
	NI6003093b	0.7034±2	2660				

sample		$^{87}Sr/^{86}Sr$	K	Rb	Sr	K/Rb	$(^{87}Sr/^{86}Sr)_0$
Kozu-shima	NI60071803	0.7032±2	56700	85.6	51	662	0.7032±2
Hachijo-zima	NI55071806	0.7032±5	5250	2.09	170	2512	0.7032±5
	NI67091704	0.7034±3	3900	8.80	250	443	0.7034±3
Chichi-zima	R382	0.7054±4	10800	24.3	115	443	0.7052±4
Haha-zima	NI69021002	0.7040±3	16300	25.6	192	637	0.7038±3
Iwo-jima	NI68082304	0.7039±1	36100	83.2	440	434	0.7039±1
Saipan	131B5	0.7041±3	12200	8.25	229	1479	0.7040±3
	7141D	0.7040±3	5900	8.04	215	734	0.7040±3
Guam	1-7	0.7037±2	4700	10.04	447	468	0.7037±2
	2-4	0.7038±4	6720	12.00	510	560	0.7038±4
Yap		0.7029±1	2460	0.42	557	5857	0.7029±1
Palau	1	0.7030±1	2700	2.28	206	1184	0.7030±1
	6-A	0.7025±2	3820	8.29	194	461	0.7024±2
	12	0.7032±1	5630	8.41	177	669	0.7031±1
	14	0.7026±3	4850	5.60	239	866	0.7026±3
Mariana trough* (mean)		0.7028±1	3547	4.51	186	786	0.7028±1

*(Hart, et al., 1972)

4. Discussions

The $(^{87}Sr/^{86}Sr)$ ratios of volcanic rocks from island arc areas have been studied by several investigators. Dickinson (1970) showed that Sr isotope ratios in 75 comagmatic basalts, andesites and dacites from central America, the Cascade, the Marianas, Japan, and New Britain are all in the range of 0.7038±0.0010. Nineteen lavas collected from Saipan, North Mariana, Ogasawara, and Izu Islands have initial $(^{87}Sr/^{86}Sr)$ ratios ranging from 0.703 to 0.705 (Pushkar, 1968), which are similar to the value for Hawaian basalt. Dickinson concluded on the basis of the narrow range in $(^{87}Sr/^{86}Sr)$ ratios that all these lavas had been derived from a source uniform in its $(^{87}Sr/^{86}Sr)$ ratio, such as the upper mantle or the oceanic third layer. Hedge (1966) had observed similar ratios in volcanic rocks from the Mariana Islands.

Our results from O-shima, and Mariana Island are all within a range of 0.7030 ~ 0.7050, which agree with the results of previous authors. However, a somewhat high ratio is obtained for the rock from Chichi-jima of Ogasawara Islands. Pushkar (1968) also reported high ratios for two lavas from Ogasawara Islands. However, since he did not give aging correction for these two samples, it is difficult to evaluate the significance of the results. Our results show that Rb/Sr ratios from Ogasawara Islands are much larger than those from other islands. Rb contents are more than two or three times of those from other islands. However, change in the $(^{87}Sr/^{86}Sr)$ ratio due to an aging effect is almost negligible because of the young age of the sample. Hence, we conclude that the rocks of Ogasawara Islands had high initial $(^{87}Sr/^{86}Sr)$ ratio.

These results indicate that the source material for basalts in Ogasawara Island must be different from those for other islands.

On the other hand, the rocks from Palau Islands show low ($^{87}Sr/^{86}Sr$) ratios. Such low ($^{87}Sr/^{86}Sr$) ratios were also obtained for the dredged sample from Mariana basin (Hart et al., 1972). As stated in precious section, oceanic ridge basalts are characterized by both low ($^{87}Sr/^{86}Sr$) ratio and high K/Rb ratio. In fig. 2 ($^{87}Sr/^{86}Sr$) ratios are plotted against K/Rb ratios. The results for rocks from the Palau Islands show the same characteristics on this diagram as the Mariana basin basalts. Though their K/Rb ratios are in the lower part of the depleted ridge basalts field, the low ($^{87}Sr/^{86}Sr$) ratios are clearly distinguished from those for the volcanic rocks from island arcs. Hence, we may conclude that Palau Islands have also been derived from a similar mantle as that of the mid-ocean spreading ridge basalts.

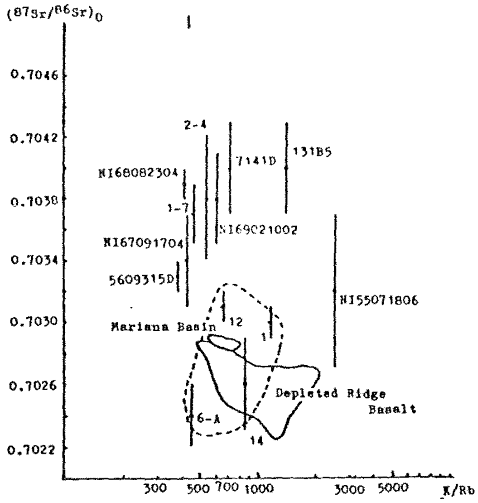

fig.2

The volcanic rocks from island arc have generally a wide spread in K/Rb ratios ranging from 150 to 1000 (Jakes & White, 1970). Meanwhile, the K/Rb ratios of mid-ocean spreading ridge basalts range over higher value (400 - 2000) (Kay et al., 1970). The K/Rb ratio for Palau are in the common range for these two basalt types. As the K/Rb ratios show such a wide range in both kinds of volcanic rocks, they cannot be a clue to identify a type of a mantle under the Palau Islands. With respect to Rb and Sr contents, the volcanic rocks from Palau Islands resemble those for tholeiite from the island arc. According to Jakes and White (1972), tholeiite with low SiO_2 from island arc have an average Rb content of 5 ppm, which is almost twice as high as that of abyssal tholeiite. The average Rb and Sr contents in rocks from the Palau Islands are about 6 ppm and 204 ppm respectively, which are also much higher than those in abyssal tholeiite.

Summarizing rocks from Palau Islands are characterized by low ($^{87}Sr/^{86}Sr$) ratio similar to oceanic ridge basalts, whereas their Rb and Sr contents are much higher than the latter, falling in ranges for island arc tholeiite.

As to the Yap Islands, the low ($^{87}Sr/^{86}Sr$) ratio implies that the rocks from the Yap Islands are of oceanic origin. It supports the results obtained from the chemical composition of rocks by Shiraki (1971).

5. Conclusion

Recently the discovery of the extinct "Philippine Ridge" which has symmetrical magnetic lineation patterns seems to complicate the problem of the origin of Philippine Sea (Ben Avraham et al., 1972). The extinct Philippine Ridge lies in the west of the Kyushu-Palau Ridge and its lateral direction is not parallel to the Kyushu-Palau Ridge (fig. 1). It seems to be difficult to explain the western Philippine Basin on the basis of extentional opening model proposed by Karig (1971; 1971). To solve these difficulties, other hypotheses were proposed (Uyeda & Ben-Avraham, 1972; Uyeda & Miyashiro, 1974). All these hypotheses assume that Ogasawara and Mariana arcs were originally part of the Kyushu-Palau "island arc".

However, results of the present study seems to suggest that mantle materials which produced volcanic rocks in Yap and Palau Islands are different from that produced rocks in Izu, Ogasawara, and Mariana Islands. Moreover, the mantle under Iwo-jima and Ogasawara Islands also seem to be different. Hence, we would like to emphasize that simple extentional models suggested by previous authors is unlikely to explain development of island arcs in the Western Pacific.

References

Ben-Avraham, Z., Bowin, C., Segawa, J., (1972) Nature 240, 453
Dickinson, W.R., (1970) Rev. Geophys. Space Phys. 8. 813
Engel, A.E.J., Engel, C.G., Havens, R.G., (1965) Geol. Soc. Am. Bull. 76, 719
Gast, P.W., (1968) Geochim. Cosmochim. Acta 32, 1057
Hart, S.R., (1970) Carnegie Inst. Yearbook 70, 353
Hart, S.R., Glassley, W.E., Karig, D.E., (1972) Earth Planet. Sci. Lett. 15, 12
Hedge, C.E., (1966) J. Geophys. Res. 71, 6119
Jakes, P., White, A.J.R., (1970) Geochim. Cosmochim Acta 34, 849
Jakes, P., White, A.J.R., (1972) Geol. Soc. Am. Bull. 83, 29
Kaneoka, I., Isshiki, N., Zashu, S., (1972) Geochem. J. 4, 53
Karig, D.E., (1971) J. Geophys. Res. 76, 2542
Karig, D.E., (1971) Bull. Geol. Soc. Am. 82, 323
Kay, R., (1970) J. Geophys. Res. 75, 1585
Peterman, Z.E., Hedge, C.E., (1971) Geol. Soc. Am. Bull. 82, 493
Pushkar, P., (1968) J. Geophys. Res. 73, 2701
Shiraki, K., (1971) Earth Planet. Sci. Lett. 13, 167
Uyeda, S., Ben-Abraham, Z., (1972) Nature Phys. Sci. 240, 176
Uyeda, S., Miyashiro, A., (1974) Geol. Soc. Am. Bull, 85, 1159

^{40}Ar - ^{39}Ar AGES OF BASALTS DREDGED FROM RIDGES IN THE LINE CHAIN AND THEIR IMPLICATIONS

Kazuo SAITO and Minoru OZIMA

Geophysical Institute, University of Tokyo
Bunkyo-ku, Tokyo 113, Japan

1. Introduction

Wilson (1963) first proposed that the linear Hawaiian volcanic chain was formed as oceanic crust moves over a magma source in the mantle. Morgan (1972) extended this hypothesis to explain other volcanic chains such as the Austral-Marshall-Gilbert and the Tuamotu-Line volcanic chains as well as the Hawaiian-Emperor chain on the basis of 'hot spots' fixed to the mesosphere. Lately Clague and Jarrard (1973) showed that the movement of the Pacific plate deduced from the analysis of the Hawaiian-Emperor chain on the basis of the hot spot hypothesis agrees with the movement expected from paleomagnetism of seamounts as well as from the sedimentation pattern in the equatorial Pacific. Radiometric ages of volcanic rocks (McDougall, 1964, Clague and Dalrymple, 1973) and ages of fossils (Scholl et al., 1971) on seamounts in the Hawaiian-Emperor volcanic chain are consistent with a hot spot origin of this volcanic chain. However, age data by which to test a hot spot origin of the Tuamotu-Line and the Austral-Marshall-Gilbert chains are scanty. This paper presents radiometric ages of volcanic rocks dredged from the ridge in the northern part of the Line volcanic chain, discusses the implications for the hot spot hypothesis of this volcanic chain.

Because of excess argon and weathering, which are rather common in submarine basalts, a conventional K-Ar age may be subject to a considerable error. Hence, we applied the ^{40}Ar-^{39}Ar dating method with a stepwise degassing technique, which is shown to be comparatively free from the disturbances due to excess argon and argon loss (Ozima and Saito, 1973).

2. Samples and experimental results

The samples are basaltic boulders dredged from the submarine ridge at two points in the Line volcanic chain. Dredging sites and other data are given in Figure 1 and Table 1. Glassy outer rims and altered portions were eliminated by hand and the least altered portions were used for dating experiments. Each Sample was then crushed into granules of a few millimeters and sealed in a quartz tube (10 x 80 mm) in vacuo of about 10^{-2} torr. The quartz tube was then put in an aluminum capsule together with a standard sample (Bern 4M muscovite), K_2SO_4 and $CaCO_3$ which also were vacuum-sealed in quartz tubes. The capsules were irradiated for 28 days in a JMTR reactor. The total neutron flux was about 10^{18} nvt and the ratio of thermal to fast neutrons was about 10.

The age of each sample was then determined from a comparison with the age of a standard sample. K_2SO_4 and $CaCO_3$ were used to obtain correction factors $(^{40}Ar/^{39}Ar)_K = 0.043$, $(^{39}Ar/^{37}Ar)_{Ca} = 0.0017$, $(^{36}Ar/^{37}Ar)_{Ca} = 0.00026$, for interfering Ar isotopes induced in the samples by the neutron irradiation. The ^{40}Ar-^{39}Ar ages of sample 133D is 84.4 ± 0.9 m.y. and of

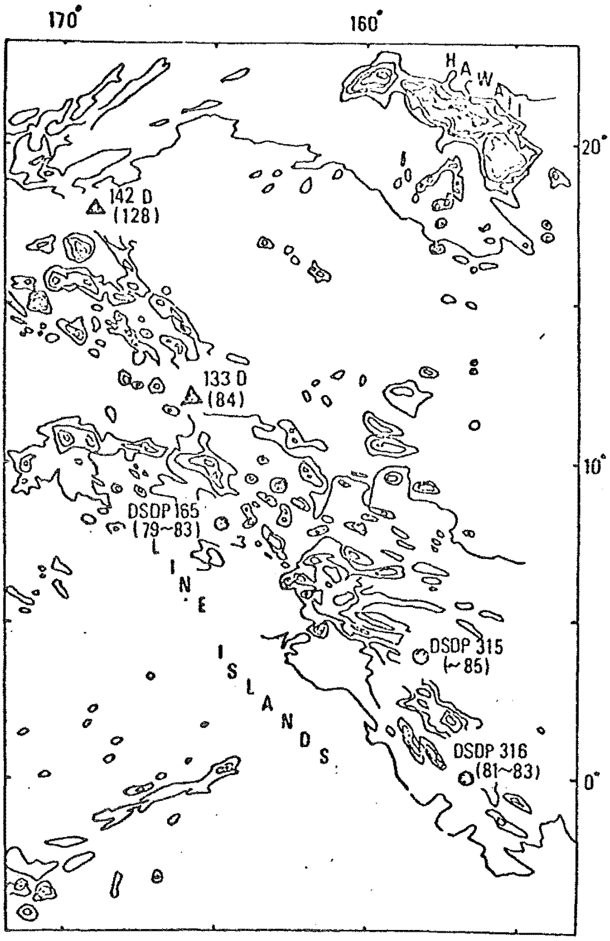

Fig. 1. Dredging sites for SEVEN-TOW 133D and 142D samples. Figures in the brackets show the ^{40}Ar -^{39}Ar ages. DSDP drill sites 165, 315 and 316 are also shown, with the basement ages of their fossils (Winterer and Ewing et al., 1973, Schlanger and Jackson et al., 1974).

sample 142D is 128 $\pm$ 5.0 m.y. An error in a final ^{40}Ar-^{39}Ar age is essentially due to errors in isotopic ratios (^{40}Ar/^{36}Ar) and (^{39}Ar/^{36}Ar). Assuming error correlation coefficient $r = 1$, we calculated standard deviations for ^{40}Ar-^{39}Ar ages and the y-intercepts by means of York's (1969) method. These are shown in Table 1.

Irradiated samples were put in a molybdenum crucible and subjected to a stepwise heating in a high vacuum extraction line. Prior to the degassing experiment, the extraction line including the sample was preheated at about 250° C for four to five hours. The samples were heated by an induction heater and several gas fractions between 600° C and the melting temperature were collected.

Isotopic ratios determined for each temperature fraction are plotted in an apparent K-Ar age plot (the left-hand diagram in Figures 2 and 3) and in an ^{40}Ar*/^{39}Ar* - ^{39}Ar*/^{36}Ar* correlation diagram (the right-hand diagrams). An asterisk in an isotopic ratio indicates that the ratio was corrected for the interfering Ar isotopes induced from K and Ca in the sample. As seen in the correlation plot, in both samples all the temperature fractions lie on a straight line. If the samples had excess argon or has lost argon straight regression

Table 1. $^{40}Ar - ^{39}Ar$ ages of submarine basalts dredged from the Line chain.

SAMPLE	WATER DEPTH(m)	Rock Type	$^{40}Ar-^{39}Ar$ age[1]	K (%)	K-Ar age[2] (m.y.)	Remarks
7-TOW-VI-133D-1 (Kapsitotwa S.M.) 165°50'W, 12°04'N	1550	altered olivine basalt with intergranular groundmass. plagioclase : relatively fresh	84.4 ± 0.9	1.23 ± 0.1		Late Cret. (Senonian) planktonic foraminifera[3]
7-TOW-VI-142D-1 169°04'W, 18°05'N	1570	fine grained trachyte plagioclase : relatively fresh	128 ± 5.0	2.80 ± 0.1		Quaternary planktonic foraminifera[3]
DSDP-165-26-3 (26~29 cm interval) 164°51.6'W, 8°10.7'N	5053	basalt		1.78 ± 0.01	67.0	Late Cret. (Santonian)[4] fossil

1) Irradiation factor $J = 0.0241$ was used to calculate the age. Errors are 1σ.

2) $\lambda_e = 0.585 \times 10^{-10} y^{-1}$, $\lambda_\beta = 4.72 \times 10^{-10} y^{-1}$; $^{40}K/K = 1.14 \times 10^{-4}$ mol/mol. Errors are 1σ.

3) E.L. Winterer (Personal communication, 1973).

4) Winterer, Ewing, et al., 1973.

line would not be expected. The situation is analogous to a conventional K-Ar dating where several separated minerals corresponding to different temperature fractions in the present experiment - give concordant K-Ar ages. We conclude that the ages obtained from the gradients of the regression lines represent the solidification ages of the samples. The apparent K-Ar ages were also calculated, (i) by assuming that non-radiogenic trapped Ar was atmospheric having $(^{40}Ar/^{36}Ar) = 295.5$ (shown by broken lines in Figure 2 and 3) and (ii) by assuming that the trapped Ar has the isotopic ratio $(^{40}Ar/^{36}Ar)$ which were determined from the y-intercepts in the correlation plots (full lines). It is seen that the latter assumption gives better age plateaus.

The correlation lines intersect with y-axis at 269 ± 3 and at 280 ± 6 respectively, which are significantly lower than the atmospheric ratio $(^{40}Ar/^{36}Ar)$ of 295.5. Since correlation lines for a standard sample always intersect with y-axis at 296 ± 4, we doubt that the low observed value of $(^{40}Ar/^{36}Ar)$ could be due to an instrumental mass discrimination. However, at present we do not know whether the low value of $(^{40}Ar/^{36}Ar)$ ratio may be characteristic of the deeper part of the mantle where hot spots are often assumed to originate (Morgan, 1972), or merely indicative of a local feature.

In Table 1, a conventional K-Ar age of DSDP-165 which was drilled from an area adjacent to the Line chain is also given as a reference. The discrepancy between the K-Ar age (67 m.y.) and the fossil age (76~82 m.y.) may be due to loss of Ar or to late fixation of K in the sample.

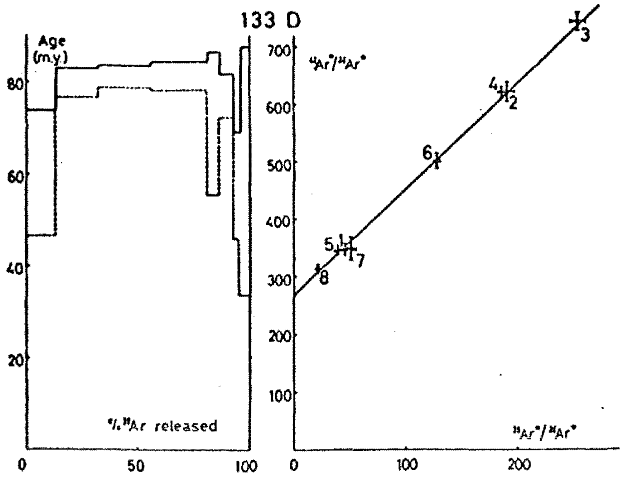

Fig. 2. Sample 133D. Apparent K-Ar age plot (left diagram) and ^{40}Ar*/^{36}Ar* - ^{39}Ar*/^{36}Ar* correlation plot (right) for stepwise degassing. The correlation line was calculated by York's method of least square fit with r (correlation coefficient) = 1 (1969). Error bars indicate 1 standard deviation. Numbers 1 to 8 indicate the lowest temperature fractions, the second lowest and so on. In the left diagram, apparent K-Ar ages were calculated (i) by assuming that non-radiogenic trapped Ar was atmospheric having (^{40}Ar/^{36}Ar) = 295.5 (shown by dotted lines) and (ii) by assuming that the trapped Ar has the isotopic ratio (^{40}Ar/^{36}Ar) which was determined from the y-intercept in the right diagram (shown by full lines).

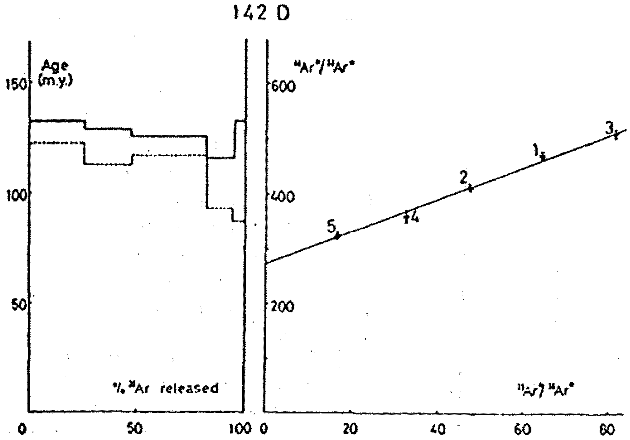

Fig. 3. Sample 142D. Notation as in Figure 2.

3. Discussion

Morgan (1972) suggested that the Line and Emperor chains formed simultaneously during the period while the Pacific plate was rotating around the "Emperor pole" at 23°N, 110°W. On the basis of additional age date Clague and Jarrard (1973) concluded that the Emperor pole is situated at 17°N, 107°W around which the Pacific plate was rotating at a rate of 0.8°/m.y. If we assume that the Line chain was formed by the mantle hot spot suggested by Morgan (1972), the present ^{40}Ar - ^{39}Ar ages may give 0.2°/m.y. for the rotation rate of the Pacific plate with respect to the 'Morgan's Emperor pole', which is about one fourth of the value estimated by Clague and Jarrard. The difference between the two estimates may be explained in the following ways.

Firstly, the Line chain may not be of a hot spot origin, or at least not of a single hot spot origin. As pointed out by Clague and Jarrard (1973), the Tuamotu chain shows better parallelism to the Emperor chain than the Line chain does. Hence, one must admit some ambiguity in Morgan's hypothesis that the Line chain was formed by a rotation around the Emperor pole, and the Tuamotu chain by a rotation around the Hawaiian pole. In addition the topography of the Line chain is not as simple as that of the Emperor chain. The northern end of the chain merges into the Mid Pacific mountains and the center of the chain is cut by the Line Cross chain. These observations suggest that the Line chain may consist of several independent short chains which may or may not be of a hot spot origin. Recently Leg 17 (Winterer and Ewing et al., 1973) and Leg 33 (Schlanger and Jackson et al., 1974) of DSDP holes in the southern part of the Line chain showed that the basement ages in these holes are almost the same ranging from 79 m.y. to 85 m.y. These simultaneous ages appear to argue strongly against a hot spot origin for the southern half of the Line chain.

Alternatively, if the northern part of the Line chain was formed by a rotation around the Emperor pole, we might argue that the rotation rate of the Pacific plate was really as slow as 0.2°/m.y. before 80 m.y. Since the oldest known age from the Emperor chain is 70 m.y. (fossils in Meiji Seamount), the rotation rate and the pole determined from the Emperor chain may only correspond to the period since 70 m.y. In regards to this, it is interesting to note that Clague and Jarrard (1973) suggested a change in the rotation pole for the Pacific plate at 70 m.y.

References

Clague, D.A. and G.B. Dalrymple (1973) Earth Planet. Sci. Letters, 17, 411.
Clague, D.A. and R.D. Jarrard (1973) Geol. Soc. Amer. Bull., 84, 1135.
McDougall, I. (1964) Bull. Geolog. Soc. Amer., 75, 107.
Morgan, W.J. (1972) Amer. Ass. Petrol. Geol. Bull., 56, 203.
Ozima, M. and K. Saito (1973) Earth Planet. Sci. Letters, 20, 77.
Schlanger, S.O. and E.D. Jackson, et al. (1974) Geotimes, 19, 16.
Scholl, D.W., J.S. Creager, R.E. Boyce, R.J. Echols, T.J. Fullam, J.A. Grow, I. Koizumi, J.H. Lee, H.-Y. Ling, P.R. Supko, R.J. Stewart, and T.R. Worsley (1971) Geotimes, 16, 12.
Wilson, J.T. (1963) Can. J. Phys., 41, 863.
Winterer, E.L. and J. Ewing, et al. (1973) Initial report of the Deep Sea Drilling Project, Vol.17, Washington, 930pp.
York, D. (1969) Earth Planet. Sci. Letters, 5, 359.

ON MANTLE - CRUST MATERIAL INTERACTION

Minoru OZIMA

Geophysical Institute, University of Tokyo
Bunkyo-ku, Tokyo 113

Introduction

Sr and Pb isotopic data on volcanic rocks appear to indicate that there has been persistent material interaction between the mantle and the crust. The material interaction is also an unescapable conclusion from an ocean floor spreading theory (OFS), in which upwelling mantle material is introduced to the crust at mid-ocean ridge (MOR) and then returns to the mantle at subduction zones. The process of the material interaction may be most conveniently expressed in terms of a transport rate. The transport rates for the upwelling mantle material were estimated on the basis of OFS and a continental growth. The transport rates are then compared with those proposed for Rb, Sr, U and Pb from their isotopic ratios by several authors, hoping that such comparison would shed more light on the understanding of the material interaction between the mantle and the crust, or of the geodynamic processes involved.

Transport rates estimated for some trace elements

On the basis of systematic variation of the isotopic ratios of Sr in basaltic rocks with age, Hart (1969) suggested that Rb/Sr ratio has continuously decreased in the mantle throughout the whole history of the earth. The continuous decrease in Rb/Sr ratio may be best understood if one consider an upward differential movement of Rb with respect to Sr, in which Rb has been more effectively removed from the mantle to the crust than Sr. Similar upward movement is also suggested for U, Pb, on the basis of Pb isotopic ratios in ore lead and oceanic basalts (Russell, 1972, Russell and Birnie, 1974). As was suggested by Armstrong (1968) and Armstrong and Hein (1973), such material interaction between the mantle and the crust may be bidirectional, since ocean floor spreading requires crustal materials to be dragged into the mantle in subduction zones. However, as shown by Russell (1972) and Russell and Birnie (1974), this return flow is likely to be at most one tenth of the upward flow. Hence, as a good approximation we may assume that the material exchange between the mantle and the crust is an unidirectional i.e. an upward flow from the mantle to the crust.

The transport process for elements may be approximated by a first order rate process, that is, the transport rate is proportional to the concentration of the elements considered. Here, the proportional coefficient is defined as a transport rate of the respective element. Below we compile the transport rates for a net upward flow estimated for some trace elements by various authors.

Table 1

Rb	$k = 0.23 \times 10^{-9}\ y^{-1}$	Hart, 1969
Sr	$k = 0.1 \times 10^{-9}\ y^{-1}$	Hart, 1969
U	$k = 2.6 \times 10^{-9}\ y^{-1}$	Russell, 1972 (Model B)
Pb	$k = 1.6 \times 10^{-9}\ y^{-1}$	Russell, 1972 (Model B)
	$k = 1.5 \sim 1.1 \times 10^{-9}\ y^{-1}$	Russell and Birnie, 1974

Transport rate estimated from the rate of the continental growth

On the basis of the Rb-Sr whole rock age values for selected rocks from several continents, Hurley (1969) showed that the age histogram can be best explained by a continuously growing crust model. The rate of the crustal accumulation was about twice as fast as 3.0 b.y. ago than for the last 0.5 - 1.5 b.y., the average value being about $10^6 \mathrm{km}^3/\mathrm{m.y.}$ The growth rate can then be related to the transport rate, if one specifies the volume of the part of the mantle involved in the mass transport. Assuming that the upper half of the mantle is involved, that is,

$$v \cong 4 \times 10^{11} \mathrm{km}^3 \left(= \frac{4}{3} \pi \left((6370)^3 - (4870)^3\right)\right)$$

we estimate the transport rate of the mantle material,

$$k_o = \frac{1}{V} \frac{dV}{dt} \sim \frac{10^6}{4 \times 10^{11}} = 2.5 \times 10^{-6}/\mathrm{m.y.}$$
$$= 2.5 \times 10^{-12} y^{-1}$$

The value of k_o is about one to two orders of a magnitude as small as the values of the transport rate for the trace elements. This may be explained that the trace elements such as U, Pb, Rb and Sr can be more effectively loaded in the upward moving material than major elements constituting the moving material. If we assume that the material transport from the mantle to the crust takes place as a magma, the transport rate for the individual element should expressed as

$$k = K \cdot k_o$$

in which K denotes a partition coefficient of the element between solid and liquid phases, that is,

$$K = (C)_L/(C)_S, \quad C = \text{concentration of the element.}$$

Since the partition coefficients for the trace elements are estimated to range from ten to one hundred, we may reasonably explain the difference between the transport rate of a bulk material and those estimated for the trace elements.

Transport rate estimated from ocean floor spreading (OFS) theory

A rate of the addition of the mantle derived material to the crust can be estimated on the basis of OFS theory. According to Sclater and Francheteau (1970), the total length of an active MOR (mid oceanic ridge) in the present earth is $L = 5 \times 10^7$ km. If we follow Sclater and Francheteau that the lithosphere which was formed upon MOR has a depth of 75 km and moves laterally with a speed at $v = 3$ cm/y, we can estimate the rate of the crustal accumulation, that is,

$$dV/dt \cong L \times v \times d = (5 \times 10^7 \times 10^5) \times 3 \times (75 \times 10^5)$$
$$\simeq 113 \times 10^6 \mathrm{km}^3/\mathrm{m.y.}$$

Assuming that the upper half of the mantle is involved in the mass transport, we can estimate the upward transport rate

$$k = \frac{1}{V} \frac{dV}{dt} \sim 0.28 \times 10^{-9} y^{-1}$$

The value is about a hundred times as large as that estimated from the data by Hurley (1969) on the basis of Rb-Sr whole rock age distribution in continents (a previous section). The difference between the two estimates must be due to the return flow, since most of the plate formed at MOR would return to the mantle in subduction zones. Assuming that the resultant upward flow or the net transport rate is the same as that estimated on the basis of a continental growth (a previous section), we may conclude that about 99% of the upwelling materials derived at MOR are dragged back into the mantle at subduction zones, or only 1% of the upwelling mantle material remains as new crustal material.

Conclusions

The transport rates estimated for U, Pb, Rb and Sr are one to two orders of a magnitude as high as that estimated for upwelling mantle material from the rate of a continental growth by Hurley (1968). The difference between the two estimates for a transport rate may be interpreted as due to large partition coefficients of the trace elements (C_1/C_s). Almost two orders of a magnitude higher transport rate estimated for upwelling material at MOR may indicate that about 99% of the upwelling material returns to the mantle, leaving only 1% as a new crust material.

References

Armstrong, R.L. (1968) Rev. Geophys., 6, 175.
Armstrong, R.L. and S.M. Hein (1973) Geochim. Cosmochim. Acta, 37, 1.
Hart, S.R. and C. Brooks (1970) Ann. Report of the Director, Dept. Terr. Magnetism, Carnegie Institution, 1968-1969, 426.
Hurley, P.M. (1969) Science, 164, 1229.
Russell, R.D. (1972) Rev. Geophys. Space Physics, 10, 529.
Russell, R.D. and D.J. Birnie (1974) Phys. Earth Planet. Interiors, 8, 158.
Sclater, J.G. and J. Francheteau (1970) Geophys. J., 20, 509.

On deficiency of water in Cytherean atmosphere.

Sadao MATSUO

Department of Chemistry, Tokyo Institute of Technology

Introduction

The chemical composition of the atmosphere of Venus has been known even for minor constituents to a certain extent. The major difference between Cytherean and terrestrial atmosphere with respect to their chemical compositions is the deficiency of water in the former. The pertinent information is summarized in Table 1.

Table 1

	Venus	Earth
surface temp.	770 K	(300 K)
surface press.	90 atm.	1 atm. (440 atm.)
CO_2	8.7×10^4 g/cm^2	4.9×10^4 g/cm^2 *
N_2	3×10^3 g/cm^2	860 g/cm^2
O_2	< 0.9 g/cm^2	210 g/cm^2
H_2O	< 0.1 g/cm^2	3.8×10^5 g/cm^2 **

* buried carbonate equivalent

** including water in the crust

Since the genetic and evolutionary situations of Venus and earth are inferred to be closely related, the deficiency of water on Venus has been a great puzzle. The challenge to this problem can be divided into two groups, viz., a) photochemical dissociation of water vapor followed by the loss of hydrogen and/or oxygen (e.g., Rasool, 1968, Smith and Gross, 1972), and b) intrinsic deficiency of water on Venus (e.g., Holland, 1964). This paper proposes one of the bases which supports the latter idea.

Disadvantage of the photo-dissociation hypothesis

When the original amount of water incorporated into the proto-Venus is the same as that of the proto-earth, and the water on Venus has been photo-dissociated for 4.5×10^9 years, the amount of oxygen produced should be as much as 180 kg/cm^2. In order to expel almost all of the oxygen produced, the exospheric temperature of the order of 10^5 K in the model-H_2O atmosphere is necessary (Smith and Gross, 1972). However, if the temperature is as high as 10^5 K, the loss of hydrogen from the exosphere is almost instantaneous. The hydrogen-dificient upper atmosphere is hard to maintain such a high temperature. This results in the retention of oxygen in the Cytherean atmosphere. On the basis of γ-ray spectrometry on the surface of Venus, K, Th and U contents were reported to be 40,000 ppm, 6.5 ppm and 2 ppm respectively (Venera VIII, TASS Sept. 9, 1972). It has been emphasized that the terrestinal analogue of the surface material of Venus is granite from this result. When we assume that the original surface material of Venus consists of basalt, and the retained oxygen oxidized basalt to granite (with the simultaneous transfer of other elements), the oxygen with the amount of 180 kg/cm^2 affects to the depth of 35 km. The affected depth thus calculated seems to be too great.

On the other hand, oxidation may have occurred only in the superficial part of Venus. If the retention of oxygen is valid, oxides such as hematite prevail in the surface materials. No positive evidence supporting the presence of hematite particles, however, has yet been obtained in the lower atmosphere of Venus (Hunt and Bartlett, 1973).

Stability of hydrous silicate in Venus site

Did the precursor material of Venus contain hydrous silicates? If this is so, the water should have been lost during the accretion process of Venus. This is not likely, since a certain amount of water has been incorporated into the proto-earth, and that the time and other parameters needed for accretion are inferred to be not much different between our planetary twin.

We may postulate here that hydrous silites had not been stable in a region of the planetary nebula where Venus was to be formed. The postulate can be extended to, hydrous silicates were unstable but carbonates were stable in the Venus site, and both of hydrous silicates and carbonates were stable in the earth site.

Chlorite is taken as a representative of hydrous silicates, and calcium carbonate as that of carbonates in this study. The line of thought is to seek the temperature condition under which hydrous silicates are unstable and carbonates are stable.

The following two chemical reactions are considered,

$$\underset{\text{chlorite}}{Mg_5Al_2Si_3O_{10}(OH)_8} + \underset{\text{quartz}}{SiO_2} \rightleftharpoons \underset{\text{enstatite}}{4MgSiO_3} + \underset{\text{spinel}}{MgAl_2O_4} + 4H_2O \quad .....(1),$$

$$\underset{}{Mg_5Al_2Si_3O_{10}(OH)_8} + CaCO_3 + 3SiO_2 \rightleftharpoons \underset{\text{forsterite}}{Mg_2SiO_4} + 3MgSiO_3 + \underset{\text{anorthite}}{CaAl_2Si_2O_8} + 4H_2O + CO_2 \qquad .....(2).$$

When the dissociation pressure of water is higher than the ambient water vapor pressure at the site, the hydrous silicate is unstable. On the basis of the temperature dependence of the equilibrium constant of reaction (1), the relationship between P_{H_2O} and temperature can be obtained. Then from reaction (2), we can also obtain the relationship between P_{CO_2} and temperature.

On the other hand, the ambient partial pressures of H_2O and CO_2 are estimated in the following manner. The atomic composition of the planetary nebula is assumed to be the same as that of the solar surface. Then, with a good approximation,

$$\frac{2P_{H_2} + 2P_{H_2O} + 4P_{CH_4}}{P_{CO_2} + P_{CO} + P_{CH_4}} = \frac{H}{C} = 2 \times 10^3 \qquad .....(3),$$

$$\frac{2P_{H_2} + 2P_{H_2O} + 4P_{CH_4}}{P_{H_2O} + 2P_{CO_2} + P_{CO}} = \frac{H}{O} = 1 \times 10^3 \qquad .....(4),$$

eqs.(3) and (4) hold. In the gaseous phase, it is assumed that the equilibrium is established for the following two reactions,

$$H_2 + CO_2 \rightleftharpoons H_2O + CO \qquad .....(5),$$

$$CO + 3H_2 \rightleftharpoons CH_4 + H_2O \qquad .....(6).$$

For the first approximation, the partial pressure of H_2 is taken to be the same as the total gas pressure of 10^{-4} atm. (Cameron 1973).

The results of calculation are given in Table 2 for both dissociation pressures and ambient partial pressures.

Table 2

	P_{CO_2} (atm.)		P_{H_2O} (atm.)	
T(K)	dissociation	ambient	dissociation	ambient
298	2×10^{-86}	1×10^{-24}	3×10^{-25}	2×10^{-7}
400	2×10^{-23}	3×10^{-17}	3×10^{-7}	2×10^{-7}
500	6×10^{-17}	1×10^{-12}	3×10^{-4}	2×10^{-7}
600	2×10^{-12}	2×10^{-10}	3×10^{-2}	2×10^{-7}

Conclusion

As seen in Table 2, the dissociation vapor pressure becomes higher than the partial pressure of water in the planetary nebula above 400 K. On the other hand, the carbonate is stable up to as high as 600 K (probably unstable above 700 K). It is to be noted that the change in the total pressure by an order of magnitude gives only the 50 K difference for the dissociation temperature for the same dissociation pressure. In reactions (1) and (2), we used clinochlore (the magnesium-rich end-number of chlorite). Actual chlorite is a solid solution of Mg- and Fe- end-members. Since we don't know the activity of clinochlore in the actual planetary chlorite-embryo, it is impossible to conclude how the occurrence of iron in chlorite exerts the effect on the dissociation pressure. Although the numerical certainty of the results given in Table 2 deserves further checks, let us try to seek the physical condition in the early planetary nebula that is indicated in Table 2.

According to Kusaka et al. (1970), the temperatures in the planetary nebula (disc) are estimated to be 405 K, 274 K, 225 K and 175 K for Mercury, Venus, earth and Mars sites respectively, at the time of the terminal stage of the glowing proto-sun ($L = 10L_\odot$).

Under this temperature condition, hydrous silicates are stable even in the Venus site. According to the results given in Table 2, the temperature of the planetary nebula at the Venus site should be higher than 400 K and probably lower than 700 K. When the temperature distribution in the planetary disc is governed mainly by the radiation energy from the proto-sun, the indicated temperature range at the Venus site corresponds to the more high luminosity stage of the proto-sun, probably $10^4 \sim 10^5$ years after the beginning of the contraction of the proto-sun.

The precursor grain of Venus may be formed under the temperature condition in the range from 400 K to 700 K. Since hydrous silicates were stable in the precursor grains of the earth, their formation temperature should have been lower than 400 K. The mean accretion temperature of earth's material has been estimated to be 470 K (10^{-4} atm. of the total pressure by Anders (1971), 450 - 470 K by Onuma et al. (1972). Although they regarded these temperatures as the accretion temperature, these temperatures should be called more adequately to be the condensation temperature. Thus, the formation temperature less than 400 K of hydrous silicates in the precursor material of the earth indicates the temperature of the terminal stage of a condensation sequence relevant to the earth could have been lower than 400 K. While the temperature of the terminal stage for Venus material could have never been below 400 K.

References

Anders, E., (1971), Ann. Rev. Astron. Astrophys., 9, 1-34.
Cameron, A.G.W., (1973), Earth Sci. Rev., 9, 125-127.
Hunt, G.E. and Bartlett, J.T., (1973), Endeavour, 32, 39-43.
Holland, H.D., (1964), The origin and evolution of atmospheres and oceans, ed. by Brancazio, P.J. and Cameron, A.G.W., pp. 86-101, John-Wiley.
Kusaka, T., Nakano, T. and Hayashi, C., (1970), Progr. Theor. Phys., 44, 1580-1595.
Onuma, N., Clayton, R.N., and Mayeda, T.K., (1972), Geochim. Cosmochim. Acta, 36, 169-180.
Rasool, S.I., (1968), J. Atmos. Sci., 25, 663-664.
Smith, L.L. and Gross, S.H., (1972), J. Atmos. Sci., 29, 173-178.

ON ESTIMATION OF PARAMETERS OF TURBULENT MOTION IN THE CORE

Hidehumi WATANABE

Geophysical Institute, University of Tokyo, Bunkyo-ku, Tokyo, Japan

1. Introduction

Geomagnetic field is believed to be maintained by a dynamo action in the earth's core. However, the concrete structure of fluid motion that plays an essential part on the feed back process from the toroidal field to a poloidal field, is rather uncertain; the characteristic scale of fluid motion, its life time and the magnitude of fluid velocity etc. By a dynamical consideration it is possible as shown below to estimate some properties of fluid motion essential for a feed back process, based on geomagnetic data(field intensity and the transition interval of polarity change). We assume a turbulent dynamo model in this paper and it is attempted to estimate the correlation length(ℓ), time(τ) and the magnitude(v) of turbulent velocity in the core.

2. Equation for a turbulent Hydromagnetic Dynamo

The dynamo equation for the mean magnetic field $\mathbf{B}$ is

$$\frac{\partial \mathbf{B}}{\partial t} = \mathrm{curl}\ (\mathbf{V}_\varphi \times \mathbf{B} + \alpha \mathbf{B}) + \eta \nabla^2 \mathrm{B}, \qquad (1)$$

where $\mathbf{V}_\varphi$ and α represent nonuniform rotation of the core and α-effect of turbulence, respectively. α composes of the two parts, $\alpha = \alpha_\omega + \alpha_m$. One is α_ω caused by Coriolis force on turbulent motion which has a gradient in the intensity of turbulence (Steenbeck, Krause and Rädler, 1966).

$$\alpha_\omega = - \frac{8}{15} \frac{\tau \ell^2}{\eta} \boldsymbol{\omega} \cdot \nabla \overline{\mathbf{v}^2}, \qquad (2)$$

where $\boldsymbol{\omega}$, η and $\mathbf{v}$ are rotation rate of the earth, magnetic diffusivity and the turbulent velocity in the core. The other is α_m caused by the reaction of magnetic field. Derivation of it is lengthy and only the result is described,

$$\alpha_m = - 1/(24\pi\rho\eta)^2 \tau \ell^2 \mathrm{B}^2 \, \mathbf{B}\ \mathrm{curl}\ \mathbf{B}, \qquad (3)$$

where ρ is the density of the fluid core. This is similar to the the result obtained by Vainshtein (1971).

3. Scheme for the Estimation of τ, ℓ and v

As equation (1) is nonlinear in **B**, the intensity of the geomagnetic dipole field in the stationary state, say 0.3 G, can be used to impose a condition on α_ω and α_m.

We consider the time interval required for the recovery after the polarity change of the geomagnetic field. Now imagine that a fluctuation in the distribution of turbulent motion reduced the field intensity and produced a small reversed field. On the next stage turbulent motion recovers rather rapidly and possesses the same α_ω as in the steady state. Then the magnetic field intensity will be increased again to the level of stationary state. The time interval required for this recovery essentially depends on both of α_ω and α_m, imposing another condition on τ, ℓ and v. Thus the estimation of τ, ℓ and v is shown to be possible.

References

Steenbeck, M., F. Krause, and K. H. Rädler (1966) Z. Naturforsch. A, 21, 369.
Vainshtein, S.I.,(1972) Sov. Phys. JETP, Engl. Transl., 34, 327.

The Melting of Pure Iron at High Pressures

Yozo Hamano

Geophysical Institute, Faculty of Science
University of Tokyo, Tokyo, Japan

1. Introduction

The estimates of the melting temperature of iron under the Earth's core conditions have been done by many authors. The ranges of the estimated values are about 2500 to 5000°K at the core-mantle boundary and about 3000 to 8500°K at the inner-outer core boundary. These discrepancies are due to the different experiments and the theories which they based on. Considering this, it seems more important to clarify the assumptions and the consequences of these estimates rather than to add a new estimate.

The purpose of this paper is to compile the estimates of the melting temperature of iron at the core pressures and to discuss the consequences of these estimates. An estimate appropriate with regard to the available data is suggested in the last section.

2. Experimental works

Experimental studies of the melting of iron at high pressures have been published by Strong(1959), Boyd and England(1963), Sterrett et al. (1965), and Strong et al.(1973).

Strong(1959) observed the fusion curve of iron up to 96,000 atmospheres by a belt type high pressure apparatus. His fusion curve gave the mean slope $dT/dP=2.35^\circ$/kb. But, because of the nonlinearity of this device, the high pressures were overestimated. Later Strong(1962) corrected the pressure scale and obtained the slope $dT/dP=2.60^\circ$/kb, but the effect of pressure on the emf of thermocouples is still necessary. Strong et al. (1973) measured the fusion curve of iron to 60 kb by using gold for an internal pressure standard. Their result gives the melting slope $dT/dP=3.5^\circ$/kb($P=0$-50kb) after the correction of the pressure effect on thermocouples. Over the δ-γ-liquid triple point, ~1718°C, ~52kb, they observed the different slope $dT/dP=3.85^\circ$/kb for γ-liquid transition. This result indicates that it is necessary to consider the effect of phase transition of iron for the estimate of the melting point at higher pressures.

Boyd and England(1963) used a piston-cylinder apparatus to determine the fusion curve of iron to about 45 kb. Their fusion curve is not smooth due to the friction of the piston-cylinder system. The mean melting slope is about 2.5°/kb.

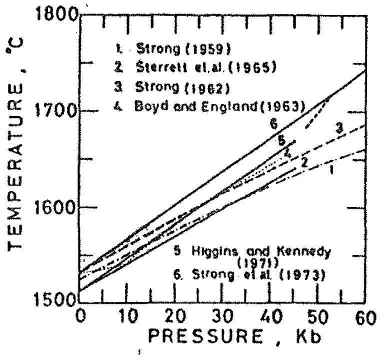

Fig.1 The fusion curves of iron observed by experiments.

Sterrett et al.(1965) determined the fusion curve to 40 kb in piston-cylinder apparatus. Their results shows the melting slope of 2.85°/kb. By applying the correction for the effect of pressure on thermocouples, it becomes 3.8°/kb. Higgins and Kennedy(1971) also corrected the above result and obtained the slope of 3.5°/kb.

Above mentioned result are shown in Fig.1. Considering the thermodynamic data at one atmosphere and the accuracy of the experiments, the melting slope of 3.5°/kb is an appropriate value for the initial 50kb range. Finally it is worth noting that a systematic error of the estimated temperatures by 1% may cause about 10% error for the melting slope.

3. The fusion curve of iron in the Earth's core

In 1950s the melting point, the volume change ΔV and the entropy change ΔS on the melting of iron at atmospheric pressure were known, but the melting temperatures of iron at high pressures were not available. Using the Clapeyron's equation $dT/dP = \Delta V/\Delta S$, the initial slope of the fusion curve was calculated to be about 3°/kb. Linear extrapolation of this slope to the core-mantle boundary($P=1.4$Mb) gave the melting temperature about 6000°K.

The Simon's equation has been much employed for extrapolating the melting curve to high pressures. This equation is expressed as

$$P/a = (T/T_0)^c - 1$$

where T_0 is the melting temperature at 1 atm., a and c are constants to be determined from experiments.

Simon(1953) and Bullard(1954) estimated the melting point of iron at the core pressures by using the Simon's equation, where they evaluated the parameters a and c by averaging the values for alkali metals and combining them with the thermodynamic data at 1 atm. Their estimates of the melting temperature of pure iron under core-mantle conditions is about 3250°K and under inner-outer core conditions their estimate is about 4000°K.

Salter(1954) and Gilvarry(1956) derived the relation

$$c = (6\gamma+1)/(6\gamma-2)$$

from the Lindemann's theory of melting, where γ is the Grüneisen ratio of the solid determined from the equation of state and c is the parameter in the Simon's equation. Gilvarry(1957) used this relation and the thermodynamic data at 1 atm. to evaluate the parameters in the Simon's equation. His melting temperature of iron is about 4200°K at the core-mantle boundary and about 6200°K at inner-outer core boundary.

Strong(1959) measured the fusion curve of iron at high pressures, and extrapolated his data to the core pressures by use of the Simon's equation. He estimated the melting temperature to be about 2500°K at the core-mantle boundary and about 2900°K at the inner-outer core boundary. His estimate is low reflecting his experimental result. Later Strong(1962) revised his experimental result. Birch(1963) used this revised data and the Salter-Gilvarry's relation to determine the parameters in the Simon's equation. His estimated values are 5000°K and 8500°K for the mantle-core and inner-outer core boundaries.

The estimates mentioned above are all based on the Simon's equation, but this equation is not a good expression for the melting of metals. Kennedy and co-workers measured the fusion curves of many metals, and proposed a new linear relationship between the melting temperature of a substance and its isothermal compression.(e.g. Kraut and Kennedy(1966), Kennedy and Vaidya(1970)) The relation is

$$T/T_0 = 1 - C(V_0-V)/V_0 \qquad (1)$$

where T_0 is the melting temperature at 1 atm. and $(V_0-V)/V_0$ is the isothermal compression. C is a constant depend on a substance.

Higgins and Kennedy(1971) used the above relation to extrapolate the fusion curve of iron to the core pressures, where they used the initial melting slope $dT/dP=3.5$°/kb. Their estimated temperatures are 4000°K and 4500°K at the core-mantle and the inner-outer core boundaries. Although the relation (1) represent the available fusion curves of metals quite well,

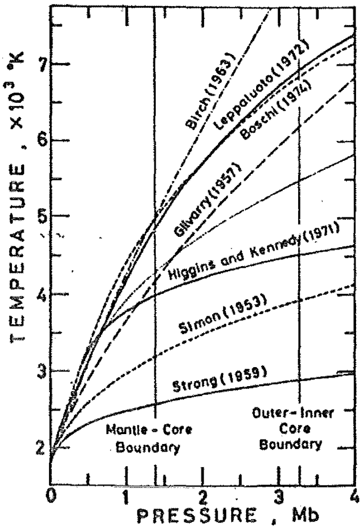

Fig.2 The fusion curves of pure iron extrapolated to the core pressures.

it does not have a theoretical basis.

Leppaluoto(1972) derived the fusion curve of iron by use of the Eyring's significant structure theory of liquid. (see e.g. Eyring and Jhon(1969)) The result of his calculation shows that the minimum value of the melting temperature of iron at the core-mantle boundary is 5000 K and the value at the inner-outer core boundary is 7000 K.

Alder(1966) calculated the melting points of the core material by two methods based on the Lindemann's theory of melting. In the first method he used the observed sound wave velocity of the core. In the second method he assumed the volume dependence of the Grüneisen ratio as $\gamma \propto \sqrt{V}$ and used the observed density of the core. Since he combined the observed data for the core and the thermodynamic data of iron at 1 atm., his estimates have some inconsistency.

Boschi(1974) also used the Lindeman's theory and assumed the Grüneisen ratio to be independent of the volume. He obtained the melting temperatures 5000°K at the core-mantle boundary and 7000°K at the inner-outer core boundary. Fig.2 shows the estimated fusion curves mentioned above. Besides these fusion curves, many other estimates have been proposed, but the estimated temperatures and the methods of estimation are not so different.

Birch(1973) considered the effect of the phase change of iron on the melting temperature. He calculated the initial slope of the fusion curve for eace phase from the thermodynamical data and applied the Kennedy's law to extend the fusion curve in each phase. His results shows that the effect of the phase change of iron from δ to γ phase at high pressures will increase the melting point by about 200°K under core conditions. This value is rather small compared to the discrepancies of the estimated melting temperatures.

4. Discussions

Since the estimates of the fusion curve of pure iron under core conditions show much scatter, it is suitable here to consider the consequences of these estimates. In this section we show two figures helpful to understand them.

In the first place we calculated the variation of $\Delta V/\Delta S$ from the fusion curves of iron. Since the volume change ΔV and the entropy change ΔS on melting depend on the volume of the material, we plotted the variation of $\Delta V/\Delta S$ as a function of the compression. For the conversion of the pressure to the compression, we used the P-V relation of solid iron derived by Higgins and Kennedy(1971) from shock wave data.

Although we can not calculate the variation of ΔV and ΔS separately, we can estimate the upper bound of the volume change on melting at high pressures, since the entropy change generally decreases with pressure. For example, since the relative volume change of iron on melting $\Delta V/V$, where V is the volume of solid iron at melting point, is about 3%, if we accept the Higgins and Kennedy's fusion curve, the relative volume change at the inner-outer core boundary can not exceed 0.2%. In this case the

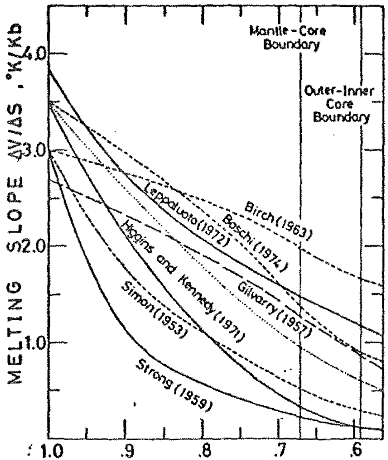

Fig.3 Iron melting curve slope versus isothermal compression. These curves are calculated from the fusion curves in Fig.2.

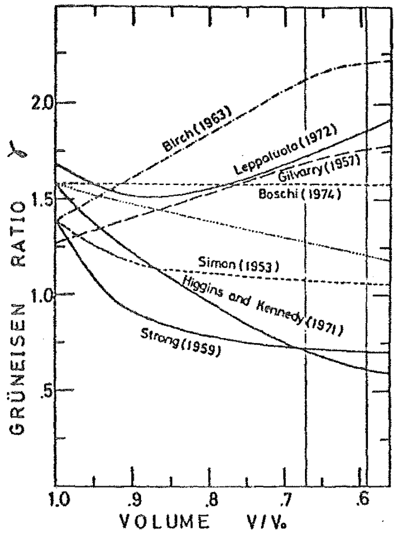

Fig.4 Grüneisen ratio versus isothermal compression.

viscosity of the liquid iron is very high and other physical properties are very close to the solid iron under the core conditions. On the other hand, if we assume the Birch's model, $\Delta V/V$ at the inner-outer core boundary can be 3%, and the viscosity of the liquid iron may have the same value as at atmospheric pressure. In this way, fusion curves of iron under core conditions exert some constraints on the core model.

In the second place, we calculated the variation of the Grüneisen ratio as a function of the compression of iron from the fusion curves in Fig.2 by use of the Lindemann's theory of melting. Since the validity of this theory is supported from both theoretical work(Lennard-Jones and Devonshire(1939)) and numerical experiments(Hoover et al.(1970)), the calculated variation of the Grüneisen constant can be compared with the equation of states of solids. The results are shown in Fig.4.

The Grüneisen ratio of solid iron at 1 atm. is calculated to be about 1.6 from the thermodynamic data, and the variation of the ratio by compression is derived from the shock wave experiments. The result shows the Grüneisen ratio decreases with the compression.(see e.g. Rice et al(1958)) If we accept the Lindemann's theory and the experimental data from shock waves, the fusion curves which give an increase of the Grüneisen ratio by compression are not acceptable.

As Alder(1966) pointed out, the variation of the Grüneisen ratio with the compression of metals is approximated as $\gamma \propto \sqrt{V}$. The variation of the ratio derived from the Higgins and Kennedy's model is too large, and the ones by Boschi(1974) and Leppaluoto(1972) are too small or have different sense.

By assuming the Grüneisen ratio is 1.6, which is derived from the themodynamic data at 1 atm., and the variation of the ratio as $\gamma \propto \sqrt{V}$, we can construct the fusion curve of iron at high pressures. The fusion curve, the variations of $\Delta V/\Delta S$ and of the Grüneisen ratio are shown by the dotted lines in Figs. 2,3 and 4. According to this model, the melting temperature is about 4300°K at the core-mantle boundary and is 5500°K at the inner-outer core boundary. The upper bound of the relative volume change on melting at the inner-outer core boundary is about 1% and the viscosity of the liquid iron under core conditions are about 10^6 poise.

5. Summary

The experimantaly determined fusion curves of iron at high pressures and the models of the fusion curves under core conditions were reviewed. The variations of $\Delta V/\Delta S$ and the Grüneisen ratio with the compression of iron were calculated from these models. The compromised fusion curve consistent with the experimental data and the observations were given.

6. References

Alder, B.J., J. Geophys. Res., 71, 4973-4979, 1966.
Birch, F., in Solids under Pressure, eds. W. Paul and D.M. Warschauer, McGrow-Hill, New York, pp 137-162,1963.
Birch, F., Geophys. J. R. astr. Soc., 29, 373-387, 1972.
Boschi, E., Geophys. J. R. astr. Soc., 38, 327-334, 1974.
Boyd, F.R., and J.L. England, Carnegie Inst. Wash. Year Book 62, 278-284, 1963.
Bullard, E., in The Earth as a Planet, ed. G.P.Kuiper, University of Chicago Press, Chicago, 1954.
Eyring,H. and Mu Shik Jhon, Significant Liquid Structures, Wiley, New York, 1969.
Gilvarry, J.J., Phys. Rev., 102, 325-331, 1956
Gilvarry, J.J., J. Atmosphric and Terrest. Phys., 10, 84-95, 1957
Higgins, G., and G.C.Kennedy, J. Geophys. Res., 76, 1870-1878, 1971.
Hoover, W.G., Ross, M., Johnson, K.W., Henderson, D., Barker, J.A. and Brown, B.C., J. Chem. Phys., 52, 4931-4939,1970.
Kennedy, G.C. and S.N.Vaidya, J. Geophys. Res., 75, 1019-1022,1970.
Kraut, E.A., and G.C.Kennedy, Phys. Rev., 151, 668-675,1966.
Lennard-Jones, J.E. and A.F.Devonshire, Proc. Roy. Soc., A169, 464-484, 1939
Leppaluoto, D.A., Phys. Earth Planet. Interiors, 6, 175-181, 1972.
Salter, L., Phil. Mag., 45, 369-378, 1954.
Simon, F.E., Nature, 172, 746-747, 1953.
Sterrett, K.F., W. Klement, Jr., and G.C.Kennedy, J. Geophys. Res., 70, 1979-1984,1965.
Strong, H.M., J. Geophys. Res., 64, 653-659, 1959.
Strong, H.M., in Modern Very High Pressure Techniques, ed. R.H.Wentorf, Jr., pp 93-117, Butterwirths, Washington, 1962.
Strong, H.M., R.E. Tuft, and R.E. Hanneman, GE report no. 73CRD017,1973.
Rice, M.H., R.G. McQueen, and J.M. Walsh, Solid State Physics, 6, 1-63, 1958.

UNIQUENESS OF THE SPHERICAL HARMONIC ANALYSIS OF THE GEOMAGNETIC FIELD BASED ON THE INCLINATION AND DECLINATION DATA : A CORRECTION

Masaru KONO

Geophysical Institute, University of Tokyo
Bunkyo-ku, Tokyo 113

In the paper published in Rock Magnetism and Paleogeophysics, vol. 1, pp. 118-123, 1973, an error was pointed out to the author by Mr. N. Sugiura and Dr. M. Saito. The proof of the theorem in pages 118 and 119 should be replaced by what follows:

Proof

The bloblem can be stated as: we are given a vector field $\underline{\underline{F}}$ which can be expressed in terms of a scalar potential

$$\underline{\underline{F}} = -\operatorname{grad} W \qquad \nabla^2 W = 0 \tag{1}$$

Can we construct another irrotational, solenoidal vector field $\underline{\underline{F'}}$ which satisfies, on the boundary S, the condition

$$\underline{\underline{F'}} = g\,\underline{\underline{F}} \tag{2}$$

where g is an arbitrary scalar function defined on S? What are the properties of the function g and the vector field $\underline{\underline{F'}}$? In the following, the term "equipotential" always refers to the potential W.

As any component of forces $\underline{\underline{F}}$ or $\underline{\underline{F'}}$ is analytic in V, g is also analytic.

If there is a finite area on the boundary S in which the equi-g lines can be drawn not parallel to the equipotential lines, we can easily show that the theorem indeed holds. To prove this consider an integral $\int_A^C F'_s\,ds$ where F'_s is the component of $\underline{\underline{F'}}$ in the direction of the line element ds (Fig. 1). As this integral does not depend on the choice of the path, we take the path ABC and see that

$$\int_A^C F'_s ds = \int_A^B g F_s ds + \int_B^C g F_s ds$$
$$= -g_2 \int_B^C \frac{\partial W}{\partial s} ds = g_2 (W_2 - W_1)$$

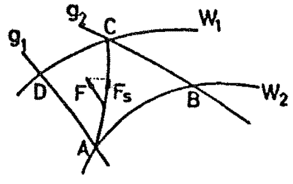

Fig. 1. Integration paths.

On the other hand, if we take the path ADC, we obtain

$$\int_A^C F'_s ds = g_1 (W_2 - W_1)$$

which shows that $g_1 = g_2$ and hence g is constant in that area. But, since g is analytic, g must be a constant on S $(g \equiv c)$ and $\underline{F'}$ can be derived from an obvious potential

$$\underline{\underline{F'}} = -\operatorname{grad} W' \qquad W' = cW + c' \tag{3}$$

where c' is another constant. As a potential is uniquely determined by its

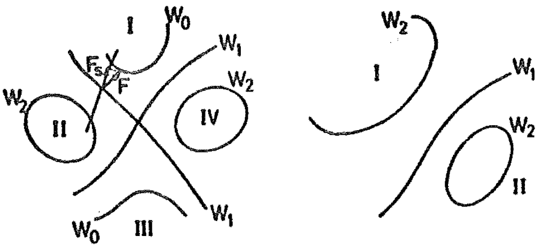

(a) (b)

Fig. 2. Cases when multiple disconnected equipotential lines exist. $W_0 < W_1 < W_2$ is assumed.

derivative $\partial W'/\partial n$ on S, where n denotes the direction normal to the boundary, (3) is the unique solution and $\underline{\underline{F}}' = c\,\underline{\underline{F}}$ holds in the entire space V.

If g depends on variables other than W, equi-g lines are not always parallel to equipotential lines on S. As we have proved that in such cases the theorem holds, it suffices to consider the cases in which the function g in eq. (2) depends only on the value of the potential W. First we show that such g is necessarily a single valued function of W, even when equipotential line form multiple disconnected pieces on S (Fig. 2). We assume that the functional form of g is $g_1(W)$, $g_2(W)$, etc. which are single valued functions of W in each region I, II, etc. separated by the equipotential line W_1. For the case of Fig. 2a, we see, from the values of F_s' and its derivatives with respect to the line element ds at the point $W = W_1$, that

$$g_1 \frac{\partial W}{\partial s} = g_2 \frac{\partial W}{\partial s}\,, \quad \frac{dg_1}{dW}\left(\frac{\partial W}{\partial s}\right)^2 + g_1 \frac{\partial^2 W}{\partial s^2} = \frac{dg_2}{dW}\left(\frac{\partial W}{\partial s}\right)^2 + g_2 \frac{\partial^2 W}{\partial s^2}\,, \quad \text{etc.} \tag{4}$$

hence (as W is analytic) $g_1(W) = g_2(W)$. Likewise we can show that $g_1(W) = g_3(W)$ and so on. When $\partial W/\partial s \equiv 0$, at W_1 as in Fig. 2b, we take the first, third, 5th etc. equations of (4) and can also show that the functional form of g is the same on both sides. Therefore g is single valued function of W.

We can write the potential function for $\underline{\underline{F}}'$ as

$$W' = G(W) + H \qquad G(W) = \int g(W)\,dW \tag{5}$$

where g(W) is now defined in the entire space, with the boundary conditions

$$\text{grad}\, H = 0 \qquad \text{on} \quad S \tag{6}$$

if we treat g (and therefore G) as a known function of W, the equation which must be satisfied by H is

$$\nabla^2 H = -\nabla^2 G \tag{7}$$

which has the general solution

$$H = P(W) + Q \tag{8}$$

where P is a particular solution of (7) depending only on W, and Q is an arbitrary harmonic function with no singular points in V. Since the part of Q which is dependent only on W can be incorporated in P, we can assume, without loss of generality, that Q is a function not only of W but also of the coordinates u, v taken in the direction of equipotential surfaces. The boundary conditions (6) are then

$$\frac{dP}{dW} + \frac{\partial Q}{\partial W} = \frac{\partial Q}{\partial u} = \frac{\partial Q}{\partial v} = 0 \qquad \text{on} \quad S \tag{9}$$

By the assumption, the first term in the first equation is a function of W only while the second does also depend on u and/or v, so that both of these two terms must be zero.

$$\frac{dP}{dW} = 0 \quad \text{and} \quad \frac{\partial Q}{\partial W} = 0 \qquad \text{on } S$$

The harmonic function with grad $Q \equiv 0$ on the boundary is a constant in V and, therefore, by equations (5) and (8), W' is a function of W only. Taking the Laplacian of W'

$$\nabla^2 W' = \operatorname{div}\left(\frac{dW'}{dW} \operatorname{grad} W\right) = \frac{d^2W'}{dW^2}(\operatorname{grad} W)^2 + \frac{dW'}{dW} \nabla^2 W$$

We see that, as W is harmonic and grad W is not zero everywhere,

$$\frac{d^2W'}{dW^2} = 0 \quad \text{or} \quad W' = cW + c' \qquad c, c' : \text{constants} \tag{10}$$

This concludes the proof of the theorem.

AUTHOR INDEX